Preclinical evaluation of TCR gene transfer in combination with arginase inhibition as a therapeutic approach in anticancer medicine

Dissertation

for the award of the degree

Doctor rerum naturalium

Faculty of Biology

Johannes Gutenberg University Mainz

Alexander Lang

Born on February 10th, 1991

in Speyer

Mainz, February 2024

Dean: Prof. Dr. Eckhard Thines

1st correspondent: [redacted]

2nd correspondent: [redacted]

Day of oral exam: April 17th 2024

Affidavit

I hereby declare that I have developed and written this Doctoral Thesis completely by myself and have not used sources or means without declaration in the text. Any thoughts from others or literal quotations are clearly marked. This Doctoral Thesis was not used in the same or in a similar version to achieve an academic grading or is being published elsewhere.

Mainz, February 2024

Alexander Lang

Table of contents

Affidavit I
Abbreviations IX
Summary XIII
Zusammenfassung XV
1. Introduction 1
1.1. Cancer Therapy 1
1.1.1. Conventional Therapy 2
1.1.2. The immune system and cancer 3
1.1.3. Targeted cancer therapy 6
1.1.4. Cancer Immunotherapy 6
1.1.4.1. Immune checkpoint inhibitors 7
1.1.4.2. Cellular therapy 8
1.1.4.3. Cancer Vaccines 11
1.1.5. Challenges in T-cell based cancer therapy 12
1.2. Arginine metabolism 15
1.2.1. Therapeutic anti-cancer strategies acting on arginine metabolism 18
2. Aim of the Study 21
3. Material and Methods 22
3.1. Material 22
3.1.1. Laboratory equipment 22
3.1.2. Cell culture 23
3.1.3. Molecular biology 26
3.2. Methods 30
3.2.1. Animals 30
3.2.2. Cell culture 30
3.2.2.1. Cell lines 31
3.2.2.2. Production of TCGF medium 31

3.2.2.3. Isolation of murine splenocytes 32
3.2.2.4. Stimulation and culture of murine T cells 32
3.2.2.5. Isolation of human PMNs 33
3.2.3. DNA construct and cloning 33
3.2.3.1. DNA restriction digest 34
3.2.3.2. Agarose gel electrophoresis and DNA extraction 34
3.2.3.3. Ligation 35
3.2.3.4. Transformation of chemocompetent bacteria 35
3.2.3.5. Bacterial ON culture and DNA preparation 35
3.2.3.6. Sequencing 36
3.2.4. Retroviral transduction 36
3.2.4.1. Murine T cells 36
3.2.4.2. Tumour cells 37
3.2.5. Flow cytometry 38
3.2.5.1. Staining procedure 39
3.2.5.2. Cell sorting 39
3.2.6. Liquid chromatography–mass spectrometry 40
3.2.7. Functional *in vitro* assays 40
3.2.7.1. Cell layer cytotoxicity assay 40
3.2.7.2. Luminescence based killing assay 41
3.2.7.3. MTS Assay 41
3.2.7.4. Thymidine incorporation assay 41
3.2.8. Western Blot 42
3.2.8.1. Cell lysis and determination of protein concentration 42
3.2.8.2. SDS-PAGE 43
3.2.8.3. Blotting 43
3.2.8.4. Protein detection 43
3.2.9. *In vivo* experiments 44
3.2.10. Software and Statistical Analysis 44

4. Results 45

4.1. MEF cells as tumour target cell line 45

4.1.1. Investigation of MHC I downregulation 45

4.1.2. Genotypic and Phenotypic characterisation of MEF cells *in vitro* 47

4.1.3. T cell transduction and restimulation 48

4.1.4. Chimeric MHC I construct increases HLA expression and recognition by antigen TCR-specific T cells 49

4.1.5. Absence of tumour formation after injection of MEF cells *in vivo* 50

4.2. MC38 cells as new tumour target cell line 51

4.2.1. ASS1 expression in diverse tumour cell lines 51

4.2.2. p53 expressing MC38 cells are eliminated by antigen specific T cells 52

4.2.3. Impact of nor-NOHA on phenotype and proliferation capacity of MC38 cells *in vitro* 53

4.3. *In vitro* characterization of p53 antigen specific T cells and impact of nor-NOHA treatment 54

4.3.1. p53-scTCR expressing T cells specifically recognize MC38_p53 tumour cells 55

4.3.2. T cell phenotype is differently reshaped depending on tumour peptide presentation 56

4.3.3. nor-NOHA treatment does not affect T cell functional characteristics 58

4.4. The impact of arginine deficiency on T cells and tumour cells *in vitro* 60

4.4.1. PMN derived arginase effectively metabolises arginine 61

4.4.2. Arginine deficiency alters T cell proliferation and immune checkpoint expression 62

4.4.3. Effects of arginine deprivation on tumour cell proliferation and surface marker expression 65

4.4.4. Killing capacity of antigen specific T cell is impaired upon arginine starvation 67

4.5. Effect of human PMNs on T cells in cell/cell contact setting 68

4.6. Impact of ACT and nor-NOHA combinatorial treatment on tumour growth *in vivo* 71

4.6.1. MC38_p53_luc/GFP tumour and p53-scTCR T cells 71

4.6.2. MC38_OVA tumour and OT-1 T cells ... 76

5. Discussion ... 82

5.1. MHC downregulation ... 82

5.2. Nor-NOHA treatment *in vitro* ... 83

5.3. Arginine deficiency on T cells and tumour cells ... 86

5.4. Investigation of ACT and nor-NOHA treatment *in vivo* ... 87

6. Bibliography ... 96

7. Appendix ... 112

7.1. Vector maps and constructs ... 112

7.1.1. pMx_puro RTV-014 vector ... 112

7.1.2. pMx-Luciferase-IRES-GFP vector ... 113

7.1.3. pMx_Katushka vector ... 114

7.1.4. p53-scTCR_pGMP93 vector ... 115

7.1.5. pMx_scA2Kb-b2M-p53_puro ... 116

7.2. Primer ... 117

Acknowledgement ... XVI

List of figures

Figure 1: Timeline of breakthroughs in cancer treatments and therapies [7] 2
Figure 2: Schematic overview of TCR structure (A) and TCR-MHC interaction stabilized by co-receptors (B) [34,35] 5
Figure 3: Principle of immune checkpoint interactions and blockade by immune checkpoint inhibitors [43] 7
Figure 4: T cell anti-tumour strategies [51] 9
Figure 5: Structure of CARs and different generations [58] 10
Figure 6: Arginine-related metabolic pathways [102] 16
Figure 7: Impact of arginine starvation on T cell immune responses [112] 17
Figure 8: Chemical structure of L-arginine, nor-NOHA, ABH and BEC [125] 19
Figure 9: PMN isolation with density gradient. [created with BioRender] 33
Figure 10: FACS analysis of HLA-A2 expression on MEF_p53$^{-/-}$_A2K^{b}_Mut.4_Cl.3_GFP 45
Figure 11: HLA-A2 expression on MEF cells 46
Figure 12: Metabolic activity of MEF cells and ASS1 expression 47
Figure 13: Representative expression of CD155/PVR and PD-L1 on MEF_p53 cells 48
Figure 14: Representative FACS staining of T cells after transduction and peptide specific... restimulation 49
Figure 15: Surface HLA_A2 expression and cytotoxicity assay with MEF cells 50
Figure 16: ASS1 expression in selected tumour cell lines 52
Figure 17: HLA-A2 expression on MC38 cells 52
Figure 18: Cytotoxicity assay of WT-MC38 and p53 expressing MC38 and MEF cells 53
Figure 19: Surface marker expression and proliferation of MC38_p53 cells upon long-term.. nor-NOHA treatment 54
Figure 20: T cell specificity and antigen recognition 56
Figure 21: T cell phenotype after tumour co-culture *in vitro* 57
Figure 22: nor-NOHA effect on TCR and immune checkpoint expression of T cells *in vitro* .. 59
Figure 23: Effect of nor-NOHA on proliferation and killing capacity of T cells 60
Figure 24: Representative control staining of isolated human PMNs. 61
Figure 25: Representative LC-MS measurement of arginine 62
Figure 26: Proliferation and cell counts of T cells under arginine starvation 63

Figure 27: FACS based analysis of immune checkpoints and TCR expression under arginine starvation 64
Figure 28: Proliferation of MC38_p53_Luc/GFP tumour cells under arginine deficiency 65
Figure 29: Surface marker expression on MC38_p53_Luc/GFP cells upon arginine deprivation 66
Figure 30: Killing capacity of antigen specific T cells upon arginine starvation 67
Figure 31: T cell proliferation in direct co-culture with PMNs 69
Figure 32: Impact on killing capacity of T cells co-cultured with PMNs 70
Figure 33: Experimental set up of in vivo experiments 71
Figure 34: Tumour growth and survival of mice received ACT ± nor-NOHA treatment 72
Figure 35: Tumour infiltrating immune cells and arginase I expression 73
Figure 36: Splenic MDSC fractions and cytotoxic T cells 74
Figure 37: Total tumour arginase I quantity and plasma arginine levels 75
Figure 38: Tumour growth and survival of mice received ACT ± nor-NOHA treatment 77
Figure 39: Investigation of circulating cytotoxic T cells in the blood 77
Figure 40: Tumour infiltrating immune cells and arginase I expression 79
Figure 41: Splenic cytotoxic T cells 80
Figure 42: Total tumour arginase I quantity 81
Figure 43: Vector map of the pMx_puro RTV-014 plasmid 112
Figure 44: Vector map of the pMx-Luciferase-IRES-GFP plasmid 113
Figure 45: Vector map of the pMx-Katushka plasmid 114
Figure 46: Vector map of the p53-scTCR_pGMP93 plasmid 115
Figure 47: Schematic representation of the sequence encoding for scA2K^{b}_β_2M_p53 117
Figure 48: Structural representation of the chimeric single chain MHC I molecule including the p53 $_{(264\text{-}272)}$ peptide 117

List of tables

Table 1: Laboratory devices 22
Table 2: Reagents for cell culture applications 23
Table 3: Peptides 24
Table 4: Culture media 25
Table 5: Buffers for cell culture applications 26
Table 6: Reagents for applications in molecular biology 26
Table 7: Buffers used in molecular biology applications 28
Table 8: Mouse strains 30
Table 9: Enzymes used in cloning applications 34
Table 10: Restriction mix 34
Table 11: Ligation mix 35
Table 12: Plasmids 37
Table 13: Antibodies and dyes used for FACS staining 38
Table 14: List of WB antibodies 44
Table 15: Primer for pMx_scA2K^{b}_β_2M_p53_puro DNA amplification 117

Abbreviations

A2K^b	Chimeric MHC-I complex (human A2 + murine K^b sequence)
ABH	(S)-2-amino-6-boronohexanoic acid
ACT	Adoptive cell transfer
ADC	Arginine decarboxylase
APCs	Antigen-presenting cells
APS	Ammoniumpersulfate
ASL	Argininosuccinate lyase
ASS1	Argininosuccinate Synthase 1
ATP	Adenosine triphosphate
Aza	Azacitidine
BEC	(S)-(2-boronoethyl)-L-cysteine
BL6	C57 black 6 mouse (C57BL/6)
BSA	Bovine serum albumin
CAR	Chimeric antigen receptor
CD	Cluster of differentiation
COVID	Corona virus disease
CTL	Cytotoxic T lymphocyte
CTLA-4	Cytotoxic T-lymphocyte-associated antigen 4
Ctrl	Control
DAMPs	Damage-associated molecular patterns
DC	Dendritic cell
DMEM	Dulbecco's modified Eagle medium
DMSO	Dimethyl sulfoxide
E:T	Effector to target ratio (T cell to tumour cell ratio)
EDTA	Ethylenediaminetetraacetic acid
FACS	Fluorescence activated cell sorting
FCS	Fetal calf serum
FITC	Fluorescein isothiocyanate
FoxP3	Forkhead-Box-Protein P3

FSC-A	Forward scatter area
GFP	Green fluorescent protein
HLA	Human leukocyte antigen
HNHA	N-hydroxy-7-(2-naphthylthio) heptanomide
hu	Human
IDO	Indoleamine 2,3-dioxygenase
IFN	Interferon
IL	Interleukin
IMC	Immature myeloid cell
iNOS	Inducible nitric oxide synthase
i.p.	Intraperitoneal
i.v.	Intravenous
K_i	Inhibitory constant
KRAS	Kirsten rat sarcoma virus
LAG-3	Lymphocyte activation gene-3
LAT1	L-type amino acid transporter 1
LB	Luria and Bertani
LC-MS	Liquid chromatography–mass spectrometry
mAB	Monoclonal antibody
MDSC	Myeloid derived suppressor cell
MEF	Mouse embryonic fibroblasts
MFI	Mean fluorescence intensity
MHC	Major histocompatibility complex
mio	Million
mRNA	Messenger ribonucleic acid
mu	Murine
NAC	N-Acetylcystein (ROS scavenger)
NEAA	Non-essential amino acids
NK cells	Natural killer cells
NO	Nitric oxide
nor-NOHA	Nω-Hydroxy-nor-L-arginine
ON	Overnight

PBMC	Peripheral Blood Mononuclear Cell
PBS	Phosphate-buffered saline
PCR	Polymerase chain reaction
PD-1	Programmed cell death protein 1
PD-L1	Programmed cell death protein 1 ligand
PE	Phycoerythrin
PEG-ADI	Pegylated arginine deiminase
PFA	Paraformaldehyde
Φ. A.	Phoenix-Ampho
PMNs	Polymorphonuclear neutrophils
PMSF	Phenylmethylsulfonylfluorid
ROS	Reactive oxygen species
RPMI	Roswell Park Memorial Institute
RT	Room temperature
s.c.	Subcutaneous
SD	Standard deviation
SDS	Sodium dodecyl sulfate
SLC	Solute carrier
SOB	Super Optimal Broth
SSC-A	Sideward scatter area
TAA	Tumour-associated antigen
TAE	Tris-acetate-EDTA
TAM	Tumour associated macrophages
TBST	Tris-buffered saline + Tween
TCGF	T cell growth factor
TCR	T cell receptor
TEMED	Tetramethylethylendiamin
TfB	Transformation buffer
TGF	Transforming growth factor
Th	T helper
TIGIT	T cell immunoglobulin and ITIM domain
TIL	Tumour infiltrating lymphocyte

TIM-3	T cell immunoglobulin-3
TME	Tumour microenvironment
TNF	Tumour necrosis factor
TRAIL	TNF-related apoptosis-inducing ligand
Treg	Regulatory T cell
VEGF	Vascular endothelial growth factor
WB	Western Blot
WT	Wild type

Summary

Despite increasing number of new precise treatment strategies, cancer remains as one of the leading causes of death worldwide. The complexity and heterogeneity of tumours with its suppressive tumour microenvironment (TME) and its inhibitory mechanisms against immune cell attack represent hurdles to new cellular therapies. However, every new therapeutic approach leads to a better understanding of tumour characteristics, the TME and the interaction between tumour and immune cells. Thus, promising results in first clinical trials were already achieved by combining different treatment aspects. Nevertheless, it is important to further investigate and target tumour suppressive mechanisms, which could lead to improved anti-tumour therapies. The enzymes arginases play an essential role in metabolic pathways of both immune and tumour cells. In particular, arginase I (Arg1) expression in the TME plays a critical role as a tumour escape mechanism by which arginine availability is reduced to block T cell effector functions. We therefore investigated the inhibition of Arg1 in the TME and its impact on adoptive cell transfer (ACT) of tumour specific T cells. As tumour model, the murine colon carcinoma cell line MC38 was used and genetically modified to express either a p53 (MC38_p53) or an ovalbumin (MC38_OVA) derived peptide for T cell receptor (TCR) recognition. We first demonstrated that direct treatment with the arginase inhibitor nor-NOHA resulted in reduced proliferation of MC38_p53 tumour cells whereas T cell phenotype (TCR and immune checkpoint expression) as well as proliferation were not affected *in vitro*. On the other hand, blocking arginase mediated arginine degradation by nor-NOHA restored TCR expression, reduced PD-1 and TIGIT expression and recovered T cell proliferation and killing capacity *in vitro*. Despite those promising results *in vitro*, *in vivo* experiments revealed controversial outcomes. In the MC38_p53 tumour model, nor-NOHA had a strong impact on reducing tumour growth and improving survival of those animals independent of injected T cells. In addition, nor-NOHA treatment strongly reduced arginase I expression in tumour infiltrating macrophages and myeloid derived suppressor cells (MDSCs). However, no synergistic effect of nor-NOHA treatment in combination with ACT was visible. In contrast, the MC38_OVA tumour model revealed a strong impact of tumour specific T cells resulting in reduced tumour growth and increased survival. Treatment with nor-NOHA even seemed to slightly worsen survival and increasing arginase I expression in tumour infiltrating macrophages and MDSCs.

Those results demonstrate the difficulty to apply the same treatment strategy to different tumour antigen models which even originated from the same tumour cell line (MC38) and only expressed a different antigen. Therefore, it is necessary to further investigate intracellular mechanisms and the TME with its cell subsets to explain the different reactions to one and the same therapeutic approach. However, mRNA vaccination, as another promising strategy in anti-cancer medicine, showed efficiency in further boosting ACT and arginase inhibition in a small mouse cohort. Those results provided promising insights, that combined treatment strategies are on the one hand necessary but on the other hand also efficient to target tumour growth.

Zusammenfassung

Trotz großer Bemühungen in der Erforschung neuer präziser Therapien sind Krebserkrankungen immer noch eine der häufigsten Todesursachen weltweit. Sowohl das komplexe und heterogene Tumorgewebe als auch das supprimierende Tumormikromilieu mit seinen inhibitorischen Mechanismen zur Unterdrückung von Immunzellen stellen eine große Herausforderung in der Entwicklung neuer effektiver Therapien dar. Jedoch wird durch neue therapeutische Ansätze das Verständnis von Tumor- und Immunzellinteraktionen immer weiter vertieft und verschiedene kombinatorische Behandlungsansätze führten bereits zu vielversprechenden Ergebnissen in ersten klinischen Studien. Es ist wichtig, inhibitorische Mechanismen weiter zu untersuchen, um neue und verbesserte Tumor-Therapien zu entwickeln. Das Enzym Arginase I hat eine essenzielle Bedeutung im Stoffwechsel von Immun- und Tumorzellen. Seine erhöhte Expression ist ein bekannter sogenannter „Tumor Evasions-Mechanismus", durch welchen Arginin im Tumormikromilieu degradiert wird. Dies führt zu reduzierter Proliferation und zur Unterdrückung von T Zell spezifischen anti-Tumor-Mechanismen. Wir untersuchten die Inhibierung von Arginase I im Tumormikromilieu mittels des Arginase Inhibitors nor-NOHA und die damit verbundenen Auswirkungen auf eine adoptive T Zell-Therapie. Als Tumormodel nutzten wir die murine Darmkrebszelllinie MC38. Diese Zellen wurden genetisch verändert, um entweder ein spezifisches p53 (MC38_p53) oder Ovalbumin (MC38_OVA) Antigen an der Zelloberfläche zu präsentieren. Somit konnten die Tumorzellen von T Zellen mit individuellen T Zell Rezeptoren erkannt und bekämpft werden. In ersten *in vitro* Versuchen konnten wir zeigen, dass die Kultivierung von MC38_p53 Tumorzellen mit nor-NOHA zu einer verringerten Proliferation führte. Bei der Kultivierung von T Zellen hatte nor-NOHA jedoch keinerlei Einfluss auf deren Phänotyp (T Zell Rezeptor- und Immuncheckpoint-Expression) und Proliferation. Durch die Inhibition der Arginase Aktivität mittels nor-NOHA konnte die Arginin Degradierung *in vitro* verhindert werden. Dies führte zum Erhalt der T Zell Rezeptor Expression und zu reduzierter PD-1 und TIGIT Expression im Vergleich zu T Zellen in Arginin Mangelmedium. Durch die Arginase Inhibierung konnte sowohl die T Zell Proliferation als auch deren anti-tumorale Zytotoxizität erhalten bleiben. Trotz dieser erfolgsversprechenden *in vitro* Ergebnisse führten *in vivo* Versuche zu kontroversen Resultaten. Im MC38_p53 Tumormodel konnten wir durch Behandlung mit nor-NOHA ein stark reduziertes Tumorwachstum und deutlich verbesserte Überlebenschancen erzielen.

Des Weiteren konnte eine signifikante Reduktion der Arginase I Expression in Tumor infiltrierenden Makrophagen und myeloischen Suppressor Zellen gemessen werden. Diese Ergebnisse waren jedoch unabhängig von den jeweils injizierten T Zellen. Durch die Kombination von nor-NOHA und adoptiver T Zell Therapie wurde kein synergistischer Effekt beobachtet. Im Gegensatz hierzu zeigte das MC38_OVA Tumormodel einen stark positiven Einfluss der tumorspezifischen T Zellen, welcher zu reduziertem Tumorwachstum und somit verbesserten Überlebenschancen führte. Die Behandlung mit nor-NOHA zeigte allerdings einen leichten Trend zu schlechteren Überlebenschancen und erhöhter Arginase I Expression in Tumor infiltrierenden Makrophagen und myeloischen Suppressor Zellen. Trotz unserer Versuche mit derselben Tumorzelllinie (MC38), die lediglich verschiedene Antigene präsentierte, erhielten wir sehr unterschiedliche Behandlungsergebnisse. Dies verdeutlicht den komplexen Zusammenhang von Tumoren, deren Mikromilieu, Immunzellen und der jeweils angewandten Therapie. Daher ist es notwendig, sowohl intrazelluläre Stoffwechselmechanismen als auch das Tumormikromilieu und seine verschiedenen Zellpopulationen intensiver zu untersuchen, um die sehr unterschiedlichen Ergebnisse erklären zu können. Wir konnten jedoch zeigen, dass mittels mRNA-Impfung, welche einen weiteren vielversprechenden Therapieansatz darstellt, eine Verstärkung der adoptiven T Zell Therapie in Kombination mit Arginase Inhibierung erreicht wurde. In einer kleinen Testgruppe konnte das Tumorwachstum, im Vergleich zur Behandlung ohne mRNA-Impfung, weiter reduziert werden. Diese Ergebnisse lieferten vielversprechende Erkenntnisse, die zeigen, dass für eine effektive Behandlung eine Kombination von Therapien nötig ist, die es dann jedoch ermöglicht das Tumorwachstum deutlich zu reduzieren.

1. Introduction

Cancer is a large group of diseases caused by an uncontrolled division of abnormal cells, which have the potential to invade nearby tissues and spread to other parts of the body. It is one of the main leading causes of premature death worldwide with a rapidly increasing incidence and mortality. An estimated 19.3 million new cases and 10 million cancer deaths occurred worldwide in 2020 [1]. External environmental factors including smoking, heavy alcohol consumption, excess body weight, physical inactivity and poor nutrition are the main preventable risk factors for malignant tumours (80-90 %). But also, genetic predisposition can contribute to the development of cancer as well as age which is the most significant unpreventable risk factor [2,3].

1.1. Cancer Therapy

With cancer cases and deaths rising continuously over the last decades, the scientific community strongly increased the effort in finding new specific therapies and treatments. As evidenced by first historical and scientific records of tumours in humans date back to the ancient Egyptian and Greek civilization. During that time, the disease was mainly treated with radical surgery and cautery, still leading to the death of patients due to ineffectiveness [4]. The first modern therapeutic approach in medical oncology was already invented during the 1890s when X-rays were used for the treatment of breast cancer [5]. In the mid-1900s, Chemotherapy revolutionized the modern therapy of tumours, building the basis of effective medical therapeutic interventions [6]. From the 1980s on, growing number of immunotherapeutic approaches have been developed which significantly increased the effectiveness of treatments and the survival rates of cancer patients [Figure 1].

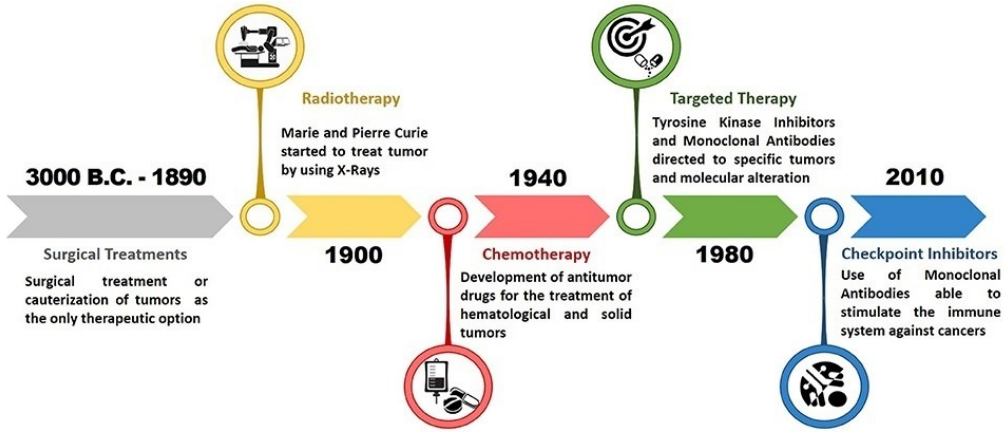

Figure 1: Timeline of breakthroughs in cancer treatments and therapies [7]

1.1.1. Conventional Therapy

Conventional cancer therapy strategies comprise surgery, radiation and chemotherapy or a combination of these options.

Approximately 50 % of all cancer patients will receive radiation therapy during their course of illness [8]. Radiation is mainly applied for the treatment of solid tumours, to generate irreparable DNA damage of the cells, thereby preventing them from growing and proliferating. Unfortunately, the surrounding healthy tissue is often affected as well. Therefore, radiation treatments were improved over the past few decades, enabling precise delivery of matching radiation doses to the exact dimension of tumour while minimizing radiation exposure of surrounding healthy tissue [9]. Additionally, recent studies revealed a multitude of immune-stimulating functions due to radiation therapy. For instance, the release of tumour-associated antigens (TAAs) and damage-associated molecular patterns (DAMPs) leading not only to immune cell priming but also to the destruction of an immunosuppressive tumour-supporting stroma [10]. Furthermore, low-dose γ irradiation was shown to program macrophage differentiation to an M1-like phenotype that can orchestrate effective T cell immunotherapy [11]. However, many tumour types acquire resistance shortly after the treatment due to tumour heterogeneity and recur. Other tumours, in particular cancer stem cells remain insensitive to radiotherapy owing to intrinsic resistance. All those factors contribute to the poor effectiveness of radiotherapy [12].

Sullivan *et al.* estimated a need of surgical intervention for 80 % of all cancers [13]. Long remission can be achieved by operative treatment in the early stage of the disease before metastases in other organs occur. However, 60 % of the newly registered cases are already in the advanced stage [14].

Therefore, cytoreductive surgery is an approach to reduce the number of cancer cells by resection of primary tumours or metastasis to facilitate further treatment strategies. Finally, surgery can have an important role in palliation for those patients whose cure is not possible.

In 2018, roughly 58 % of new cancer cases globally required chemotherapy [15]. There are several chemotherapeutic agents mainly used to inhibit cell proliferation and tumour multiplication. It was shown that chemotherapy is effective in the treatment of various types of cancer, even in later stages. In other types of cancer, however chemotherapy may only prolong overall survival while a curative effect is not achieved. To produce more effective responses a common choice is combination chemotherapy, preventing the development of resistant clones [16,17]. Thereby, a wide range of cancer cells with different genetic abnormalities can be targeted and the development of drug resistance can be prevented or at least reduced [18]. As most chemotherapy drugs show general activity in rapidly multiplying cells, also healthy cells, like bone marrow cells, cells from the gastrointestinal tract or hair follicles are affected. Side effects associated with such agents include nausea, vomiting, alopecia and a strong risk of infections due to immunosuppression. Some chemotherapeutics are even reported to induce secondary malignancies a few years after the drug exposure [16].

In summary, most conventional strategies are not specifically directed to tumour cells and may also affect healthy tissue resulting in severe side effects. Therefore, efforts on conventional therapy approaches stagnated in the late 1980s and the need for more specific and targeted cancer immunotherapies arose.

1.1.2. The immune system and cancer

Cytotoxic macrophages, natural killer cells (NK cells), neutrophils as well as dendritic cells (DCs) and T cells represent the main subset of tumour fighting immune cells.

As part of the innate immune response, tumour associated macrophages (TAMs) are among all tumour infiltrating cells one of the most abundant immune cells [19]. TAMs are classified into two phenotypes. Proinflammatory M1-like macrophages play a relevant role during carcinogenesis as they execute an anti-tumour immune response through the expression of high levels of tumour necrosis factor (TNF), inducible nitric oxide synthase (iNOS) or major histocompatibility complex (MHC) class II molecules.

Whilst the tumour progresses, the tumour microenvironment (TME) induces a polarization of macrophages towards a pro-tumourigenic M2-like subtype participating in the process of tumour cell growth, metastasis, immunosuppression, and inhibition of inflammation [20,21]. Therefore, strong tumour infiltration of M2-TAMs correlates with poor prognosis and reduced overall survival [22].

NK cells are also innate immune cells with a broad spectrum of inhibitory and stimulatory receptors on their surface which are used for immune surveillance [23]. Together with cytotoxic T cells they represent the two major killer cell subsets. NK cells are characterized amongst others by the expression of CD56 and CD16 whereas they do not express CD3 as compared to T cells [24]. In contrast to cytotoxic T cells, NK cell activation does not rely on peptide presentation via MHC class I complex. Moreover, MHC class I expression acts as an inhibitory molecule for NK cells. They express NKIR proteins, the ILT-2 protein and the lectin-like CD49/NKG2 complex, which deliver inhibitory signals upon binding to various HLA subtypes [25]. In contrast, CD16 facilitates antibody-dependent cellular cytotoxicity (ADCC) by binding to the Fc portion of various antibodies, triggering lysis by NK cells [25]. Upon direct binding of stimulatory cell surface receptors, like CD16 and CD56, to their tumour-derived ligands, NK cells get activated and release cytotoxic perforin and granzyme ultimately leading to tumour cell death [26]. Furthermore, NK cells are able to trigger apoptotic pathways in tumour cells by releasing cytokines such as TNF-α or via direct cell-cell contact through activation of TNF-related apoptosis-inducing ligand (TRAIL) and Fas-ligand (FASL) pathways [27].

To elicit an adaptive immune response to cancer, DCs represent the interface between innate and adaptive immunity. They sample and present endogenous and exogenous antigens to T cells. To express antigen-derived peptides on the surface, DCs have to receive activation signals to mature and differentiate [28]. As a next step, DCs must migrate to lymphoid organs where they present the processed antigens in the context of MHC for recognition by T cells. MHCs also known as human leukocyte antigens (HLAs) can be subdivided into two classes. MHC class I complexes are presented on almost all nucleated cells, whereas MHC class II complexes are exclusively expressed by antigen-presenting cells (APCs) such as DCs. Both classes share an overall similar structure. The peptide binding cleft is composed of two domains, formed by a single heavy α-chain in the case of MHC class I and by two chains in the case of MHC class II (α-chain and β-chain). Immunoglobulin-like domains support the peptide binding unit and transmembrane helices anchor the complex in the membrane [Figure 2B] [29].

T cells are the second most frequent immune cell type found in human tumours and belong to the adaptive immune system. The two main sub-classes of T cells are CD8 and CD4 T cells which express a highly specific TCR recognizing peptides presented on MHC I or II, respectively. The natural TCR consist of an α/β heterodimer or a less prominent γ/δ heterodimer on the surface [30]. Each chain consists of a constant and variable domain. A disulfide bond between the constant alpha and beta domain stabilizes the complex [Figure 2A]. The two extracellular variable domains contribute to the MHC affinity and the peptide interaction [31]. The TCR is stabilized at the cell membrane by noncovalent association with the transmembrane cluster CD3, which transmits an intracellular activation signal upon TCR binding [32]. Furthermore, the TCR-MHC interaction is stabilized by the CD8 or CD4 co-receptor which binds to the α-chain of MHC class I or II respectively [33] [Figure 2B]. T cell activation is additionally executed by the interaction between the costimulatory CD28 molecule and B7 (CD80 and CD86).

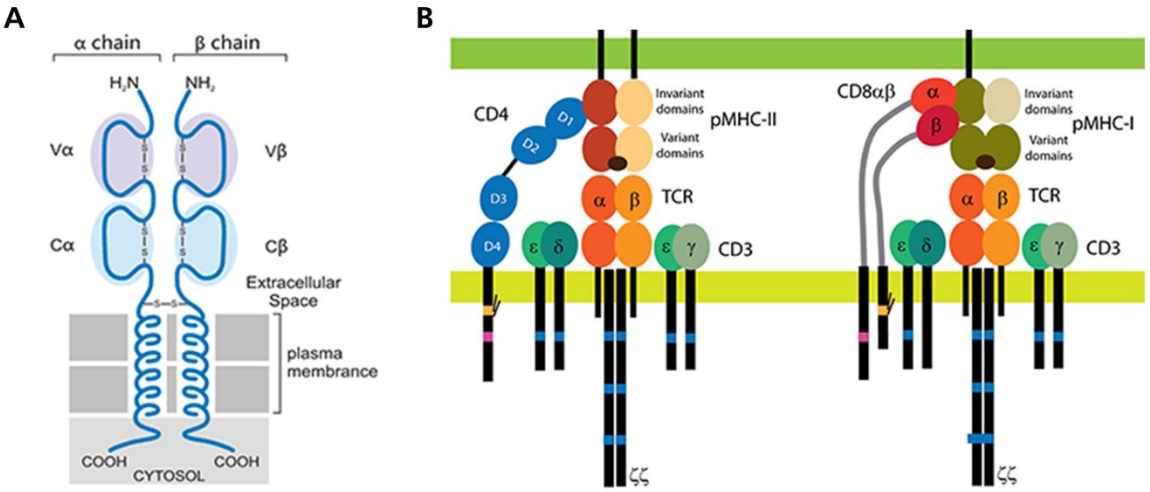

Figure 2: Schematic overview of TCR structure (A) and TCR-MHC interaction stabilized by co-receptors (B) [34,35]

During tumour development, DCs prime and stimulate naïve T cells to generate a protective effector T cell response against immunogenic cancer cells. CD8 T cells as the most prominent anti-tumour cells differentiate into cytotoxic T lymphocytes (CTLs). Soluble factors as reactive oxygen species (ROS), nitric oxide (NO), IL-12, interferon-γ (IFN-γ) and IL-1β recruit those CTLs to the TME where they can exert an efficient anti-tumoural response by the exocytosis of perforin- and granzyme-containing granules [36]. Additionally, also CD4 T cells especially of the T helper 1 (Th-1) subset are able to mediate an anti-tumoural response.

By the secretion of proinflammatory cytokines such as IL-2, TNF-α, and IFN-γ, Th-1 cells promote not only T-cell priming, activation and CTL cytotoxicity but also the anti-tumoural activity of macrophages and NK cells and an overall increase in the presentation of tumour antigens [37]. In many malignancies, the overall survival, and a disease-free survival correlates with the presence of infiltrating CD8 T cells and Th-1 cytokines in the tumour micromilieu [38]. In contrast, regulatory T cells (Tregs) which maintain immune homeostasis in healthy individuals are involved in tumour development and progression by inhibiting antitumour immunity [39].

1.1.3. Targeted cancer therapy

Already in the 1980s, the era of targeted cancer therapies started as molecular and genetic approaches revealed new signalling networks that regulate cellular activities such as proliferation and survival [40]. Like conventional chemotherapy, targeted cancer therapies interfere with proteins involved in tumour growth, progression and spread of cancer cells. By focusing on specific molecular changes, which are unique to a particular cancer, targeted cancer therapies are of great advantage in comparison to conventional chemotherapy. It is now possible to design customised treatments to an individual patient's tumour. There are two main types of targeted cancer therapy, monoclonal antibodies, and small molecule inhibitors. Monoclonal antibodies (mAbs) exert their anti-cancer effects through various mechanisms. They inhibit ligand-receptor interactions crucial for cell survival, directly stop proliferation of cancer cells or cause them to self-destruct. Others carry a lethal toxin to cancer cells. On the other hand, small molecule inhibitors act on specific enzymes and growth factor receptors which are involved in cancer cell proliferation [41].

1.1.4. Cancer Immunotherapy

Immunotherapies can provide specificity and lower toxicity, opening new therapeutic possibilities in cancer treatment. Immunotherapeutic strategies focus on the stimulation of the host's anti-tumour response by increasing the effector cell number and the production of soluble mediators as well as decreasing the host's suppressor mechanisms. Further approaches are to activate T cells, prevent exhaustion and reshape phenotypes towards anti-tumour effector cells.

1.1.4.1. Immune checkpoint inhibitors

Remarkable advances in cancer immunotherapy were developed in recent years. In 2011, the first immune checkpoint inhibitor (ICI) (ipilimumab) was approved. These inhibitors are immunotherapeutic mAbs designed to block tumour proteins or T cell protein receptors located in the membrane surface of T cells and cancer cells, respectively. The main targets of those inhibitors are proteins or receptors that are responsible for the dampening of the immune response. Specifically, cytotoxic T-lymphocyte-associated antigen 4 (CTLA-4) and programmed cell death protein 1 (PD-1) as well as its ligand PD-L1 are currently the targets for which approved inhibitors are available for therapy [42] [Figure 3].

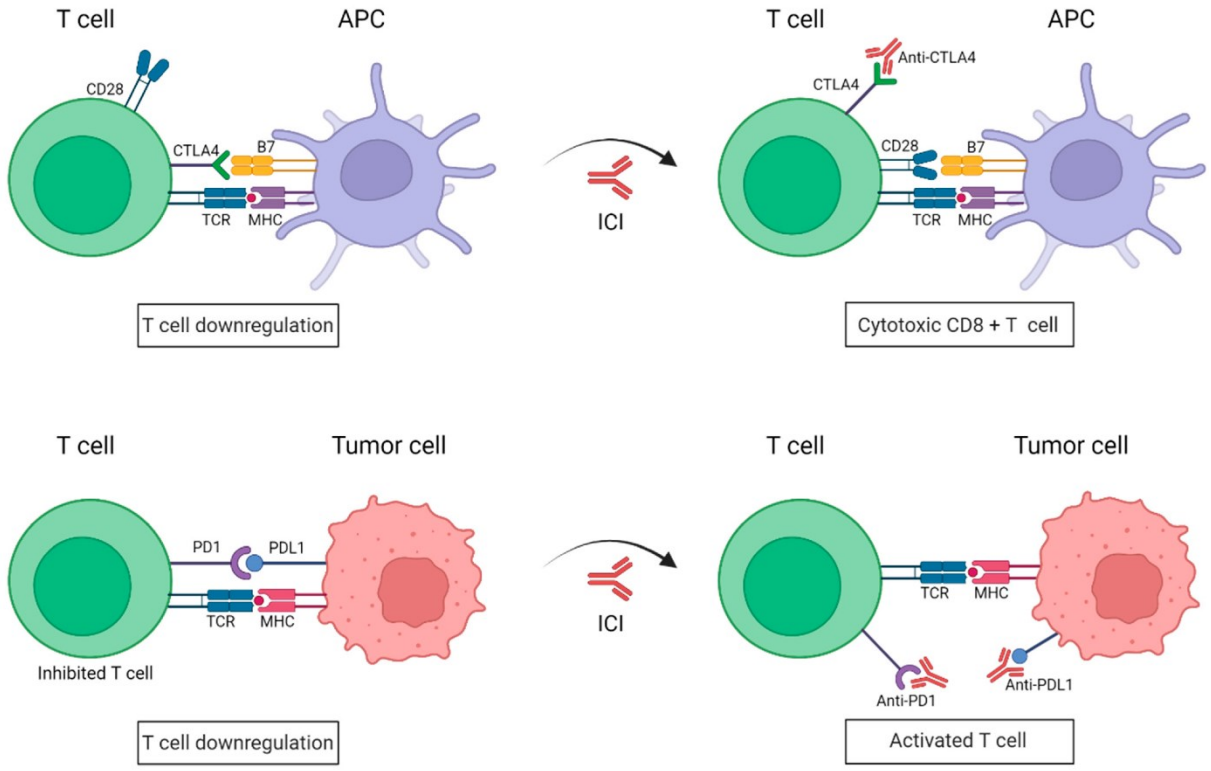

Figure 3: Principle of immune checkpoint interactions and blockade by immune checkpoint inhibitors [43]

Administered in combination with each other or in combination with chemotherapeutic agents results in effective treatments and a prolongation of progression-free survival as well as overall survival mainly in melanoma but also Hodgkin lymphoma, renal cell carcinoma and cutaneous squamous cell carcinoma [42,44]. More important, these drugs have revolutionized the treatment for previously incurable tumours such as metastatic melanoma and non-small cell lung carcinoma [7,45]. However, it is estimated that only about 13 % of cancer patients respond to immune checkpoint inhibition [46]. Those low response rates have several reasons.

Immune checkpoint inhibitors act on blocking T cell inhibition and thereby re-activate anti-cancer processes executed by T cells. Therefore, antigen specific T cells capable of infiltrating the tumour are necessary to achieve responses. It was shown that tumours with low numbers of endogenous tumour infiltrating lymphocytes (TILs) are unlikely to respond to immune checkpoint blockade (ICB). Furthermore, loss of antigen presentation and low mutational burden and neoantigen load (poorly immunogenic tumours) correlate with poor treatment outcome. Other resistance mechanism in the TME, like immune suppressive cells and their cytokine milieu are additional factors that contribute to therapeutic resistance to ICB [47]. Biomarkers to better characterise tumours and predict responses to ICB treatment are strongly investigated. To capture the full genetic complexity of a tumour, next-generation sequencing (NGS) of cancer tissue is performed to reveal its genetic profile. This helps to guide personalized treatment decisions based on the analysis of multiple targets simultaneously [48].

1.1.4.2. Cellular therapy

The use of cellular therapy emerged as an effective cancer treatment strategy over the past decade. This approach uses living immune cells as a drug to treat disease. Mainly two strategies of ACT, focusing on T cells, are investigated and already approved or in clinical testing. i) Endogenous TILs from a patient's tumour can be isolated, expanded ex vivo, activated and re-infused back into the patient. Those cells can traffic to the tumour site after reinfusion as they have an intrinsically heightened ability to recognize and attack cancer cells by their natural TCR repertoire [49] [Figure 4A]. ii) Another approach involves genetically engineered T cells equipped with a receptor (TCR or CAR) to recognise and target specific molecules expressed on cancer cells [50] [Figure 4B]. Those engineered T cells hold great promises for improving existing therapeutic strategies.

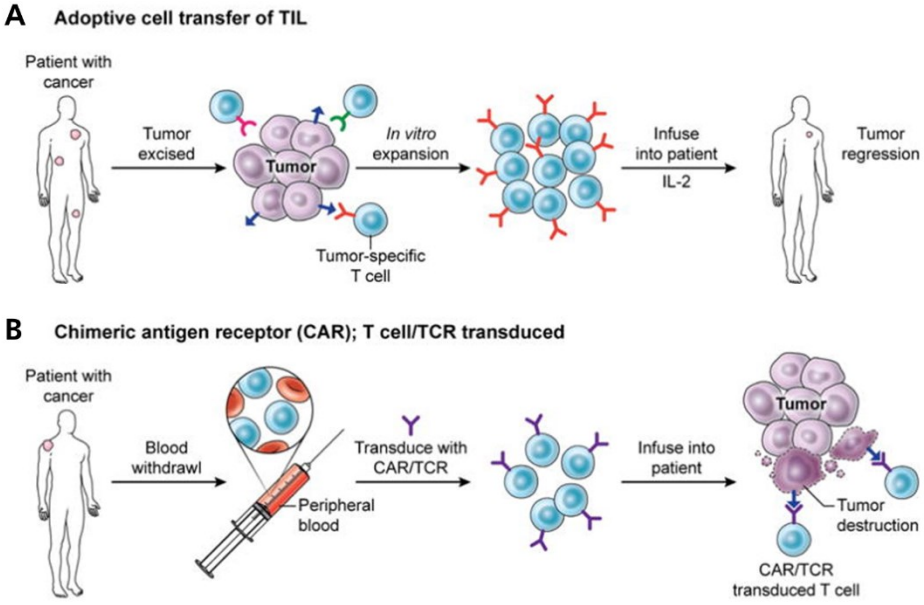

Figure 4: T cell anti-tumour strategies [51]

To achieve effective T cell responses and efficiently target cancer cells, T cells must recognize specific antigens. Those proteins are either located on the surface or processed intracellularly and presented as peptides via MHC on the surface of tumour cells or DCs. Through those specific antigens, immune cells can distinguish cancer cells from healthy cells. Tumour antigens can be classified into two major groups. i) Tumour-specific antigens (TSAs), like cancer neoantigens, derive from somatic genomic mutations in cancer cells resulting in the expression of altered proteins which are only present on cancer tissue, or ii) Tumour-associated antigens (TAAs) which are non-mutated self-antigens overexpressed on cancer cells but also presented on healthy cells [52]. Identifying antigens which are expressed among different tumours could help to design a single receptor beneficial for the treatment of various cancer types.

Theobald and colleagues generated a TCR with high affinity towards a p53 peptide presented by HLA-A2.1 on tumour cells [53]. The p53 protein, known as a master tumour suppressor protein, regulates cell division and replication. It is one of the best studied transcription factors involved in the prevention of cancer cell formation. However, impairment or loss of function due to genetic alterations lead to abnormal cell growth. Overall, p53 is mutated in 50 % of all human cancer types [54]. As wild type (wt) p53 is rapidly degraded in healthy tissue and mutated p53 accumulates in cancer cells, it provides a promising target for immunotherapy [54].

The TCR [55] binds to an unmutated peptide comprising the amino acids 264-272 of wt p53 and is therefore suitable for all HLA-A2.1 patients harbouring a p53 positive cancer type. This peptide represents a broadly expressed TAA in many malignancies. T cells transduced with the p53-scTCR have proven to recognize and eliminate $p53^+$ cancer cells *in vitro* and *in vivo* [55].

To circumvent MHC dependent recognition of tumour antigens, as it is the case for TCRs, chimeric antigen receptors (CARs) were developed. Those synthetic receptors are composed of an extracellular tumour-specific antibody fragment, a transmembrane domain, and a cytoplasmic signalling domain and are MHC-independent [56,57]. CARs are classified by their intracellular domain into several generations [Figure 5]. The first generation has a single CD3-derived immunoreceptor tyrosine-based activation motif (ITAM) signalling chain (mostly CD3 zeta), whereas the second generation has the CD3 zeta domain plus an additional costimulatory domain, mainly 4-1BB or CD28. Those costimulatory domains enhance both cell proliferative and cytotoxic capacities of CAR T cells. Further generations include multiple costimulatory domains, cytokine expression domains like IL-12 inducer for universal cytokine-mediated killing or IL-2Rβ domain to activate JAK and STAT3/5 [58].

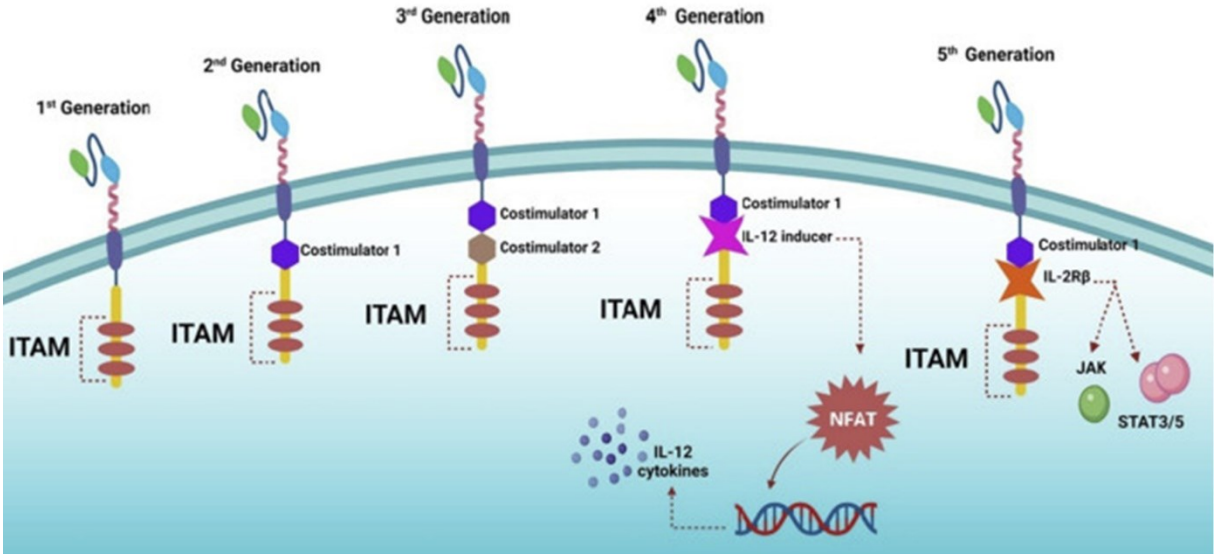

Figure 5: Structure of CARs and different generations [58]

The first US Food and Drug Administration (FDA) CAR treatment therapy was approved in 2017. Novartis designed a CAR targeting CD19 on B cells in young patients with acute lymphoblastic leukaemia (ALL) [59]. Ever since, six CAR-T cell products were approved by the FDA, all for the treatment of haematological malignancies targeting CD19 or B-cell maturation antigen (BCMA) [60,61]. However, to date there is no approved CAR treatment therapy for solid tumours.

1.1.4.3. Cancer Vaccines

Other attractive alternative immunotherapeutic options are cancer vaccines. Preventive, or prophylactic cancer vaccines have the potential to reduce cancer prevalence. Currently, five vaccines protecting against two cancer-promoting viral infections, such as hepatitis B (HBV) and human papillomavirus (HPV), are approved by the FDA. Those viral infections are associated with several different types of cancer including cervical and oral cancer (HPV) or hepatocellular cancer (HBV) [62]. The most promising therapeutic vaccine platform is nucleic acid based and even more specific mRNA based. In general, mRNA vaccination facilitates APC activation due to intracellular tumour antigen expression consequently stimulating the innate and adaptive immune response. In comparison to other cancer vaccine strategies, mRNA vaccination has a stronger potency, a safer administration, rapid development potentials, and cost-effective manufacturing. As already demonstrated successfully in the prevention of COVID-19 and in several clinical trials against multiple aggressive solid tumours, mRNA vaccination strategies will be a key player in the future not only in cancer therapy but also in the treatment of infectious diseases [63].

Especially the combination of mRNA vaccination and adoptive CAR T cell transfer or immune checkpoint blockade proved to be very effective in the treatment of solid tumours. After adoptive transfer of cancer-antigen specific CAR T cells, liposomal antigen-encoding RNA was administered which delivered the antigen to APCs and thereby initiated an immune stimulatory program. This promoted priming and strong expansion of antigen specific CAR T cells [64]. A phase 1/2 clinical trial of CAR T cell administration in combination with mRNA vaccination (CARVac) delivered promising data with strong response and disease control rates in solid tumours [65]. In another clinical phase 1 trial, the combination of anti PD-L1 immunotherapy and individualized neoantigen mRNA vaccination was tested. It was shown, that intravenously delivered mRNA, encoding for up to 20 patient-specific neoantigens, induced a high-magnitude of neoantigen-specific T cells in those patients. This resulted in a longer median recurrence-free survival in patients with pancreatic ductal adenocarcinoma [66,67]. Those results emphasize the strong potential of combinatorial mRNA vaccine treatment strategies.

1.1.5. Challenges in T-cell based cancer therapy

Although, a tremendous development of anti-cancer immunotherapies was achieved during the past few decades, there are still many challenges which need to be overcome.

One of the main problems in tumour therapy is intra-tumour heterogeneity. Tumour cells exhibit multiple phenotypes both in terms of morphology and physiology, resulting in heterogeneity in cell surface molecule expression, proliferation and angiogenic potential [68]. Accordingly, tumour cells express a broad spectrum of antigens which are unevenly distributed on tumour subpopulations and induce different immune responses to the same determinant [69]. For diagnosis, treatment efficacy, and the identification of potential targets, such heterogeneity has important implications.

In addition, many tumour escape mechanisms were reported and characterized. Those mechanisms are specific strategies by which cancer cells evade immune surveillance to survive and replicate in the microenvironment of the host. Examples are MHC-I downregulation, antigen loss variants, upregulation of inhibitory immune checkpoints, recruitment of suppressive cells like Tregs, MDSCs, macrophages or neutrophils, and metabolic starvation. It is important to consider those mechanisms, when designing new therapies and treatment protocols for cancer patients.

In the context of immune evasion, DC maturation and differentiation is important for antigen presentation and initiation of a proper T cell response. This process is inhibited by vascular endothelial growth factor (VEGF), IL-10 and Transforming growth factor β (TGF-β) secreted by tumour cells and immune suppressive cells. DCs retain an immature phenotype and present antigens in a tolerogenic manner resulting in anergic / tolerant T cells. Those tolerogenic or regulatory DCs display low expression of costimulatory molecules such as CD80 and CD86 and in contrast high expression of immunosuppressive factors and molecules such as PD-L1, TGF-β, IL-10 and indoleamine 2,3-dioxygenase (IDO) [70–72].

Antigen presentation for T cell priming following tumour recognition and killing is pivotal for an adaptive immune response. Tumours have developed the ability to down-modulate the antigen processing machinery, resulting in reduced or complete loss of tumour antigen expression on the surface by MHC class I. The tumours become “invisible” for T cells and their tumour antigen specific TCR repertoire which also strongly impairs T cell therapy [73].

Moreover, T cell activity is further regulated by checkpoint receptors which are upregulated upon T cell stimulation and initiate self-regulation.

Such immune checkpoints are important mechanisms to restrict unwanted immunity as well as to diminish responses after an infection. In cancer, however stimulation of checkpoint receptors is often chronic, leading to an inhibition of T cell effector functions also called exhaustion [74]. PD-1 is one of those inhibitory molecules upregulated on T cells after activation, while its ligand (PD-L1) is often expressed on tumour cells. PD-1/PD-L1 interaction leads to a counteraction of positive signals from the TCR as well as CD28 co-stimulation, and downstream signalling pathways are inhibited. This results in decreased T cell activation, proliferation, survival, and cytokine production [75]. On the other hand, it was shown that PD-L1 on cancer cells acts as an immunosuppressive receptor, mediating anti-apoptotic signalling. This causes resistance to cytolysis by CTLs and Fas-mediated killing [76]. After TCR engagement, CTLA-4 is upregulated, which binds to B7 with much higher avidity and affinity compared to CD28. This binding generates inhibitory signals in T cells, hindering proliferation and activation [77]. Consequently, CTLA-4 and PD-1 / PD-L1 are targeted by immune checkpoint inhibitors which have received approval for treatment of several cancer types as breast, bladder, colon, liver, lung and many more. Nevertheless, further co-inhibitory molecules such as Lymphocyte activation gene-3 (LAG-3), T cell immunoglobulin-3 (TIM-3) and T cell immunoglobulin and ITIM domain (TIGIT) have emerged as promising targets for blockade therapy. They all have in common that after binding to their respective ligand (mainly expressed on tumour cells), the effector T cell response is blocked. More in detail, those receptor-ligand interactions lead to inhibited T cell activation, suppressed metabolism and cytokine production as well as decreased proliferation potential [78–81].

Another mechanism evading immune surveillance is via production of several immune suppressive cytokines. TGF-β is a key player in tumour formation as it acts as a tumour suppressor in normal cells by inhibiting cell growth or by promoting cellular differentiation or apoptosis. During the transition towards malignancy, tumour cells become resistant to TGF-β growth inhibition due to mutations of the TGF-β signalling pathway. In addition, tumour cells secret large amounts of TGF-β which weakens the immune system and contributes to tumour evasion and metastasis [82]. Other pivotal cytokines such as IL-6 and IL-10 further induce an immunosuppressive microenvironment.

Furthermore, the TME presents a dynamic and complex system of tumour-fighting and tumour-promoting immune cells. Pro-tumourigenic immune cells assist tumours to evade or silence immune responses by various strategies resulting in inefficient therapeutic treatments and further progression of the disease. Several immune cells play a crucial role in tumour progression and immune suppression. Mainly Tregs, TAMs and MDSCs infiltrate the TME and execute their immunosuppressive functions.

In response to IDO, IL-10 and TGF-β, naïve CD4 T cells differentiate into Tregs in mice and human. Those Tregs can be subdivided into natural occurring Treg (nTregs) or peripherally derived Treg (pTregs) subsets. While nTregs reside in the thymus and express CD25 and Foxp3, pTregs do not express CD25 and are generated after antigenic stimulation in the periphery. Additionally other suppressive regulatory T cell subsets have been described. Those cells are FoxP3 negative and can be classified in $CD4^+$, IL-10-producing type 1 Treg (Tr1) cells and TGF-β-expressing Th3 cells [83]. Tregs either positively participate in immune tolerance or have a negative contribution by hampering cancer immunity. Attracted by chemokines and their receptors [84], Tregs infiltrate the TME and promote tumour growth and metastasis. Tregs inhibit T cell activation and proliferation by releasing IL-10 and TGF-β as well as enhance the expression of inhibitory receptors such as PD-1, LAG-3 and TIM-3 promoting TIL exhaustion [85,86]. In addition, it was shown, that Tregs can suppress NK cell function [87] and execute cell lysis of T cells and APCs upon release of perforin and granzyme [88].

TAMs, especially the anti-inflammatory and tumour supportive M2-type are another major key player in immune suppression, tumour migration, invasion, and angiogenesis. By secretion of lactic acid, tumour cells contribute to a M2-like polarization of TAMs in the TME [89]. Via the secretion of IL-10 and TGF-β, TAMs suppress T cells, NK cell functions, inhibit DC migration and promote differentiation of CD4 cells into Tregs and their recruitment into the TME [90]. Furthermore, TAMs (hu/mu) not only express PD-L1 but also produce and release arginase I (induced by lactic acid) and IDO, leading to inhibited T cell function and metabolic starvation [91]. In line with the release of arginase I, TAM-mediated oxidative stress induces downregulation of the CD3-ζ chain resulting in non-functional TCR expression [92,93].

MDSCs promote tumour cell evasion and metastases, and are an important regulator of immune responses, especially in cancer. MDSCs are a heterogeneous group of immature myeloid cells (IMCs) with potent immunosuppressive activity originating from the bone marrow.
Under pathological conditions, IMCs have failed to further differentiate into macrophages, granulocytes or DCs in the peripheral organs. Instead, they are attracted by chemokines produced in the TME [94], accumulate at the tumour side, get activated, and exhibit their immunosuppressive function [95]. In mice, MDSCs are generally characterized as Gr-1 / CD11b positive cells. As they share phenotypical and morphological characteristics with either monocytes or neutrophils, MDSCs can be further subdivided into two major groups: $CD11b^{+}Ly6G^{-}Ly6C^{hi}$ M-MDSCs and $CD11b^{+}Ly6G^{+}Ly6C^{lo}$ PMN-MDSCs [96]. In the TME, MDSCs are activated by various molecular factors such as VEGF, IFN-γ, TGF-β, IL-6, IL-10, and many others [95]. Upon activation, they highly express IDO, thereby inducing T cell apoptosis [97] and reducing NK cell-mediated tumour killing [95]. MDSCs also contribute to the inhibition of T cell tolerance as they increase the expression of PD-L1 and CTLA-4. Another immunosuppressive mechanism executed by MDSCs is the attraction and stimulation of Tregs which additionally requires tumour-associated antigens [95]. PMN-MDSCs mainly release ROS to induce immunosuppression, whereas M-MDSCs secrete ROS, inducible nitric oxide synthase (iNOS) and arginase I and have therefore the more powerful immunosuppressive potential [74]. These multi-potent immunosuppressive mechanisms of MDSCs make these cells among the major obstacles against effective anti-tumour immunity in solid tumours. Therefore, I focused in this thesis on MDSC-mediated T cell suppression via arginase I.

1.2. Arginine metabolism

Metabolic pathways and their intermediates have been shown to play an important role in the immunosuppressive tumour features. Thus, excluding immune cells from the TME or impairing their anti-tumour response. Manipulation of these metabolic aspects can revert immunosuppression and strengthen anti-tumour responses by recovering the functions of T cells [98]. Hence, metabolic modulations of the TME to promote the immune system in fighting tumours, emerged as an attractive treatment option in cancer research.
In this context, the crucial role of arginine metabolism for T cell function and proliferation has been established. But also, cellular metabolism in most mammalian cells and tumour progression is dependent on the accessibility of arginine.

Availability of arginine is mediated via three major resources: i) arginine-enriched nutrition, ii) protein catabolism (approximately 80 % of the circulating arginine) and iii) endogenous synthesis from citrulline mainly in the kidney [99] (15 % of the total arginine production) [100]. Arginine is therefore a semi-essential amino acid as normal cells do not completely depend on external arginine. Arginine is taken up mainly through two types of solute carrier (SLC) transporters, the cationic amino acid transporters, and the system y^+L amino acid transporters [101]. Within the cell, arginine, as part of the urea cycle, is metabolized into different products [Figure 6]. The enzyme nitric oxide synthase (NOS) metabolizes arginine into nitric oxide (NO) and citrulline, whereas arginase converts it into ornithine and urea, and agmatine results of enzymatic activity of arginine decarboxylase (ADC) [102].

Both ornithine and agmatine are the main sources for putrescine, which is a crucial precursor for polyamines [103]. They play multiple roles in cell growth, proliferation, differentiation, and survival [104]. In addition, arginine can stimulate secretion of hormones and is strongly involved in immunoregulation [105]. Another key player in the urea cycle is citrulline, mainly present in the gut [99]. Normal cells exhibit the intrinsic ability to synthesize arginine from citrulline and aspartate via argininosuccinate synthase 1 (ASS1) and argininosuccinate lyase (ASL) [106]. Citrulline in turn can be imported by the cells or synthesized from glutamine [107], glutamate [108], or proline [109]. It is noteworthy that arginine is the most consumed amino acid in the inner necrotic core of tumour mass. As in over 70 % of tumours, ASS1 expression is suppressed, those tumour cells are auxotrophic to external arginine. Accordingly, to saturate their high arginine demand, tumour cells frequently overexpress specific types of SLCs [102].

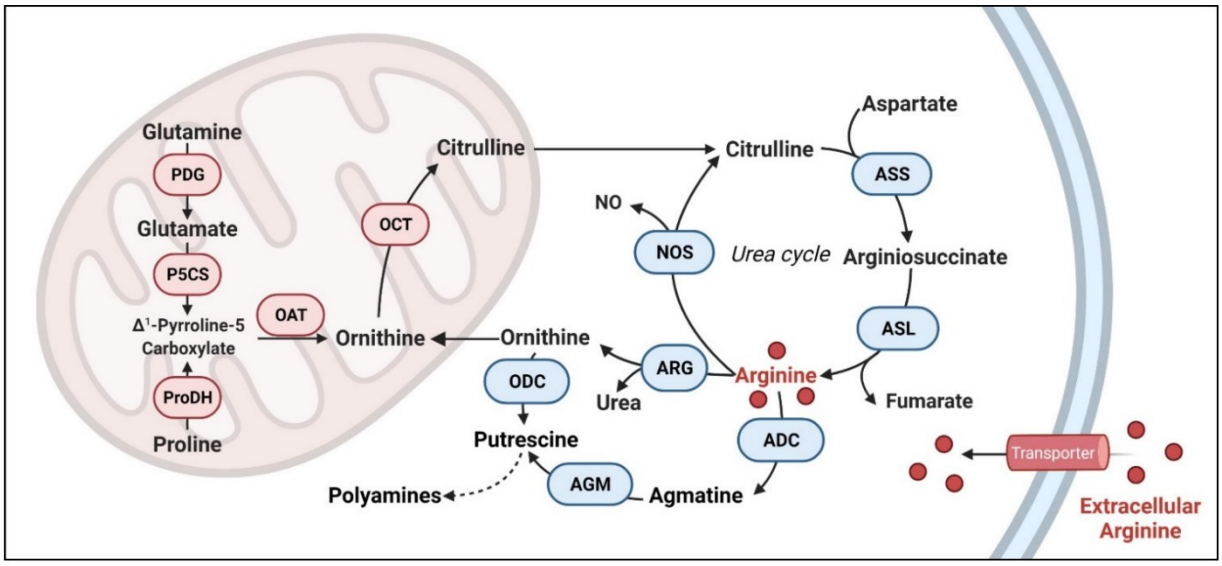

Figure 6: Arginine-related metabolic pathways [102]

In the TME, extracellular arginine is metabolized by high amounts of arginase released mainly from M2-macrophages and MDSCs [105]. Reduced arginine concentration in the circulatory system strongly impairs T cell function [Figure 7]. For example, CD3 ζ chain expression is downregulated resulting in deprived T cell interaction with antigens following reduced TCR-induced activation. Additionally, it was demonstrated that arginine deficiency impairs cofilin dephosphorylation with consecutive inhibition of actin reorganization necessary to create immune synapses and T cell proliferation [110]. Since actin reorganization is also involved in cytokine synthesis, IFN-γ secretion is significantly reduced upon arginine depletion [110]. Arginine deficiency in the microenvironment induces T cell arrest in the G_0-G_1 phase of the cell cycle hindering T cell proliferation. This is due to suppressed translation of the mRNA-binding and -stabilizing protein HuR leading to reduced cyclin D3 mRNA stability [111].

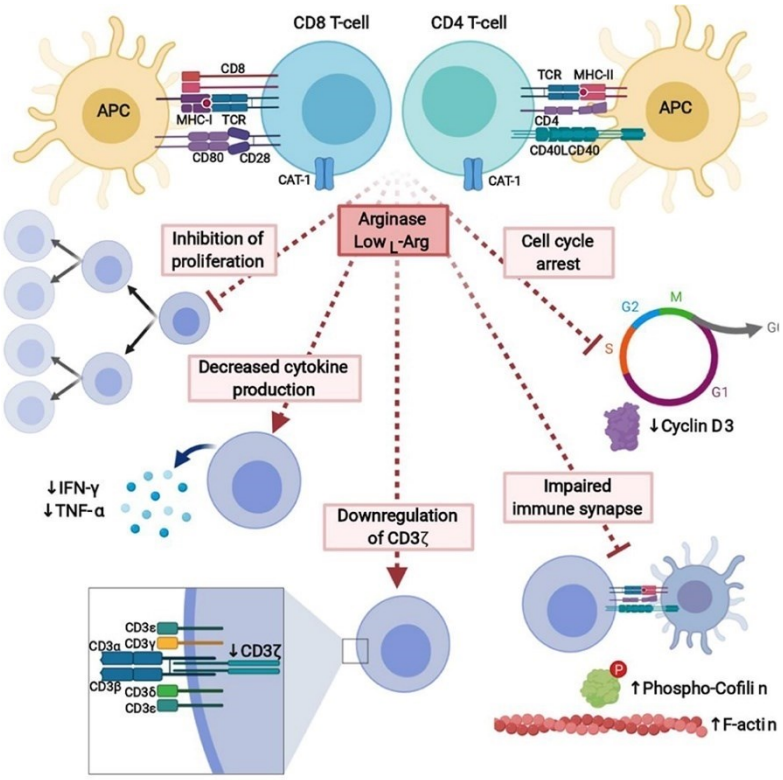

Figure 7: Impact of arginine starvation on T cell immune responses [112]

1.2.1. Therapeutic anti-cancer strategies acting on arginine metabolism

Multiple therapeutic strategies acting on arginine metabolism have been developed to support anti-cancer immunity and induce tumour cell death.

Two opposing treatment options are under investigation focusing on arginine elimination in the TME or arginine supplementation / arginase inhibition.

Some tumours rely on exogenous arginine as they are totally or particularly devoid of ASS1 expression and are therefore arginine auxotrophic. Arginine elimination from the circulatory system by specific enzymes such as pegylated arginine deiminase (PEG-ADI) was developed as a therapeutic approach. The efficacy of ADI-PEG20 therapy has been confirmed in clinical trials to target arginine auxotrophic tumours like hepatocellular carcinoma, melanoma, prostate cancer, and recently small cell lung cancer and acute leukaemia [113–117].

On the other hand, endogenous arginine depletion is addressed pharmacologically by either arginine supplementation or by inhibition of the enzyme arginase. It was reported that arginine treatment reduces cell proliferation in patients with colorectal adenocarcinoma [118], an effect that is most likely related to increased NO concentrations detected in the serum, as high NO concentrations have been reported to induce cytostasis and cytotoxicity in some tumour cells [119]. However, using arginine supplementation ameliorates non-auxotrophic cancer therapy by mainly improving the anti-tumourigenic properties of the immune system. This is in contrast to arginine deprivation strategies which result directly in autophagy and apoptosis of auxotrophic tumour cells. Upon increased arginine supplementation, murine as well as human T cells showed an increase in intracellular arginine level resulting in improved proliferation and survival. Interestingly, NO levels did not increase, indicating that in T cells arginine is mainly catabolized through arginase. In addition, increased intracellular arginine levels shifted T cell metabolism from glycolysis toward mitochondrial oxidative phosphorylation which is more efficient in producing adenosine triphosphate (ATP). T cell differentiation was limited and a central memory-like T cell state with enhanced anti-tumour activity in a mouse model was maintained [120]. Despite those results and other publications following the same direction, too few clinical studies were performed assessing the effectiveness of this treatment strategy. Therefore, no clear advantage of arginine supplementation regarding clinical outcome emerged so far. Further studies demonstrated extensive arginine metabolism by gut and liver arginases [121] and by liberated arginase from MDSCs and M2-TAMs.

A potential metabolic bypass for T cells under conditions of arginine limitation could be the oral administration of citrulline. As shown in Figure 6, arginine can be recycled from citrulline via the enzymes ASS1 and ASL in T cells. The supplementation of citrulline was already tested as an alternative to arginine showing no intestinal degradation [122]. In addition, a study could demonstrate a significant increase of arginine plasma concentrations after oral administration of citrulline [123]. Further proof of concept was presented, as activated human primary T cells upregulated ASS expression in response to low extracellular arginine concentrations. Upon supplementation of citrulline, a reconstitution of T cell proliferation was demonstrated. Citrulline uptake was facilitated by increased expression of the L-type amino acid transporter 1 (LAT1) which was induced upon T cell activation. However, this reconstitution of T cell proliferation was only achieved when low extracellular arginine concentrations were still available. In the complete absence of extracellular arginine, no relevant induction of ASS expression was detectable [124].

Strong efforts were also directed towards arginase inhibitors for clinical use. Almost all drugs are competitive inhibitors of arginase and are in the vast majority arginine analogues [125]. Molecules such as N-hydroxy-nor-L-arginine (nor-NOHA) [126], (S)-2-amino-6-boronohexanoic acid (ABH) [127] and (S)-(2-boronoethyl)-L-cysteine (BEC) [128] belong to the first generation of arginase inhibitors [Figure 8]. They reversibly inhibit the enzymatic activity of arginase by binding to the enzyme with a much higher affinity than its usual substrate arginine [126]. Nor-NOHA became the most potent molecule (K_i = 0.5 μM) of the first generation of arginase inhibitors [129].

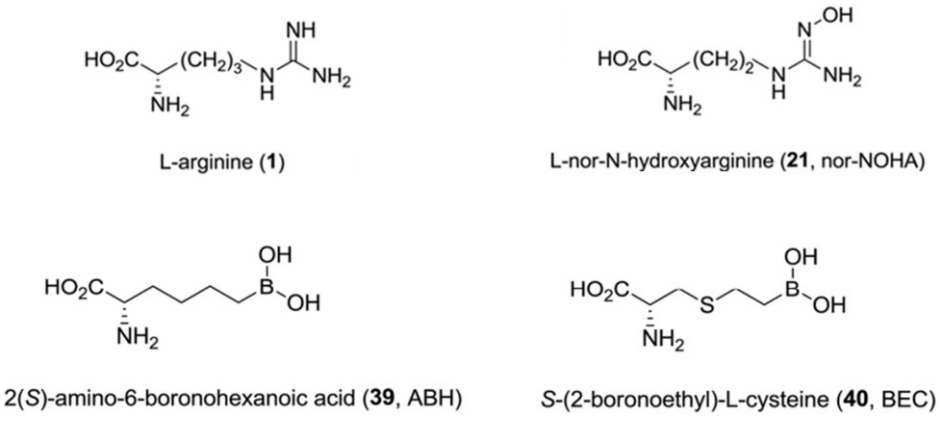

Figure 8: Chemical structure of L-arginine, nor-NOHA, ABH and BEC [125]

Nevertheless, second generation compounds proved to have better pharmacokinetic and pharmacodynamic properties. As an example, the growth of KRAS mutated murine lung tumours was decreased by compound 9 [I-2-amino-6-borono-2-(2-(piperidin-1-yl)ethyl)hexanoic acid] treatment [130]. In addition, the orally available small-molecule compound CB-1158 is being clinically evaluated in the treatment of cancer, both solid tumours and multiple myeloma. It is tested as single agent treatment as well as in combination with immune checkpoint inhibitors in solid tumours. Partial responses were seen in patients with monotherapy and combination therapy with overall response (ORR)/disease control rate (ORR + stable disease) of 3 % / 28 % (n = 32) and 6 % / 37 % (n = 35), respectively [131,132]. CB-1158 was first shown to exert immune-based anti-tumour effects in syngeneic mouse tumour models [133].

Yet, nor-NOHA is commercially available and is used widely from cell culture models to clinical investigations in humans not only in the field of cancer research but also in many other diseases affected by high arginase expression like respiratory [134,135] and cardiovascular diseases [136–139]. Daily systemic administration of nor-NOHA in mice and rats did not result in toxicity during 2-month long treatment [140]. In mouse models, nor-NOHA has shown effectiveness in inhibiting local tumour growth in a T cell (endogenous) dependent manner [141,142] as well as in reducing metastatic burden [143]. In addition, the expression of arginase was markedly decreased in tumour associated MDSCs [141]. In another study, nor-NOHA blocked the downregulation of MHC class II expression on DCs during the tumour bearing state [142]. Preclinical and initial clinical evidence support the idea of targeting arginase activity as a promising option in cancer treatment. Those studies also show that inhibiting arginase might serve as a potent combination treatment with other immunotherapeutic strategies rather than as an effective single agent.

2. Aim of the Study

Our group could demonstrate that adoptive transfer of T cells equipped with an established high affinity scTCR against $p53_{(264-272)}$ was able to recognize and kill $p53^+$ tumour cells in syngeneic and xenograft mouse models. However, when T cells were injected in advanced tumour-bearing mice, only a delay of tumour growth could be achieved, indicating the need of further investigation regarding potential tumour escape mechanisms in mouse models with advanced tumours. A strong infiltration of MDSCs in the TME in conjunction with high levels of arginase I were evidenced in our p53-tumour model *in vivo*. Several reports have already shown the effectiveness of nor-NOHA in reducing tumour growth in murine cancer models. To boost the immunological anti-tumour response, a promising translational therapeutic strategy could be the support of ACT by inhibiting the arginase-mediated tumour immune escape. Therefore, p53-scTCR transduced T cells were used to investigate anti-tumour responses in addition to arginase inhibition via nor-NOHA treatment.

To that aim, the following questions were addressed in this thesis:

(I) How does nor-NOHA treatment affect the function of T cells and tumour cells *in vitro*?

(II) How does arginine starvation affects T cells and tumour cells functional activities *in vitro*?

(III) Does direct co-culture of T cells and PMNs alters T cell effector function?

(IV) What are the effects of arginase I expressing PMNs on T cell function?

(V) Is there a synergistic effect of combining nor-NOHA treatment and ACT *in vivo*?

3. Material and Methods

3.1. Material

3.1.1. Laboratory equipment

Table 1: Laboratory devices

Device	Identification	Manufacturer
Balance	L2200S	Sartorius, Göttingen (GER)
Caliper (digital)	n.a.	n.a.
Centrifuge	5417R	Eppendorf, Hamburg (GER)
Centrifuge	Biofuge fresco	Heraeus, Hanau (GER)
Clean bench	S2020 1.8	Thermo Fisher Scientific, Langenselbold (GER)
CO_2 incubator	Heracell	Heraeus, Hanau (GER)
CO_2 incubator	Hfunction line	Heraeus, Hanau (GER)
Electrophoresis power supply	EPS600	Pharmacia Biotech, München (GER)
Electrophoresis power supply	PowerPac HC	BioRad, Hercules (California, USA)
Flow Cytometer	Canto II	Becton Dickinson, Heidelberg (GER)
Flow Cytometer	Aria	Becton Dickinson, Heidelberg (GER)
Harvester	Mach 3	Tomtec, Unterschleissheim (GER)
Heating block	Thermo Stat plus	Eppendorf, Hamburg (GER)
Homogenizer	TissueLyser LT	Qiagen, Hilden (GER)
Imaging system	iBright CL750	Thermo Fisher Scientific, Langenselbold (GER)
In vivo imaging system	IVIS SpectrumCT	PerkinElmer, Waltham (USA)
Irradiation device (animals)	OB58/905-2	Buchler, Braunschweig (GER)
Irradiation device (cells)	Gammacell 2000	Mølsgaard Medical, Hørsholm (DEN)
Microscope	Axiostar	Zeiss, Jena (GER)
Microscope	Wilovert	Hund, Wetzlar (GER)
PCR cycler	MasterCycler Gradient	Eppendorf, Hamburg (GER)
pH meter	Knick pH-Meter 766	Calimatic, Zweibrücken (GER)

Plate reader	FluostarOmega	BMG Labtech, Ortenberg (GER)
Scintillation beta-counter	MicroBeta TriLux	PerkinElmer, Waltham (USA)
Tissue dissociator	GentleMACS™ Dissociator	Miltenyi Biotec, Bergisch-Gladbach (GER)
Transmitted light camera	DCF 480	Leica, Wetzlar (GER)
UV exposure unit	Transilluminator	Biostep GmbH, Jahnsdorf (GER)
UV/VIS-spectrometer	NanoDrop One	Thermo Fisher Scientific, Waltham (USA)
Water bath	1003	Gesellschaft für Labortechnik, Burgwedel (GER)
Western Blotting System	Trans-Blot cell	BioRad, Hercules (USA)

3.1.2. Cell culture

For cell culture applications the chemicals in Table 2 were used.

Table 2: Reagents for cell culture applications

Reagent	Manufacturer
anti-CD3/CD28 beads (murine)	Thermo Fisher, Dreieich (GER)
Brefeldin A	Abcam, Cambridge (GB)
BSA	Sigma-Aldrich, Deisenhofen (GER)
Concanavalin A	Calbiochem, Darmstadt (GER)
Crystal violet solution	Merck, Darmstadt (GER)
Dextransulfat	Roth, Karlsruhe (GER)
D-Luciferin	BioVision, Milpitas (USA)
DMEM	Gibco, Eggensheim (GER)
DMEM/F12	Gibco, Eggensheim (GER)
DMSO	Roth, Karlsruhe (GER)
EDTA	Sigma-Aldrich, Deisenhofen (GER)
FCS	PAA, Linz (A)
Fugene 6	Promega, Madison (USA)
Geneticin (G418)	Gibco, Eggensheim (GER)
HCl	Roth, Karlsruhe (GER)
HEPES-Buffer	BioWhittaker, Verviers (B)

Histopaque	Sigma-Aldrich, Deisenhofen (GER)
IntraPrep Permeabilization Reagent	Beckman Coulter, Krefeld (GER)
$KHCO_3$	Roth, Karlsruhe (GER)
L-Glutamine	BioWhittaker, Verviers (B)
Methyl-α-D-mannopyranoside	Sigma-Aldrich, Deisenhofen (GER)
β-Mercapthoethanol	Sigma-Aldrich, Deisenhofen (GER)
Na_2EDTA	Sigma-Aldrich, Deisenhofen (GER)
NaOH	Sigma-Aldrich, Deisenhofen (GER)
Na-Penicillin/Streptomycin	Gibco, Eggensheim (GER)
NEAA	BioWhittaker, Verviers (B)
NH_4Cl	Roth, Karlsruhe (GER)
nor-NOHA	Bachem, Bubendorf (CH)
PBS (1x)	Gibco, Eggensheim (GER)
Perm/Wash buffer	Becton Dickinson, Heidelberg (GER)
PFA	Sigma-Aldrich, Deisenhofen (GER)
Polybrene	Sigma-Aldrich, Deisenhofen (GER)
Puromycin	Sigma-Aldrich, Deisenhofen (GER)
RetroNectin	Takara Bio Europe, Saint-Germain-en-Laye (FR)
RPMI1640	Sigma-Aldrich, Deisenhofen (GER)
Sodium Pyruvat	Sigma-Aldrich, Deisenhofen (GER)
Trypan blue	Sigma-Aldrich, Deisenhofen (GER)
Trypsin-EDTA	Gibco, Eggensheim (GER)
Tumour Dissociation Kit (mouse)	Miltenyi Biotec, Bergisch-Gladbach (GER)
^{3}H-thymidine solution	PerkinElmer, Waltham (USA)

Peptides listed in Table 3 were used for antigen specific restimulation of TCR-transgenic T cells as explained in chapter 3.2.2.3.

Table 3: Peptides

Peptide	Sequence	MHC-restriction
$p53_{264-272}$	LLGRNSFEV	HLA-A*02:01
$OVA_{257-264}$	SIINFEKL	H2-K^b

All peptides were purchased from Biosynthan, Berlin (GER) and dissolved according to their solubility character in sterile DMSO or sterile aqua dest.

Cell culture media were prepared as mentioned in Table 4. Ingredients with manufacturer are listed in Table 2.

Table 4: Culture media

Medium	Additives	Recipe
DMEM compl.	DMEM	500 ml
	Penicillin / Streptomycin	1 x
	FCS	10 %
	L-Glutamine	1 x
DMEM/F12	DMEM/F12	500 ml
	FCS	5 %
	L-Glutamine	1 x
	Penicillin / Streptomycin	1 x
MEF medium	DMEM	500 ml
	Penicillin / Streptomycin	1 x
	FCS	10 %
	Hepes	25 mM
	L-Glutamine	1 x
	Non-essential amino acids	100 µM
	β-Mercapthoethanol	50 µM
Φ. A. medium	DMEM	500 ml
	Penicillin / Streptomycin	1 x
	FCS	10 %
	Hepes	25 mM
	L-Glutamine	1 x
Rat medium	RPMI 1640	500 ml
	Penicillin / Streptomycin	1 x
	FCS	10 %
	Hepes	10 mM
	L-Glutamine	2 mM
	β-Mercapthoethanol	50 µM
	Concanavalin A	5 µg/ml
RPMI compl.	RPMI 1640	500 ml
	Penicillin / Streptomycin	1 x
	FCS	10 %
	L-Glutamine	2 mM

T cell medium	RPMI 1640	500 ml
	Penicillin / Streptomycin	1 x
	FCS	10 %
	Hepes	20 mM
	L-Glutamine	1 x
	Sodium Pyruvat	1 mM
	Non-essential amino acids	100 µM
	β-Mercapthoethanol	50 µM

Erythrocytes lysis buffer and PFA were prepared as mentioned in Table 5.

Table 5: Buffers for cell culture applications

Buffer	Reagent	Recipe
Erythrocyte lysis buffer	NH_4Cl	174 mM
	$KHCO_3$	10 mM
	Na_2EDTA	0.1 mM
	H_2O	add 500 ml
	HCl	pH=7.3
2 % / 4 % PFA	Paraformaldehyde (powder)	20 / 40 g
	PBS	add 1 l
	NaOH (until dissolved)	dissolve at 60 °C
	HCl	pH=6.9

All buffers were prepared with Millipore bi-distilled water and if necessary sterile filtered with Steritop™ Filter Units (Merck Millipore, Darmstadt, Germany).

3.1.3. Molecular biology

Buffers which were used for applications in molecular biology are listed in Table 7 and containing chemicals are listed in Table 6.

Table 6: Reagents for applications in molecular biology

Reagent	Manufacturer
Acetic acid	Sigma-Aldrich, Deisenhofen (GER)
Acrylamide/ Bisacrylamide solution (30%)	Roth, Karlsruhe (GER)
Agar	Roth, Karlsruhe (GER)
Agarose	Starlab, Hamburg (GER)
Ampicilin	Sigma-Aldrich, Deisenhofen (GER)
APS	Sigma-Aldrich, Deisenhofen (GER)

Bactotryptone	Roth, Karlsruhe (GER)
Bradford reagent kit	BioRad, Hercules (USA)
Brij O10	Sigma-Aldrich, Deisenhofen (GER)
$CaCl_2$	Sigma-Aldrich, Deisenhofen (GER)
Cobalt acetate	Sigma-Aldrich, Deisenhofen (GER)
Cut-Smart Buffer	New England Biolabs, Frankfurt a.M. (GER)
DNA ladder (100bp / 1kb)	New England Biolabs, Frankfurt a.M. (GER)
dNTPs	New England Biolabs, Frankfurt a.M. (GER)
Western Lightning Plus ECL solution	Perkin Elmer, Boston (USA)
Ethanol	Roth, Karlsruhe (GER)
Gel Loading Dye (6x)	New England Biolabs, Frankfurt a.M. (GER)
Glycerine	Roth, Karlsruhe (GER)
Glycine	Sigma-Aldrich, Deisenhofen (GER)
HCl	Roth, Karlsruhe (GER)
KCl	Merck, Darmstadt (GER)
LB-Medium	Roth, Karlsruhe (GER)
Laemmli buffer	Sigma-Aldrich, Deisenhofen (GER)
Leupeptin	Sigma-Aldrich, Deisenhofen (GER)
β-Mercaptoethanol	Roth, Karlsruhe (GER)
Methanol	Roth, Karlsruhe (GER)
MgCl2	Roth, Karlsruhe (GER)
Milk powder	Roth, Karlsruhe (GER)
$MnCl_2$	Sigma-Aldrich, Deisenhofen (GER)
Mops-Na	Roth, Karlsruhe (GER)
NaCl	Roth, Karlsruhe (GER)
Na_2EDTA	Sigma-Aldrich, Deisenhofen (GER)
NaF	Sigma-Aldrich, Deisenhofen (GER)
Natriumorthovanadat	Sigma-Aldrich, Deisenhofen (GER)
NEB marker (1 kb)	New England Biolabs, Frankfurt a.M. (GER)
Nitrocellulose membrane	Perkin Elmer, Boston (USA)
Peg green DNA dye	VWR, Radnor (USA)
Pepstatin	Sigma-Aldrich, Deisenhofen (GER)

PMSF	Sigma-Aldrich, Deisenhofen (GER)
Precision Plus Protein Western C ladder	BioRad, Hercules (USA)
SDS	Sigma-Aldrich, Deisenhofen (GER)
T4 Ligase Buffer	New England Biolabs, Frankfurt a.M. (GER)
TEMED	AppliChem, Darmstadt (GER)
Tetracycline	Sigma-Aldrich, Deisenhofen (GER)
Tris	Roth, Karlsruhe (GER)
Tween20	Roth, Karlsruhe (GER)
XL-1 Blue stock solution	New England Biolabs, Frankfurt a.M. (GER)
Yeast extract	Sigma-Aldrich, Deisenhofen (GER)

Table 7: Buffers used in molecular biology applications

Buffer	Reagent	Recipe
Cell lysis buffer	Leupeptin	2.34 µM
	NaF	10 mM
	Natriumorthovanadat	1 mM
	Pepstatin	2.19 µM
	PMSF	1 mM
	Brij in Tris/HCl (50 mM)	5 ml
Blotting buffer	Tris	2.43 g
	Glycine	11.25 g
	Methanol	200 ml
	H_2O	adjust to 1 l
LB agar	Agar	15 g
	LB medium	1 l
LB medium	LB	20 g
	ampicillin (for selection)	100 µg/ml
	H_2O	1 l
SDS-Running buffer (10x)	Tris	30.3 g
	Glycine	144 g
	SDS	10 g
	H_2O	1 l
Separating gel (12 %)	H_2O	3.5 ml
	Acrylamide/ Bisacrylamide solution (30 %)	4 ml
	Tris buffer (lower)	2.5 ml
	APS (10 %)	100 µl
	TEMED	7 µl

SOB medium	NaCl Bactotryptone Yeast extract KCl (250 mM) $MgCl_2$ (2 M) H_2O	0.5 g 20 g 5 g 10 ml 5 ml adjust to 1 l pH=7.0
Stacking gel	H_2O Acrylamide/ Bisacrylamide solution (30 %) Tris buffer (upper) APS (10 %) TEMED	3.05 ml 650 µl 1.25 ml 25 µl 5 µl
TAE buffer (50x)	Tris Na_2EDTA solution (0.5 M, pH=8) Acetic acid H_2O	242 g 100 ml 57.1 ml adjust to 1 l
TBST buffer	Tris NaCl Tween20 H_2O	1.2 g 8.765 g 0.1 % 1 l
TfB I	Cobalt acetate $MnCl_2$ $CaCl_2$ Glycerin	30 mM 50 mM 100 mM 15 % pH=5.8
TfB II	Mops-Na (pH=7.0) $CaCl_2$ KCl Glycerin	10 mM 75 mM 10 mM 15 %
Tris buffer (lower)	Tris 10 % SDS-solution H_2O	91 g 20 ml adjust to 500 ml pH=8.8
Tris buffer (upper)	Tris 10 % SDS-solution H_2O	6.05 g 4 ml adjust to 100 ml pH=6.8

All buffers were prepared with Millipore bi-distilled water and if necessary sterile filtered with Steritop™ Filter Units (Merck Millipore, Darmstadt, Germany).

3.2. Methods

3.2.1. Animals

All animal experiments were approved by local authorities (state investigation office Rhineland-Palatinate, approval ID: 23 177-07/G16-1-016) and conducted according to the German Animals Protection Law for care and use of experimental animals. All animals were raised and kept in individually ventilated cages under specifically pathogen-free conditions in the Translational Animal Research Centre (TARC) at the University Medical Centre (UMC) of the Johannes Gutenberg University Mainz.

For experiments the following mouse strains were used:

Table 8: Mouse strains

Strain	Description	Origin
C57BL/6J (BL6)	wild-type	Janvier Labs, Laval (France)
CyA2K^b	HLA-A2/K^b transgenic (BL6 genetic background)	TARC, UMC, Mainz (Germany)
OT-1	Transgenic for TCR-Vα2Vβ5 specific for SIINFEKL peptide	TARC, UMC, Mainz (Germany)

Additionally, rats (female, 8-10 weeks old) [Janvier Labs, Laval, France] were used to produce T cell growth factor (TCGF) medium (see chapter 3.2.2.2).

Mice were sacrificed by cervical dislocation, while rats were sacrificed by CO_2 inhalation.

3.2.2. Cell culture

All cells were cultured in an incubator with humidified atmosphere with 5 % CO_2 at 37 °C. Unless otherwise noted, all standard centrifuge steps were performed at 550 x g for 5 min. For freezing of cell backups, cells were centrifuged and taken up in 1 ml freezing media (FCS + 10 % DMSO) per Cryovial. Cell concentrations varied between 2 and 10 mio cells per vial dependent on cell type.

3.2.2.1. Cell lines

Cells were maintained in RPMI 1640 or DMEM with cell line specific supplements.

Hep-55.1c	Murine hepatocellular carcinoma cell line provided by Strand laboratory, UMC Mainz [DMEM/F12]
Jurkat_A2 (JA2)	Human acute T cell leukaemia cell line (originally obtained from Sherman laboratory) transduced with HLA-A2.1 [RPMI compl. + 280 µg/ml G418]
MC38	Murine colon adenocarcinoma cell line provided by Schild laboratory, UMC Mainz [DMEM compl.]
MC38_OVA_mb_EGFP	MC38 transduced with membrane bound Ovalbumin (OVA) peptide (SIINFEKL$_{257-264}$) and EGFP. Provided by Schild laboratory, UMC Mainz [DMEM compl.]
MC38_scA2K^b_β_2M _p53_Luc/GFP_Cl.2	MC38 transduced with a retroviral vector encoding for a chimeric single chain MHC I / p53$_{264-272}$ peptide [see Figure 47] and a vector encoding for Luciferase_GFP [see 7.1]. [DMEM compl.]
MEF_p53$^{-/-}$_A2K^b _Mut.4_Cl.3_GFP	This mouse embryonic fibroblast cell line has been described previously [55]. [MEF medium]
Phoenix-Ampho	Packing cell line purchased from Nolan Laboratory, Stanford University (USA). [Φ. A. medium]
RMAS	Murine leukaemia cell line, deficient in antigen processing. Obtained from Sherman laboratory, Scripps Research San Diego (USA). [RPMI compl.]

3.2.2.2. Production of TCGF medium

TCGF medium, composed of cytokines and growth factors is used as a supplement for long term *in vitro* culture of murine T cells. It was produced by culturing rat splenocytes of female Lewis-Rats (8-10 months) under specific condition. First, rats were euthanized by CO_2 inhalation. Afterwards splenocytes (average 250 mio per spleen) were collected as described below (see 3.2.2.3), counted and cultured at 7 mio cells/ml in a T75 flask with a total of 50 ml rat medium. Cells were incubated at 37 °C and 5 % CO_2 for 24 hrs, harvested, centrifuged (10 min, 320 x g, RT) and cell-free supernatant was collected and stored at 4 °C. Splenocytes were resuspended in 50 ml rat medium and again cultured for another 24 hrs.

Supernatant was collected as the day before and both supernatants were pooled. 1g Methyl-α-D-mannopyranoside per 100 ml supernatant was added. After dissolving, supernatant was sterile filtered and stored as aliquots at -20 °C.

3.2.2.3. Isolation of murine splenocytes

This protocol is used to isolate splenocytes of 4–6-month-old mice, for either T cell transduction or T cell culture purposes.

Mice (CyA2K^b, C57BL/6J or OT-I) were sacrificed by cervical dislocation. Coat was disinfected and a small cut next to the spleen was applied. Afterwards spleen was removed using forceps, freed from fat and transferred into 5 ml T cell culture Medium or RPMI only. Spleen was meshed through a 100 µm cell strainer into a 50 ml falcon and cell strainer was washed twice with 10 ml T cell culture medium. After centrifugation and discarding the supernatant, the cell pellet was resuspended in 3 ml erythrocyte lysis buffer, incubated for 3 min at RT and topped up by 8 ml T cell culture medium. Following a centrifuge step, pellet was diluted with 20 ml T cell culture medium, fat clumps were removed with a pipet tip and cells were counted (approx. 80 mio cells per spleen). Afterwards cells were ready to use for restimulation of cultured murine T cells or for transduction purposes.

3.2.2.4. Stimulation and culture of murine T cells

Murine T cells were weekly restimulated (after transduction with the p53-scTCR) with peptide-pulsed APCs and feeder cells. JA2 cells were used as APCs. Cells were counted and adjusted to the number of cells needed for restimulation (0.5 mio / 24-well). Afterwards, cells were centrifuged, supernatant was decanted and 10 µg peptide ($p53_{264-272}$), was added to the dead volume. Cells were vortexed and incubated in the incubator for 1 hour. In the meantime, feeder cells were prepared using BL/6 splenocytes (see 3.2.2.3), taken up in 20 ml T cell medium and counted. After incubation, JA2 cells were resuspended in 10 ml T cell medium and irradiated with 200 Gy and BL/6 splenocytes with 30 Gy. Finally, peptide-pulsed APCs were used at 0.5 mio cells/well, together with feeder cells (6 mio cells/well) and TCR-specific T cells (0.3-0.5 mio cells/well) in a total volume of 2 ml T cell medium containing 10 % TCGF per 24-well plate.

3.2.2.5. Isolation of human PMNs

Human peripheral whole blood was provided by the Transfusion Center of the UMC Mainz. First, blood was mixed with PBS/EDTA (1 mM) 2:1. Afterwards, 15 ml Histopaque (RT) was provided in a 50 ml tube and 35 ml blood were slowly added on top without interrupting the Histopaque layer. Tubes were centrifuged at 1200 x g for 15 min at RT and without break. The lowermost layer after centrifugation contains the erythrocyte and PMN cell fraction [see Figure 9]. The other layers were discarded by aspiration and the erythrocyte/PMN layer was transferred into a new 50 ml tube and mixed 1:1 with PBS/EDTA. A 3 % dextran solution (in PBS, 4 °C) was added in a 1:1 ratio, inverted several times and incubated for 30 min at RT. The upper PMNs enriched phase was collected and centrifuged at 550 x g for 5 min at 4 °C. The supernatant was aspirated, the pellet was resuspended in 20 ml erythrocyte lysis buffer (4 °C) and incubated for 5 min at RT. Tubes were filled up with 30 ml PBS/EDTA and centrifuged at 550 x g for 5 min at 4 °C. Pellet was washed twice with PBS/EDTA and cells were counted. To check the purity of isolation, cells were stained (see 3.2.5.1) with α-human CD66b antibody and measured by flow cytometry. PMNs were either used for direct co-culture experiments with T cells or cultured for 3 days (under specific conditions) and supernatant was used for further experiments.

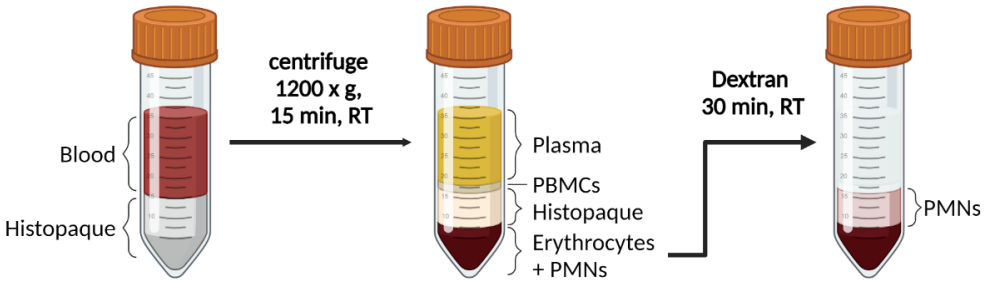

Figure 9: PMN isolation with density gradient. [created with BioRender]

3.2.3. DNA construct and cloning

This protocol was used to clone our designed DNA fragment (scA2K^b_β_2M_p53) into the pMx_puro vector. The construct is flanked by a 5′ BamHI and a 3′ NotI restriction side. We furthermore included a Kozak sequence followed by a signal peptide to shuttle the construct to the cell membrane. The main construct starts with the p53 peptide sequence followed by a 3x G4S linker sequence, the β2m sequence, another 3x G4S linker sequence, the α1-α2-α3 sequence and terminated with the transmembrane and cytoplasmic sequence.

The construct was codon optimized and synthesized by GeneArt (Thermo Fisher Scientific). Further details of the vector maps and the DNA constructs are shown in the appendix.

Table 9: Enzymes used in cloning applications

Enzyme	Manufacturer
BamHI-HF	New England Biolabs, Frankfurt a.M. (GER)
NotI-HF	New England Biolabs, Frankfurt a.M. (GER)
T4 ligase	New England Biolabs, Frankfurt a.M. (GER)

3.2.3.1. DNA restriction digest

DNA fragment was resolved in nuclease free H_2O (20 ng/µl) and incubated for 1 hour at RT. The DNA construct and the pMx_puro plasmid were digested separately with BamHI-HF and NotI-HF at 37 °C ON.

Table 10: Restriction mix

Component	Amount
pMx_Puro or scA2K^b_β_2M_p53	1 µg
BamHI-HF (20 U/ml)	1 µl
NotI-HF (20 U/ml)	1 µl
Cut-Smart Buffer (10x)	5 µl
H_2O	up to 50 µl

3.2.3.2. Agarose gel electrophoresis and DNA extraction

DNA samples (digested insert and vector) were mixed 6:1 with loading dye (6x) and loaded on a 1 % (w/v) agarose gel in TAE buffer (30 ml + 6 µl Peg green). DNA bands were separated by gel electrophoresis at 100 V for 40 min. After a clear separation was visible by UV light exposure, insert and vector bands were cut out and purified using the QIAquick Spin kit (QIAGEN, Venlo, NL). DNA concentrations were measured via Nanodrop (Thermo Fisher, Dreieich, GER) at 230 nm.

3.2.3.3. Ligation

A molar insert to vector ratio of 5:1 was used for the ligation reaction and the ligation mix was prepared as listed in Table 11 and incubated ON at 16 °C. The online NEBioCalculator tool was used to determine the amount of insert DNA.

Table 11: Ligation mix

Component	Amount
Vector DNA (pMx_puro)	100 ng
Insert DNA (scA2K^b_β_2M_p53)	X ng
T4 ligase buffer (10x)	2.5 µl
T4 ligase	1 µl
H_2O	up to 25 µl

3.2.3.4. Transformation of chemocompetent bacteria

For transformation 10 cm petri dishes with 20 ml LB agar containing 100 µg/ml Ampicillin were prepared. One aliquot (100 µl) of chemocompetent cells (XL1-Blue) was thawed on ice. Afterwards, 10 µl of ligation mix (Table 11) was added and incubated on ice for 30 min. Cells were heat shocked at 42 °C for 90 sec and subsequently incubated on ice for another 3 min. After adding 1 ml of LB medium, cells were incubated for 1 h at 37 °C in a shaker. Finally, 800 µl were plated on LB agar and petri dishes were sealed with parafilm and incubated ON upside down at 37 °C.

3.2.3.5. Bacterial ON culture and DNA preparation

The next day, bacterial colonies (single clones) were picked from the plates using a 10 µl tip and transferred each in a 15 ml Falcon tube containing 3 ml LB medium with 100 µg/ml Ampicillin. Cultures were incubated at 37 °C in a shaker (240 rpm) ON. From each ON culture, 100 µl were taken and stored at 4 °C. The plasmid DNA isolation and purification from the 2 ml ON cultures was performed according to the manufacturer´s protocol of the QIAprep Spin Miniprep kit (QIAGEN, Venlo, NL). A test restriction digest using 5 µl purified DNA in a total volume of 25 µl (see Table 10) was conducted for 1 hr. To verify the correct ligation of the insert into the vector sample size was analysed on an agarose gel. Positive clones were further processed to obtain large-scale DNA preparation. Few µl from the bacterial ON (mini)culture (positive for correct ligation) were further incubated in 100 ml LB medium at 37 °C in a shaker (240 rpm) ON.

Subsequent DNA isolation and purification were performed using EndoFree Plasmid Maxi Prep kit (QIAGEN, Venlo, NL) and DNA concentration was measured by nanodrop.
To prepare a bacterial glycerol stock, 3 ml of ON culture were centrifuged at 2000 x g for 15 min at 4 °C and pellet was resuspended in 1 ml LB medium containing 10 % glycerol. Stock can be stored at -80 °C.

3.2.3.6. Sequencing

DNA sequencing was carried out by StarSEQ GmbH (Mainz, GER). For that, a mix of 1 µl sequencing primer (see 7.2) and 0.6 µg of Maxi Prep plasmid DNA filled up to 7 µl with nuclease free water was prepared.

3.2.4. Retroviral transduction

3.2.4.1. Murine T cells

To equip murine T cells with an antigen specific TCR and therefore produce specific effector cells against our tumour cell lines, retroviral transduction was used.
The packaging cell line Φ. A. was thawed (day 0) and cells were cultured with 1.25 mio per T75 flask in 15 ml Φ. A. medium. Three days later (day 3) Φ. A. cells were trypsinized, counted and plated with a density of 1.2 mio cells per 10 cm petri dish containing 8 ml Φ. A. medium. The next day (day 4), medium of Φ. A. cells was replaced with 6 ml per dish, 4 hrs prior to transfection. For transfection of one petri dish, 800 µl DMEM only was prepared in a 1.5 ml Eppendorf tube. 35 µl FuGENE 6 were added and mixture was incubated for 5 min at RT. Afterwards, 10 µg p53-TCR-DNA (pGMP93) [Figure 46] and 7 µg helper plasmid (pCL_Eco) was added, tube was slowly rotated and mixture was incubated for 15 min at RT. DNA mix solution was slowly dropped on Φ. A. cells in the petri dish and incubated ON. The following day (day 5), medium of Φ. A. cells was refreshed with 8 ml T cell medium in the late afternoon. Additionally (day 5), 6-well plates were coated with 2 ml/well RetroNectin (25 µg/ml) and stored at 4 °C ON. Isolated primary splenocytes (see 3.2.2.3) from CyA2K^b mice were cultured with 12 mio cells in 4 ml T cell medium per 6-well plate with 10 % TCGF and 2 µg/ml Concanavalin A to pre-activate cells for 24 hrs (day 5). One day later (day 6), RetroNectin was removed (can be used again up to 4 times, store at -20 °C) and 2 ml/well of 2 % BSA in PBS was added and incubated for 30 min at RT. BSA was removed, wells were washed once with PBS and kept moist.

Splenocytes were collected (from ON culture), counted and seeded with 3 mio cells/ml pre-conditioned T cell medium with 1 ml per RetroNectin coated 6-well. Furthermore, retroviral supernatant of Φ. A. culture was collected and centrifuged at 890 x g, for 10 min at 32 °C. Last, 1 ml retroviral supernatant per 6-well was added and plate was centrifuged at 890 x g for 60 min at 32 °C without break. The next day (day 7), T cells were either directly used for in vivo ACT experiments or expanded in vitro using 5 µl murine anti-CD3 / CD28 beads per 1 mio cells and 20 % TCGF in T cell medium with 2 ml per 24-well. For further weekly expansion and culture the protocol explained in 3.2.2.4 was used.

3.2.4.2. Tumour cells

The packaging cell line Φ. A. was used as described in 3.2.4.1 to produce retroviral supernatant. Tumour cells were seeded with 0.2 mio per 6-well one day prior transduction. On the day of transduction, 2 ml virus supernatant per 6-well, containing 5 µg/ml polybrene, was used. Plate was centrifuged at 890 x g for 60 min at 32 °C with no break. Cells were cultured ON and subsequently transferred into a T75 flask. Transduced cells with a plasmid containing a puromycin resistance cassette were selected with 5 µg/ml puromycin.

Table 12: Plasmids

Plasmid	Function
pColt-Galv	Retroviral helper plasmid (human cells)
pHit60	Retroviral helper plasmid (human cells)
pCL-ECO	Retroviral helper plasmid (murine cells)
pGMP93	Retroviral expression vector
pMx_puro	Retroviral expression vector
pMx_Katushka	Retroviral expression vector
pMx_Luciferase_GFP	Retroviral expression vector
pMx_scA2Kb_β2M_p53_puro	Retroviral expression vector

Vector maps of all plasmids are enclosed in the appendix (Chapter 7).

3.2.5. Flow cytometry

Flow cytometry (Fluorescence activated cell sorting, FACS) is a technique for characterizing and examining individual cell populations based upon the specific light scattering of each cell and the fluorescence signal of specific antibodies that are used to stain diverse markers in the cells. Therefore, it is possible to analyse morphological characteristics, such as cell size (FSC-A) and granularity (SSC-A), but also the expression of specific molecules on the cell surface or within the cells.

Table 13: Antibodies and dyes used for FACS staining

Antibody / Dye	Fluorochrome	Clone	Manufacturer
hu CD66b	FITC	G10F5	Becton Dickinson, Heidelberg (GER)
hu HLA-A2	APC	BB7.2	Becton Dickinson, Heidelberg (GER)
hu TCRVβ3	PE	REA646	Miltenyi, Bergisch Gladbach (GER)
Live / Dead	FITC	/	Thermo Fisher, Dreieich (GER)
Live / Dead	Pacific Blue	/	Thermo Fisher, Dreieich (GER)
mu arginase I	APC	A1exF5	Thermo Fisher, Dreieich (GER)
mu CD3	APC	17A2	Thermo Fisher, Dreieich (GER)
mu CD3	PE	145-2C11	Thermo Fisher, Dreieich (GER)
mu CD4	APC	RM4.5	Becton Dickinson, Heidelberg (GER)
mu CD8	APC-Cy7	53-6.7	Becton Dickinson, Heidelberg (GER)
mu CD8	FITC	53-6.7	Becton Dickinson, Heidelberg (GER)
mu CD8	Per-CP	53-6.7	Becton Dickinson, Heidelberg (GER)
mu CD11b	Pacific Blue	M1/70	Biolegend, San Diego (USA)
mu CD155	PE	3F1	Becton Dickinson, Heidelberg (GER)
mu CD223 / LAG-3	PE	C9B7W	Becton Dickinson, Heidelberg (GER)
mu CD226 / DNAM-1	AF647	10E5	Becton Dickinson, Heidelberg (GER)
mu CD274 / PD-L1	Pe-Cy7	10F.9G2	Biolegend, San Diego (USA)
mu CD279 / PD-1	APC	HA2-7B1	Miltenyi, Bergisch Gladbach (GER)
mu CD366 / TIM-3	BV421	5D12	Becton Dickinson, Heidelberg (GER)
mu F4/80	Pe-Cy7	BM8	Biolegend, San Diego (USA)
mu Ly-6C	PE	HK1.4	Biolegend, San Diego (USA)
mu Ly-6G	APC-Cy7	1A8	Becton Dickinson, Heidelberg (GER)

mu TIGIT	BV421	1G9	Becton Dickinson, Heidelberg (GER)
mu TCRVα2	BV421	B20.1	Biolegend, San Diego (USA)
mu TCRVα2	FITC	B20.1	Thermo Fisher, Dreieich (GER)
mu TCRVβ5	PE	MR9-4	Becton Dickinson, Heidelberg (GER)

3.2.5.1. Staining procedure

For FACS staining 0.2-0.5 mio single cells were transferred in FACS tubes and washed once with PBS (550 x g, 2 min, RT). Tumour samples from mouse studies were first cut in small pieces and mouse tumour dissociation kit (Miltenyi, Bergisch Gladbach, GER) was used according to manufacturer's instructions, to generate a single-cell suspension. Suspension was distributed in FACS tubes and washed once with PBS. Cells were resuspended in 100 µl PBS containing the fluorochrome-coupled antibodies or dyes (Table 13) and incubated at RT for 15 min in the dark. Afterwards, cells were washed once again and taken up in 200 µl PFA (1 %). For intracellular staining procedure, the IntraPrep kit (Beckman Coulter, Brea, USA) was used as described in the protocol. Until measurement, samples were stored at 4 °C for maximum 3 days.

3.2.5.2. Cell sorting

A common variation of flow cytometry involves linking the analytical capability to a sorting device, to physically separate and thereby purify cells of interest based on their optical properties. Such a process is called cell sorting and it is able to sort one cell at a time. We used in our case different antibodies to specific molecules on the cell surface to separate target cells from other cells or even isolate cells with higher or lower expression of a surface molecule of interest. Cells were sorted at the FACS Core Facility of the UMC with an Aria device (Becton Dickinson, Heidelberg, GER).

3.2.6. Liquid chromatography–mass spectrometry

In LC-MS, the physical separation of multiple components (liquid chromatography) is combined with the mass analysis (mass spectrometry) which provides spectral information to identify those separated components. HILIC-LC/MS (Agilent Technologies, Santa Clara, USA) was used for metabolomics, to identify and quantify molecules like arginine in samples from *in vitro* and *in vivo* experiments. All samples were sent to the Helmholtz Centre in Munich and processed by the team of Dr. Michael Witting (Deputy Head of Metabolomics and Proteomics Core).

3.2.7. Functional *in vitro* assays

3.2.7.1. Cell layer cytotoxicity assay

To measure the cytolytic activity of T cells, 0.1 mio adherent target tumour cells were seeded in a 24-well plate and cultured ON. The cell-free media was removed, and effector cells (T cells) were added in their usual culture medium in different E:T ratios. The plate was incubated at 37 °C until experiment was terminated (usually between 4-8 hrs). The supernatant containing T cells and lysed/dead tumour cells was aspirated, wells were washed once with PBS and remaining viable tumour cells were fixed with 4 % PFA for 10 min at RT. PFA was discarded, cells were washed again with PBS, crystal violet solution (0.5 %, 400 µl/well) was added to stain the cells and plate was incubated for 10-15 min at RT. Afterwards, crystal violet solution was removed, cells were washed once with PBS and a 5 % SDS/PBS solution was added (500 µl/well) to solubilise the violet dye. Lastly, 2 x 200 µl per well were transferred in a 96-well (flat bottom) as duplicates and absorbance was measured using a plate reader with endpoint detection at 570 nm. Wells with tumour cells only were used as controls (maximal dye intensity) and defined as 100 % viable cells. Viability of tumour cells (in %) was calculated as the following: $\frac{\text{absorbance of well with T cells}}{\text{absorbance of control well}} \times 100$

3.2.7.2. Luminescence based killing assay

This assay was used to determine the killing capacity of T cells against different target tumour cells (adherent or suspension) under specific conditions. For this assay, a luciferase expressing target cell line is required.

Prior to the assay, D-Luciferin (0.3 mg/ml) was added to Luciferase positive target cells (100,000 cells/ml) and cells were seeded as triplicates per condition with 100 µl per 96 well (10,000 cells per well). Therefore, black, 96-well, flat-bottom plates were used. Effector cells (T cells) were added at different E:T ratios in 100 µl per well. The 96-well plate was centrifuged at 140 x g for 2 min and incubated for the indicated time. Plate was measured at individual time points with a plate reader (heated to 37 °C) detecting Luminescence. Tumour cells only were used as control to detect the maximal luminescence signal and tumour cell viability (in %) was calculated as the following: $\frac{\text{luminescence of well with T cells}}{\text{luminescence of control well}} \times 100$

3.2.7.3. MTS Assay

The MTS assay is a colorimetric assay for assessing cell metabolic activity and thereby an indirect measure of proliferation. Cells were seeded as triplicates with 25,000 tumour cells per well or 250,000 T cells per well in a 96-well plate (100 µl/well) under different stimulation conditions and incubated ON. Wells with medium only were used as blank for the measurement the next day. To each well, 20 µl MTS solution (Promega, Madison, USA) was added and reaction was incubated at 37 °C until colour change (from yellow to brownish) was visible. The incubation time varies according to the intrinsic metabolic activity of the cells. Colour intensity was measured by a plate reader with endpoint detection at 490 nm.

3.2.7.4. Thymidine incorporation assay

This assay is used for a direct measure of proliferation. The assay utilizes a strategy wherein a radioactive nucleoside, ^{3}H-thymidine, is incorporated into new strands of chromosomal DNA during mitotic cell division.

Cells were transferred or directly seeded with 200 µl medium in a 96-well plate as triplets. Following the addition of 20 µl thymidine (4.5 µCi/ml) cells were incubated for 16 hrs. Afterwards, plate was frozen at -20 °C to lyse the cells and to release radioactive labelled DNA into the supernatant.

For measurement, plate was thawed again, and samples were transferred by a specific harvester to a membrane. This membrane was loaded into a scintillation beta-counter and radioactivity in DNA recovered from the cells was detected and expressed as counts per minute (cpm).

3.2.8. Western Blot

Western blot is an analytical technique to detect specific cellular proteins. After a gel electrophoresis step and the transfer of the proteins to a membrane, the membrane is incubated with antibodies specific for the target proteins. If the specific protein is present, it can be visualized by a stained band on the western blot.

3.2.8.1. Cell lysis and determination of protein concentration

All steps were performed on ice. Cell pellets (5 mio T cells / 2-3 mio tumour cells) were washed once with PBS and resuspended in 100 µl cell lysis buffer (see all buffers in Table 7). Lysate was incubated for 30 min and in between vortexed. Tumour samples (50 mg) were transferred in 500 µl cell lysis buffer, mixed 3x with homogenizer (1 min and 50 Hz) with 10 min break on ice in between. Afterwards, samples were centrifuged at 13900 x g at 4 °C for 10 min and supernatant was transferred into a new 1.5 ml tube. Lysate can be stored at -20 °C. For the determination of the protein concentration (Bradford assay) a BSA standard curve titrated from 0 µg/ml (blank) to 20 µg/ml was used.

For each concentration, a master mix (1 ml) consisting of H_2O, lysis buffer and BSA solution was prepared and 100 µl of each BSA solution were pipetted as triplicates into a 96-well plate. For the samples, 98 µl H_2O were provided for a duplicate measurement and 2 µl protein lysate were added. Afterwards, 100 µl Bradford solution (BioRad, Hercules, USA) were added to each well, air bubbles were removed and reaction mixtures were incubated for 5 min at RT. The absorption was measured at 595 nm in a spectrophotometer. The standard curve was used to determine the protein concentration of each sample.

3.2.8.2. SDS-PAGE

Protein fractions were separated on a 12 % polyacrylamide separation gel. Therefore, the gel chamber was filled first to ¾ with the separation gel and covered with Isopropanol. After polymerisation (15-20 min), Isopropanol was decanted and chamber was washed with bi-distilled H_2O. The chamber was filled up with the stacking gel, a 1.5 mm comb was inserted, and after the polymerisation process, gel was either used directly or stored moist at 4 °C.

Sample mixes were calculated to a volume of 30 µl using 20 µg protein, 1x Laemmli buffer and H_2O. The samples were boiled at 95 °C for 5 min, shortly centrifuged and loaded onto the gel. Additionally, 5 µl protein marker were added to an empty slot, to determine the protein sizes at the different positions on the gel. Prior to loading, the gel was transferred into the running tank and the tank was filled up with SDS-running buffer (1x). The conditions for the SDS-PAGE were set as followed:

~15 min at 85 V (at separation gel)

~1.5-2 h at 130 V (at running gel)

3.2.8.3. Blotting

Two pieces of Whatman filter paper and 1 piece of a nitrocellulose membrane (GE Healthcare, Buckinghamshire, GB) were cut to the size of the gel. Both, the membrane and the Whatman papers were saturated with blotting buffer. Beginning from the negative pole, one Whatman paper was placed to the blotting chamber followed by the gel, the nitrocellulose membrane and the second Whatman paper. The blotting chamber was closed and transferred into the blotting tank which was filled up with blotting buffer (wet blotting). The blot was running at 100 V and 4 °C for 1.5 hrs.

3.2.8.4. Protein detection

The membrane was shortly washed with TBST and blocked with 5 % milk in TBST for 30 min – 1 h on a shaker at RT. Afterwards, membrane was washed 3 x 5 min with TBST and incubated with the primary antibody (diluted in 5 % milk in TBST) at 4 °C ON. The next day, membrane was washed 3 x 10 min with TBST at RT and incubated with the secondary antibody and Strep-Tactin-HRP conjugate (diluted in 5 % milk in TBST) for 1 h at RT. The membrane was again washed 3 x 10 min with TBST and ECL solution was used to detect protein bands by chemiluminescence. The results were analysed and quantified with the iBright analysis software (Thermo Fisher, Dreieich, GER).

Table 14: List of WB antibodies

Antibody	Host	Concentration	Manufacturer
GAPDH	rabbit	1:5,000	Cell Signaling Technology, Cambridge (UK)
pan-Akt	rabbit	1:5,000	Cell Signaling Technology, Cambridge (UK)
arginase I	goat	1:5,000	Abcam, Cambridge (GB)
ASS I	rabbit	1:2,000	Sigma-Aldrich, Deisenhofen (GER)
Precision Protein StrepTactin-HRP Conjugate	/	1:5,000	BioRad, Hercules (USA)
α-goat	donkey	1:5,000	Santa Cruz
α-rabbit	goat	1:5,000	Cell Signaling Technology, Cambridge (UK)

3.2.9. *In vivo* experiments

For *in vivo* experiments, tumour cells (in 100 µl PBS) were injected s.c. into the right flank of the mice. T cells (in 100µl PBS) were injected i.v. while the arginase I inhibitor nor-NOHA (in 100 µl 0.9 % NaCl) was s.c. administered in the vicinity of TME. The tail i.v. injection was supported by warming up the vein with an infrared lamp. Tumour volume was either measured by a digital calliper (length x width^2) and/or by detection of luminescence derived from luciferase positive tumour cells. Therefore, 150 µl D-Luciferin (16.6 mg/ml) was applied i.p., mice were anesthetized with Isoflurane and luminescence signal was detected by an IVIS SpectrumCT In Vivo Imaging System (Perkin Elmer, Boston, USA) after 5 min. Detailed experiment specific conditions are explained in the result section.

3.2.10. Software and Statistical Analysis

The analysis of flow cytometric data was performed using the FlowJo analysis software (version V10) (Becton Dickinson, USA). Clone Manager 5 was used to visualize cloning strategies and create vector maps. For the evaluation of western blot data, iBright analysis software (Thermo Fisher Scientific, Langenselbold, GER) was used.

Statistical analysis was carried out with GraphPad Prism 6 using the unpaired two tailed t-test to compare differences between two groups. Probability-values (p) of ≤ 0.05 were considered significant and data are usually presented as mean ± Standard Deviation (SD).

4. Results

4.1. MEF cells as tumour target cell line

To investigate the interaction between tumour cells and T cells, immortalized mouse embryonic fibroblasts (MEF_p53$^{-/-}$_A2K^{b}_Mut.4_Cl.3_GFP; short: MEF_orig) [3.2.2.1] were used as tumour target cell line. This cell line presents the human p53$_{(264-272)}$ epitope via HLA-A2 (MHC class I) on the surface and was used by our group already in earlier studies [55]. For following experiments, if not stated otherwise, murine T cells were equipped with our optimized p53-scTCR [Figure 46] by retroviral transduction and used as effector cells.

4.1.1. Investigation of MHC I downregulation

During long-term culture, a downregulation of the MHC I complex was observed by regular analysis of HLA-A2 expression by FACS [Figure 10]. It's already well known and published [144], that MHC downregulation is a key tumour escape mechanism which was reported in many types of cancer.

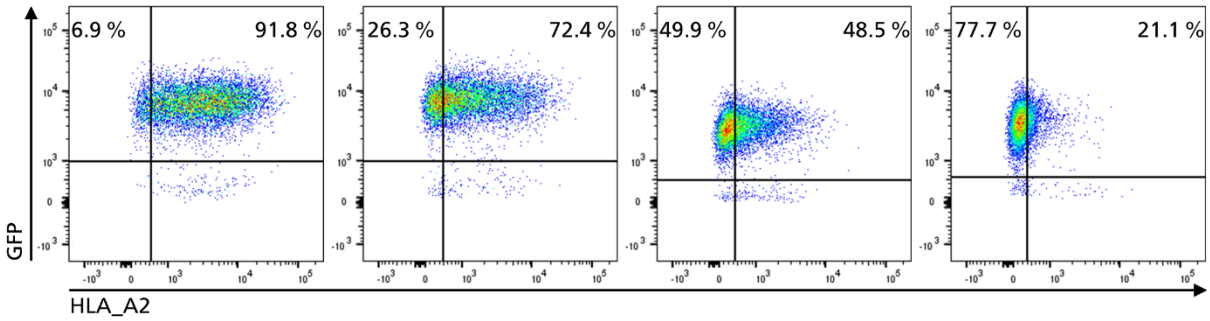

Figure 10: FACS analysis of HLA-A2 expression on MEF_p53$^{-/-}$_A2K^{b}_Mut.4_Cl.3_GFP
MEF cells were cultured for several weeks and FACS evaluation of HLA-A2 expression was performed. Blots are showing representative staining starting from freshly thawed cells (1. Plot) followed by snapshots during following weeks of culture (2.-3. Plot).

Therefore, the downregulation of HLA-A2 on MEF cells *in vitro* was further investigated and different potential mechanisms that may be involved in this downregulation were evaluated. Not only the addition of β2-microglobulin to stabilize the MHC complex, NAC and the impact of irradiation but also the inhibition of epigenetic factors by histone deacetylase inhibitors like Panobinostat, HNHA and 5-aza was analysed. None of these treatments showed a clear up-regulation of the MHC I complex *in vitro* (data not shown). Only IFNγ treatment was able to restore HLA-A2 expression. To overcome this problem, a chimeric single chain HLA-A2 molecule with directly linked $p53_{(264-272)}$ peptide [Figure 47 and Figure 48] was designed (thereafter named scA2K^b_β$_2$M_p53). Due to the single chain structure, it was secured that the linked β2-microglobulin as well as the linked antigen are in close contact to the main structure of the MHC I molecule. This arrangement resulted in MHC class I overexpression on the cell surface with ensured p53 peptide expression in the binding cleft. MEF_p53$^{-/-}$_A2Kb_Mut.4_Cl.3_GFP cells [3.2.2.1] were retroviral transduced with this construct and sorted for high HLA-A2 expression (MEF_scA2K^b_β$_2$M_p53_GFP; short: MEF_p53). Transduction resulted in 55.6 % HLA_A2 expression which was further increased after cell sorting to 88.4 % [Figure 11].

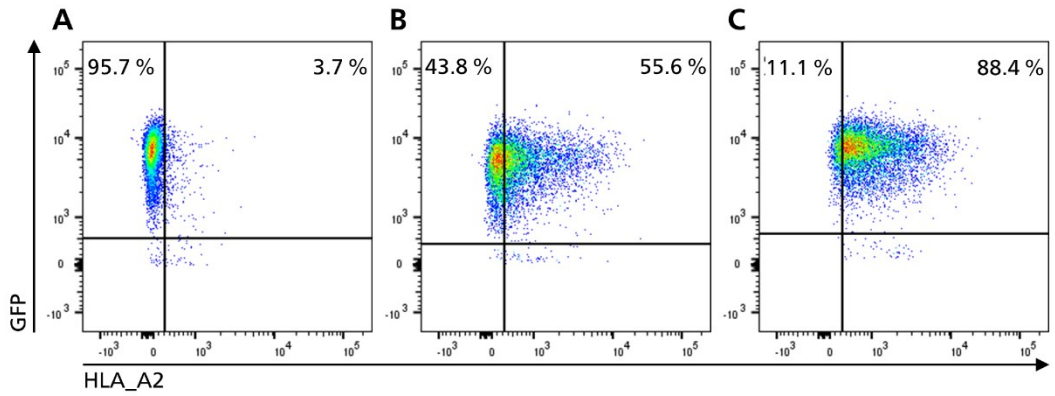

Figure 11: HLA-A2 expression on MEF cells
MEF cells were transduced with the scA2Kb_β2M_p53 construct and FACS sorted. FACS measurement of HLA-A2 expression (and GFP) is shown of MEF_p53-/-_A2Kb_Mut.4_Cl.3_GFP cells **(A)** prior transduction, **(B)** 3 days post transduction and **(C)** post sorting.

4.1.2. Genotypic and Phenotypic characterisation of MEF cells *in vitro*

For later experiments, a possible treatment strategy with administration of citrulline [as explained in 1.1.5] in the context of arginine auxotrophic tumours was planned. To determine the arginine auxotrophy of MEF tumour cells, ASS1 expression was investigated by performing an MTS assay. MEF cells were cultured ON in complete medium (+Arg), arginine deficient medium (-Arg) and arginine deficient medium supplemented with Citrulline (1 mM). As shown in Figure 12A, metabolic activity of cells was reduced in arginine deficient medium, as arginine is necessary for cell metabolism and proliferation [145]. The addition of Citrulline did not reconstitute the metabolic activity of the cells, indicating the lack of ASS1. This lack of ASS1 was additionally confirmed by western blot [Figure 12B].

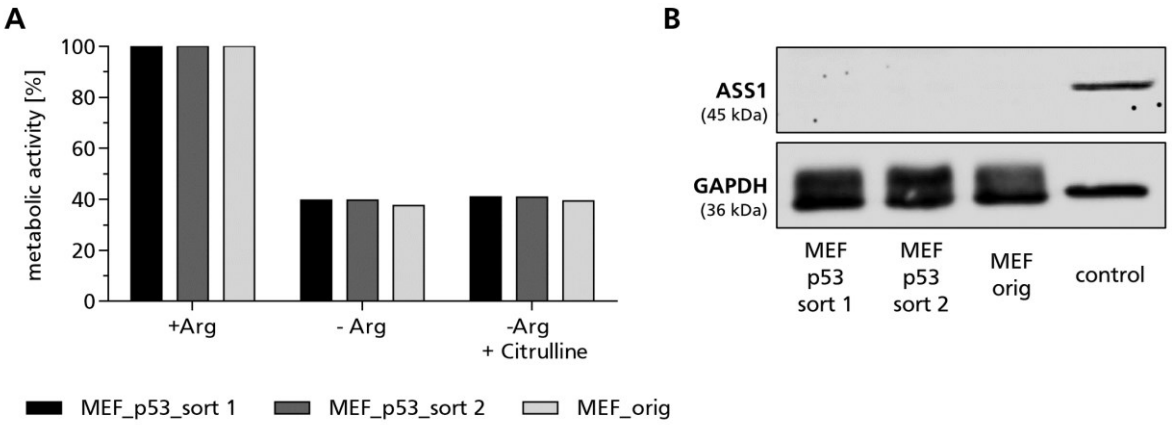

Figure 12: Metabolic activity of MEF cells and ASS1 expression
MEF cells transduced with the chimeric scA2K^b_β_2M_p53 construct and sorted for HLA-A2 expression (MEF_p53) and MEF_orig cells were used. **(A)** MTS assay of MEF cells cultured in standard medium (+Arg), arginine deficient medium (-Arg) and arginine deficient medium plus Citrulline (1 mM) ON. **(B)** Western blot against ASS1 of MEF cells. EA.hy cells (human vein endothelial cell line) were used as positive control and GAPDH as internal loading control.

Furthermore, MEF_p53 cells were phenotypically characterised by FACS analysis for their surface expression of ligands binding to immune inhibitory receptors on T cells. CD155/PVR the ligand to TIGIT and CD226/DNAM-1 as well as PD-L1 were always strongly expressed with 100 % CD155 expression and PD-L1 expression ranging between 70-90% [Figure 13].

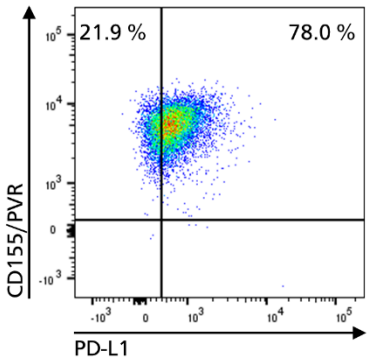

Figure 13: Representative expression of CD155/PVR and PD-L1 on MEF_p53 cells
Cells were analysed by FACS staining.

4.1.3. T cell transduction and restimulation

As explained in 3.2.4.1, T cells were transduced with the p53-scTCR. Those cells were weekly stimulated with peptide ($p53_{(264-272)}$) pulsed JA2 cells [see 3.2.2.4] and used for different assays as described in the following chapters. In Figure 14, representative FACS staining of T cells are shown. In general, always more CD8 positive cells than CD4 positive cells were obtained from murine spleens, with animal dependent variabilities. Transduction efficiency strongly relied on the potency of the produced viral supernatant. In the representative staining, TCR expression of 85 % in CD4 and 54 % in CD8 T cells was achieved 1 day after transduction. Transduction efficiency was on average 1.5-fold higher in CD4 compared to CD8 T cells as well as MFI values one day after transduction. However, already after the first peptide specific restimulation the CD8 population strongly increased whilst the CD4 population decreased even stronger. After the second restimulation, almost all CD4 positive T cells were gone and TCR expression in CD8 T cells increased to 80 %. With this procedure, usually a 100 % pure CD8 / TCR positive T cell population was obtained after 3-4 rounds of weekly restimulation.

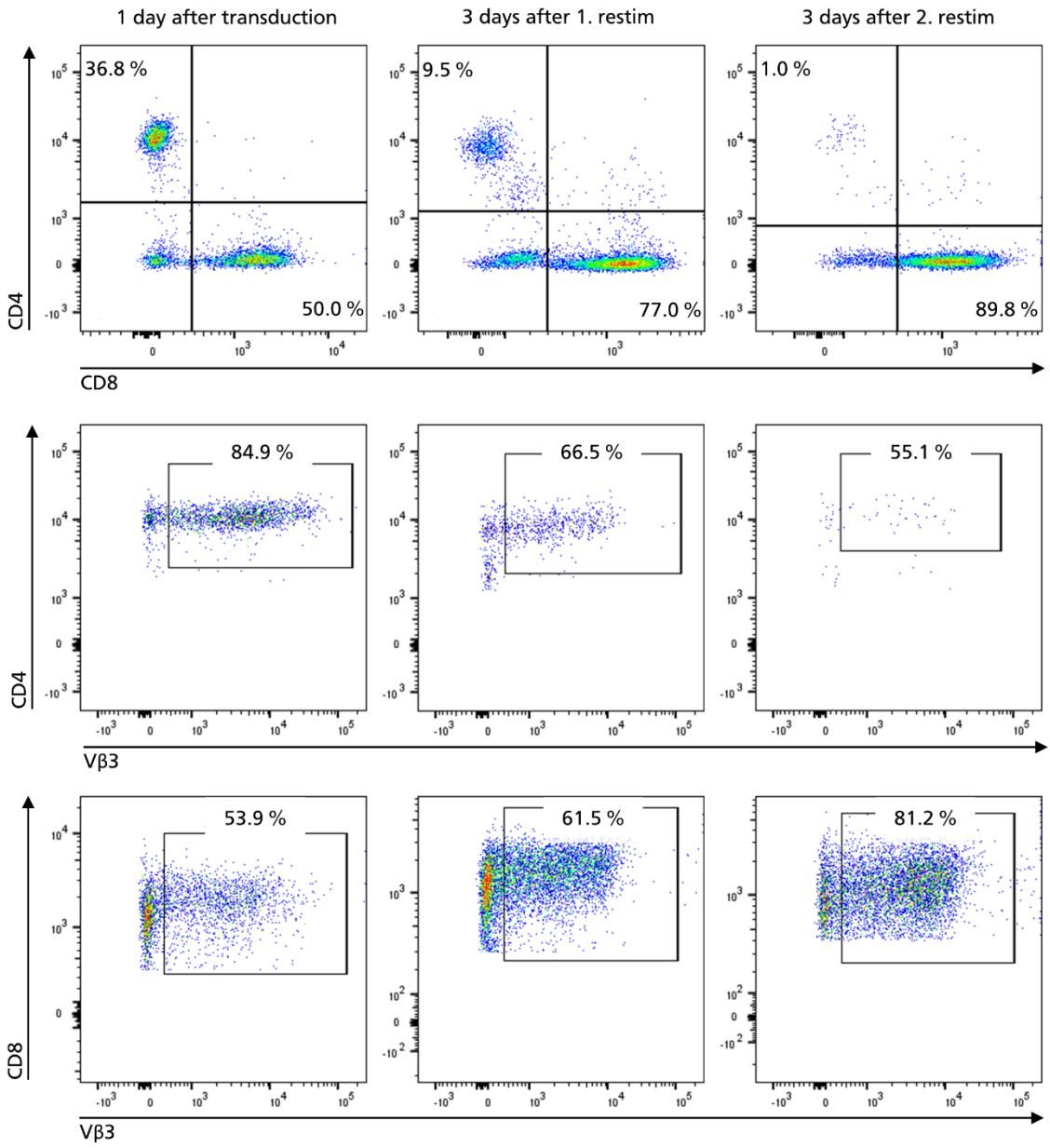

Figure 14: Representative FACS staining of T cells after transduction and peptide specific restimulation
T cells were transduced with the p53-scTCR. TCR expression on CD4 and CD8 T cells was analysed by Vβ3 staining. Analyses were performed 1 day after transduction and 3 days after peptide specific restimulation. Two rounds of restimulation are shown.

4.1.4. Chimeric MHC I construct increases HLA expression and recognition by antigen TCR-specific T cells

To test the killing capacity of T cells against MEF cells, a cell layer cytotoxicity assay was performed using both original and transduced MEF cells as target cells. A significant higher expression of the MHC I complex (HLA_A2 staining) was detected [Figure 15A] on the genetically modified MEFs (MEF_p53) resulting in increased p53 peptide expression on the cell surface.

Therefore, also a significant increased killing of MEF cells transduced with the chimeric MHC I construct was observed (MEF_p53) [Figure 15B]. Both ratios of T cells to tumour cells (1:1 and 2:1) showed 90 % of MEF_p53 cytolysis whereas only 3 % (1:1) and 7 % (2:1) of MEF_orig were lysed.

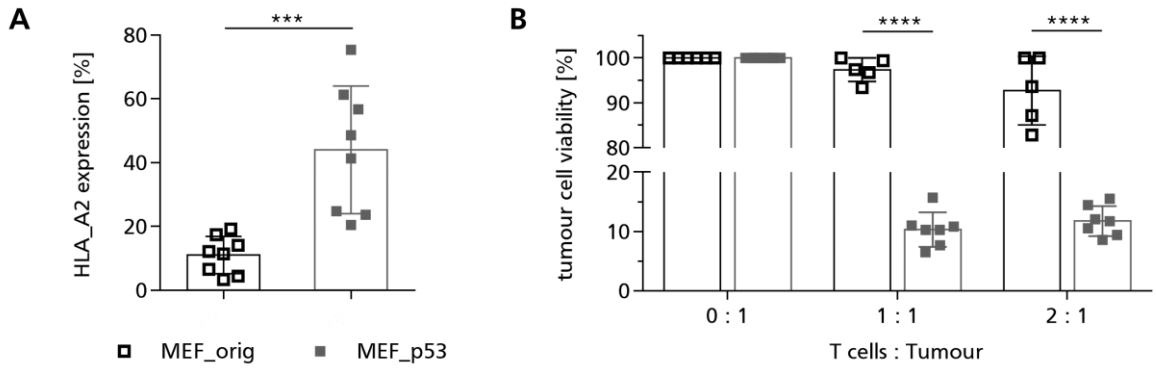

Figure 15: Surface HLA_A2 expression and cytotoxicity assay with MEF cells
(A) FACS measurement of HLA_A2 expression in MEF_orig and MEF_p53 cell lines over time in culture (n=8). **(B)** Cytolysis assay ON using MEF_orig and MEF_p53 cells as target cells and p53-scTCR transduced murine T cells as effector cells with E:T ratios of 0:1, 1:1 and 2:1 (n=5-8); Data are presented as mean ± SD. *** $p<0.0005$, **** $p<0.0001$

4.1.5. Absence of tumour formation after injection of MEF cells *in vivo*

First experiments were performed to investigate the capacity of p53-scTCR expressing T cells to recognize and eliminate MEF_p53 cells *in vivo*, with the final aim to combine TCR transfer therapy with nor-NOHA treatment. For tumour engraftment, 0.2 mio MEF_p53 cells per mouse (CyA2K^b) were injected s.c. and tumour growth was monitored. Animals received a daily injection (s.c. in the tumour area) of nor-NOHA (1 mg/mouse) whilst the control group received 0.9 % NaCl control solution starting on day 7 after tumour inoculation.

Surprisingly there was no tumour formation palpable in both groups after three weeks, even after tumour rechallenge. Further approaches, including total body irradiation (5.5 Gy) pre-conditioning with following tumour injection of MEF_p53 or MEF_orig, or injection of increasing tumour cell numbers (2 and 5 mio) did not result in tumour engraftment.

Taken together, these data showed, that our designed chimeric single chain MHC I molecule is able to overcome MHC downregulation, as it was stably expressed on the cell surface. In addition, we could show, that MEF tumour cells represent a suitable target cell line for *in vitro* assays with p53-TCR expressing T cells. However, it turned out, that this cell line was not suitable for *in vivo* experiments as no successful engraftment was achieved.

4.2. MC38 cells as new tumour target cell line

To overcome the absence of engraftment of MEF cells in CyA2K^b mice it was necessary to search for an alternative tumour model. To that aim, several criteria were to be considered. For following *in vivo* experiments, it was essential to choose cell lines from a BL6 background as a syngeneic mouse model was necessary to study our approach in the presence of a functional immune system. Another important aspect which needed to be considered was ASS1 expression in the tumour cell lines. We needed arginine auxotrophic cell lines for our experimental setup. This was necessary as for future experiments also citrulline administration as treatment option was considered. In addition, the availability of those cells from collaborators was taken into consideration.

4.2.1. ASS1 expression in diverse tumour cell lines

Different potential tumour cell lines were selected and screened for ASS1 expression by MTS assay and western blot to identify arginine auxotrophic tumours. As shown in Figure 16, RMAS (murine leukaemia), MC38 (colon adenocarcinoma) and Hep-55.1c (hepatocellular carcinoma) [3.2.2.1 Cell lines] were tested. MEF_p53 cells were used as a negative control for ASS1 expression. The RMAS cell line showed the strongest dependency on arginine with a reduction of metabolic activity to 8 % after arginine starvation. However, the RMAS cell line was able to recover metabolic activity to almost 90 % after supplementation of citrulline (arginine non-auxotrophic). MEF_p53, MC38 and Hep-55.1c cells showed all an approximately 2-fold decrease of metabolic activity after arginine starvation. This reduction in metabolic activity was not rescued by the supplementation of citrulline suggesting a non-functional ASS1 activity in those cell lines. MTS results were additionally confirmed by ASS1 expression analysis via western blot [Figure 16B]. MEF_p53 cells which were used as control, as well as MC38 cells and Hep-55.1c cells proved to be arginine auxotrophic as they were ASS1 negative. The RMAS cell line clearly expressed ASS1, confirming its capacity to use citrulline for endogenous arginine production to overcome reduced metabolic activity under arginine starvation conditions. For further experiments, we decided to use the MC38 cell line, as this cell line is extensively investigated in cancer research. In addition, it is also used by colleagues within our collaborative research centre.

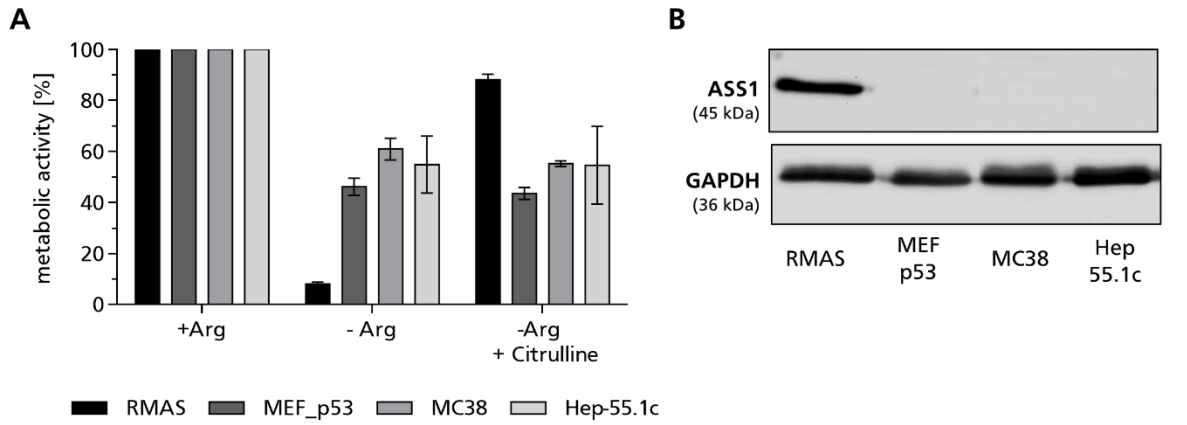

Figure 16: ASS1 expression in selected tumour cell lines
(A) MTS assay of different tumour cells cultured in standard medium (+Arg), arginine deficient medium (-Arg) and arginine deficient medium plus Citrulline (1 mM) ON. n=3 (technical replicates); Data are presented as mean ± SD. **(B)** Western blot analysis of ASS1 expression in different tumour cells. MEF_p53 and RMAS cells were used as negative and positive controls (respectively) for ASS1 expression.

4.2.2. p53 expressing MC38 cells are eliminated by antigen specific T cells

First, MC38 cells were transduced with the chimeric single chain MHC I molecule linked to the HLA-A2-restricted p53(264-272) peptide [Appendix, Figure 47 and Figure 48] to generate a tumour target cell line (MC38_scA2K^b_β$_2$M_p53; short: MC38_p53) for p53-scTCR recognition. Transduction resulted in 23.5 % of HLA-A2 expression on MC38 cells and was further increased after FACS based HLA-A2 sort to 62.7 % [see Figure 17].

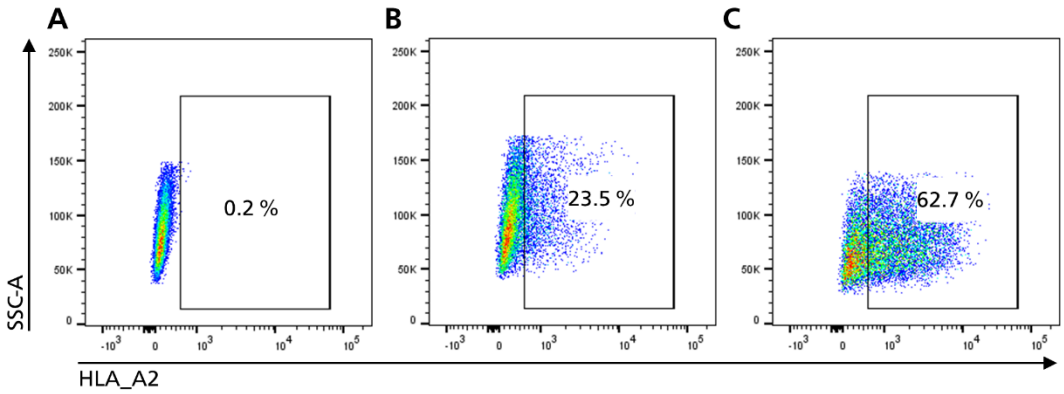

Figure 17: HLA-A2 expression on MC38 cells
MC38 cells were transduced with the scA2Kb_β2M_p53 construct and FACS sorted. FACS measurement of HLA-A2 is shown of MC38 cells **(A)** prior transduction, **(B)** 3 days post transduction and **(C)** post sorting.

Following FACS based sorting for HLA-A2 expression, cell layer cytotoxicity assays were performed to determine the recognition and killing capacity of antigen specific CD8 T cells. Wild type MC38 cells were not recognized, whereas transduced MC38 cells were recognized and killed with the same efficacy as transduced MEF cells. In both ratios of T cells to tumour cells, approximately 65 % of MC38_p53 cells and 75 % of MEF_p53 were lysed [Figure 18].

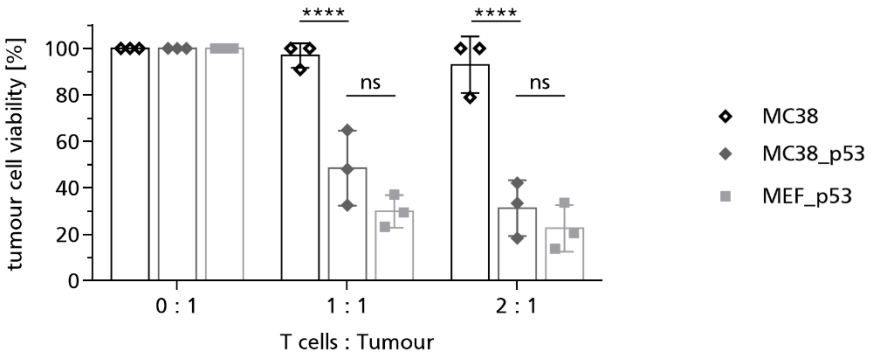

Figure 18: Cytotoxicity assay of WT-MC38 and p53 expressing MC38 and MEF cells
Killing assay over 5 hrs using wt MC38, MC38 and MEF cells expressing scA2Kb_β2M_p53 as target cells and p53-scTCR transduced CD8 T cells as effector cells with E:T ratios of 0:1, 1:1 and 2:1. n=3; Data are presented as mean ± SD. **** p<0.0001; ns=not significant.

4.2.3. Impact of nor-NOHA on phenotype and proliferation capacity of MC38 cells *in vitro*

After the new tumour cell line was established, the effect of nor-NOHA treatment on those cells *in vitro* was investigated. Therefore, the phenotype of MC38_p53 cells was analysed focusing on MHC class I (HLA-A2), PD-L1 and CD155/PVR expression. Tumour cells were cultured over several weeks ± 1 mM nor-NOHA addition to the standard medium. Surface molecule expressions were regularly checked by FACS staining.

No significant differences were detected upon nor-NOHA treatment. HLA-A2 expression ranged around 40 % (± 30 %) in non-treated cells (Ø) and 50 % (± 25 %) in treated cells (+ 1 mM nor-NOHA) whereas PD-L1 expression was rather low in both groups (~10 %). Both groups showed high CD155/PVR expression (100 %) [Figure 19A]. In addition, proliferation capacity via thymidine incorporation was examined. MC38_p53 cells treated with 1 mM nor-NOHA exhibited a significant reduction in proliferation of approximately 50 % [Figure 19B].

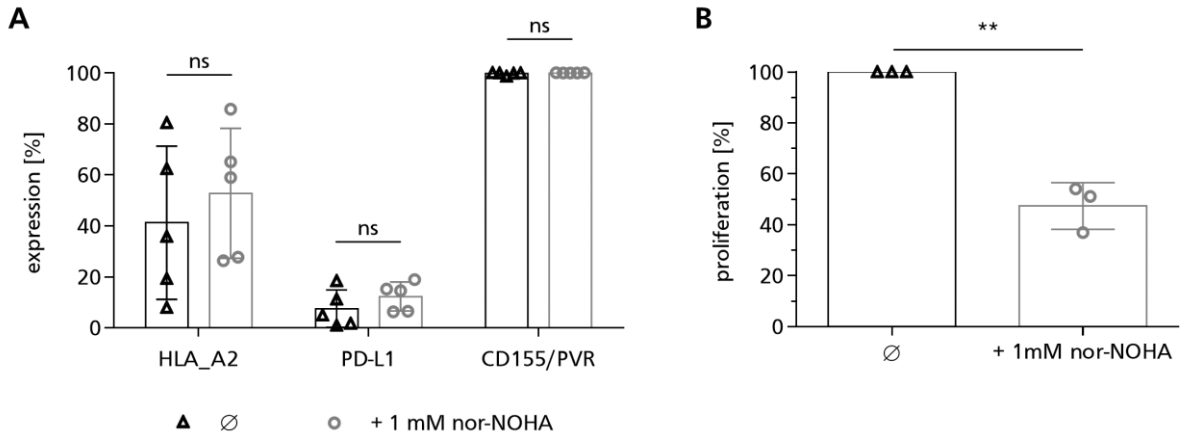

Figure 19: Surface marker expression and proliferation of MC38_p53 cells upon long-term nor-NOHA treatment Tumour cells were cultured over several weeks ± 1 mM nor-NOHA. **(A)** HLA-A2, PD-L1 and CD155/PVR expression was measured by FACS analysis. n=5 **(B)** Proliferation capacity was investigated by thymidine assays. Cells were incubated with thymidine for 16 hrs. Cpm-values of untreated cells were set to 100 % proliferation. n=3; Data are presented as mean ± SD. ns = not significant; ** $p<0.005$

Transduced (chimeric single chain MHC-I complex) MC38 cells proved to be a suitable new target cell line for following experiments. Furthermore, the findings in this chapter indicate that long-term effect of nor-NOHA treatment on MC38 cells reduces proliferation capacity but does not change the expression of inhibitory immune ligands and HLA-A2 on the cell surface.

4.3. *In vitro* characterization of p53 antigen specific T cells and impact of nor-NOHA treatment

In order to confirm and validate the peptide specificity of the newly generated tumour antigen model MC38_p53 cell line, further killing experiments were performed. Therefore, MC38 wild type cells were transduced with the same chimeric single chain MHC I construct as previously described [4.2.2] but the p53 $_{(264\text{-}272)}$ peptide was replaced by another HLA-A2 restricted peptide (MDM2$_{(81\text{-}88)}$ peptide) as irrelevant peptide for our p53-scTCR specific T cells.

After FACS based sorting for HLA-A2 expression, two comparable cell lines were available expressing either the p53 (MC38_p53) or the MDM2 (MC38_MDM2) peptide via the MHC class I complex on the surface. Both cell lines were additionally transduced with a luciferase-IRES-GFP construct (MC38_p53_Luc/GFP and MC38_MDM2_Luc/GFP) [Figure 44]. GFP expressing cells were of interest for the *ex vivo* discrimination of tumour cells from other cells of the TME in fluorescence-based analyses. Luciferase expression was used for luminescence based killing assays in vitro and for monitoring tumour growth in live animals in real-time using bioluminescence imaging detection device.

4.3.1. p53-scTCR expressing T cells specifically recognize MC38_p53 tumour cells

In a luminescence based killing assay, TCR specificity was analysed. Luminescence intensity was measured which correlates with the number of viable tumour cells. Thus, p53 as well as MDM2 expressing MC38 tumour cells were pretreated ON with 50 ng/ml IFNγ to increase MHC expression [146]. The next day, the killing assay was performed as described in chapter 3.2.7.2 and T cells equipped with the p53-scTCR were used as effector cells. Tumour cell viability was measured after 19 hrs incubation time. Only a slight "background" killing of MC38_MDM2_Luc/GFP cells was detected, whereas MC38_p53_Luc/GFP cells were strongly killed, represented by 70 % (2:1) and 85 % (4:1) of tumour lysis [Figure 20A]. To further validate, that the MC38_p53_Luc/GFP cell line is specifically recognized by T cells expressing the cognate TCR, another killing assay was performed. In this experiment MC38_p53_Luc/GFP cells as target cells were co-cultured for 3 hrs with either p53-TCR T cells or OT-1 T cells isolated from an OT-1 mouse [147]. As shown in Figure 20B, p53-scTCR specific T cells proved strong killing of target tumour cells with an E:T ratio related increase from 20 % (1:1) to 55 % (5:1) lysis. In parallel, OT-1 T cells were not able to recognize and kill the MC38_p53_Luc/GFP tumour cells. T cells which are in culture for several weeks (several rounds of restimulation) show reduced killing activity compared to freshly transduced T cells. Therefore, the assay explained in Figure 20A was evaluated after 19 hrs ("old" T cells were used), whereas the assay explained in Figure 20 B was incubated only for 3 hrs as new transduced T cells were used.
Those experiments demonstrated the antigen specificity of our model as only p53 presenting tumour cells were recognized by the p53-scTCR. Hence, MC38_p53 tumour model appeared as a suitable model for *in vivo* experiments as only p53-scTCR T cells were able to recognise and lyse those cells without any recognition and lysis by unspecific T cells.

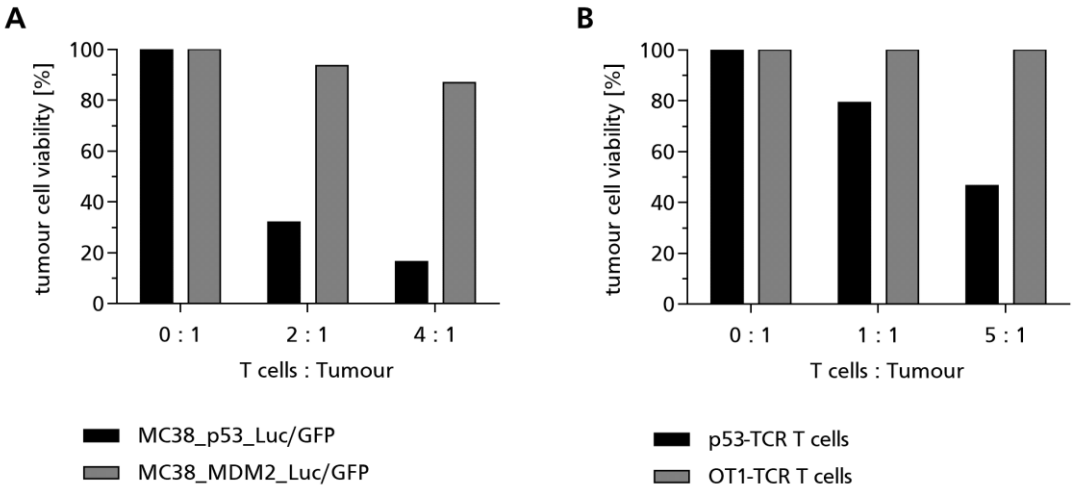

Figure 20: T cell specificity and antigen recognition
(A) Luminescence based killing assay using MC38_p53_Luc/GFP and MC38_MDM2_Luc/GFP cells as target cells and p53-scTCR transduced T cells as effector cells with E:T ratios of 0:1, 2:1 and 4:1. Evaluation after 19 hrs of incubation time. Tumour cells were pretreated ON with 50 ng/ml IFNγ. **(B)** Luminescence based killing assay with MC38_p53_Luc/GFP tumour cells and p53-scTCR or OT-1 T cells, co-cultured for 3 hrs. E:T ratios are 0:1, 1:1 and 5:1.

4.3.2. T cell phenotype is differently reshaped depending on tumour peptide presentation

To further examine any potential modulatory effects of tumour cells on the phenotype and function of T cells, co-culture experiments were performed. P53-scTCR transduced T cells were co-cultured for several days with MC38 cells either expressing the cognate p53 or the irrelevant MDM2 peptide to mimic the impact of the tumour cells on the expression of T cell effector markers. After 24 hrs incubation, T cells were harvested and cultured for another 24 hrs with fresh antigen expressing tumour cells. The procedure was repeated for 3 days consecutively. Again, tumour cells were pre-incubated ON with 50 ng/ml IFNγ, before T cells were added. T cells were analysed by FACS at time point 0 and after 24, 48 and 72 hrs of co-culture. The expression of different surface molecules is depicted in Figure 21. Results are indicated as % of expression or MFI. MFI calculation was used when 100 % of T cells where positive for the described surface molecule. Expression of the p53-scTCR (by detection of the TCR Vβ 3 domain) was slightly reduced over time but stagnated at around 83 % in T cells co-cultured with MC38_p53 whereas it further decreased to 67 % in T cells co-cultured with MC38_MDM2. PD-1 and LAG-3 expression was constantly high in T cells co-cultured with MC38_p53 and strongly decreased by approximately 50 % when co-cultured with MC38_MDM2.

Both T cell cultures demonstrated a downregulation of CD226 over time while only T cells in contact with the p53 peptide upregulated TIGIT expression to about 12-fold. However, Tigit expression was still rather low after 72 hours (14 %). TIM-3 expression in MC38_p53 co-cultured T cells showed a 2.5-fold increase after 24 hrs, which decreased almost to baseline level after 72 hrs. Expression in MC38_MDM2 co-cultured T cells did not change. In general, co-culture with p53 presenting tumour cells led to an increase or maintained high expression of inhibitory molecules on the surface of p53-scTCR T cells, whereas MDM2 presenting tumour cells had no effect on inhibitory molecules or even led to a downregulated expression.

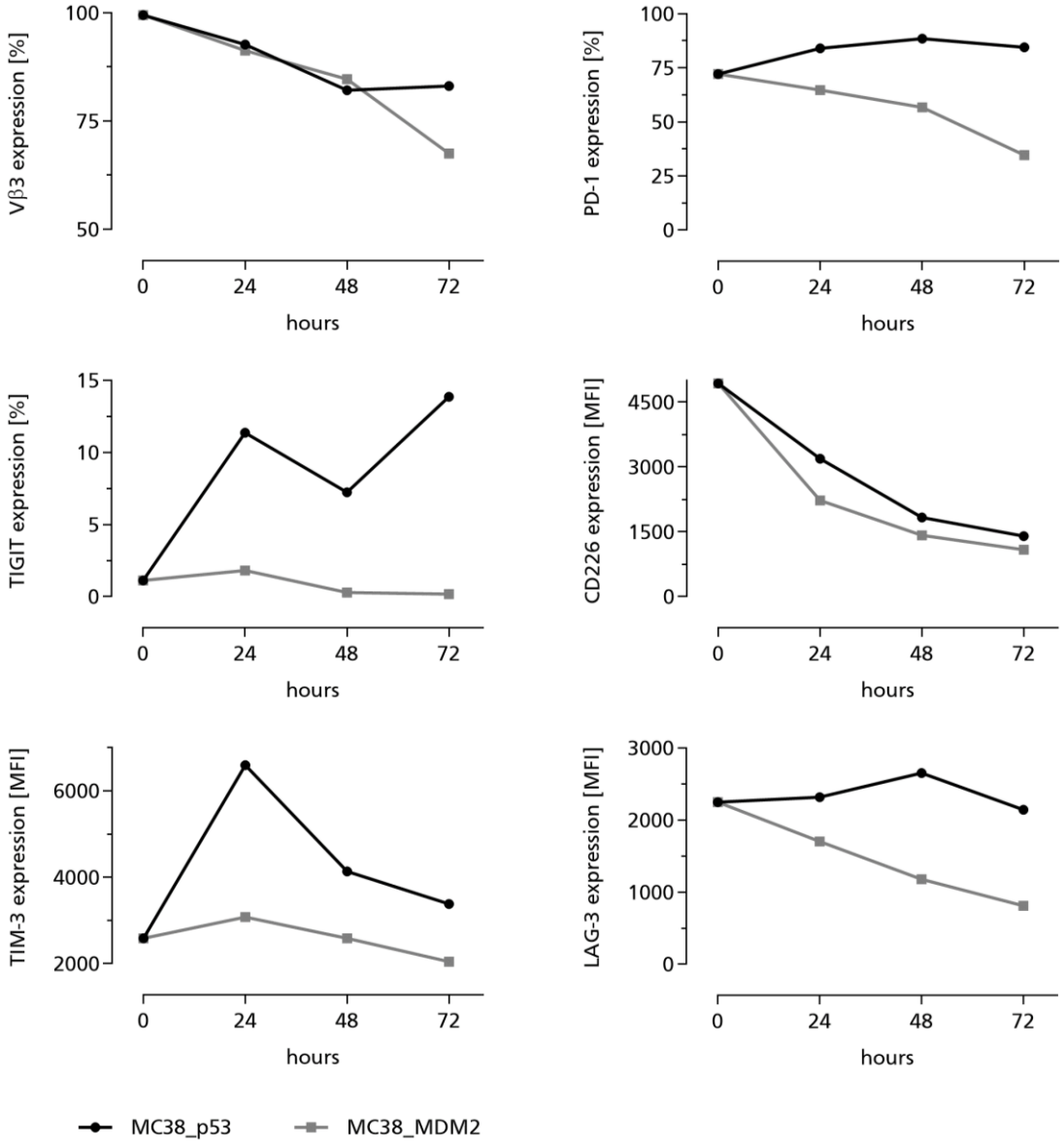

Figure 21: T cell phenotype after tumour co-culture *in vitro*
p53-scTCR expressing T cells were co-cultured with MC38 cells either expressing the p53 or MDM2 peptide. T cells were co-cultured with new tumour cells every 24 hrs. Tumour cells were pre-treated with 50 ng/ml IFNγ ON prior incubation with T cells. Surface marker expression of Vβ3, PD-1, CD226, TIGIT, TIM-3 and LAG-3 was analysed by FACS staining at time points 0, 24, 48 and 72 hrs.

4.3.3. nor-NOHA treatment does not affect T cell functional characteristics

To complement the data, nor-NOHA impact on T cells was investigated. Thus, focusing on immune checkpoint expression, proliferation and killing capacity. T cells were cultured over several weeks in standard medium ± 1 mM nor-NOHA. Regular FACS based analyses were conducted to determine Vβ3 (TCR), CD226, TIGIT, PD-1, LAG-3 and TIM-3 surface expression. No significant effect of nor-NOHA was detected as demonstrated in the representative measurement [Figure 22A, B] where (A) shows T cells in standard culture and (B) nor-NOHA treated T cells. In Figure 22C, MFI values are shown from three different measurements three days after restimulation within a time span of 8 weeks. Those values additionally demonstrate that immune checkpoint expression and TCR expression on T cells are not affected by long-term nor-NOHA treatment.

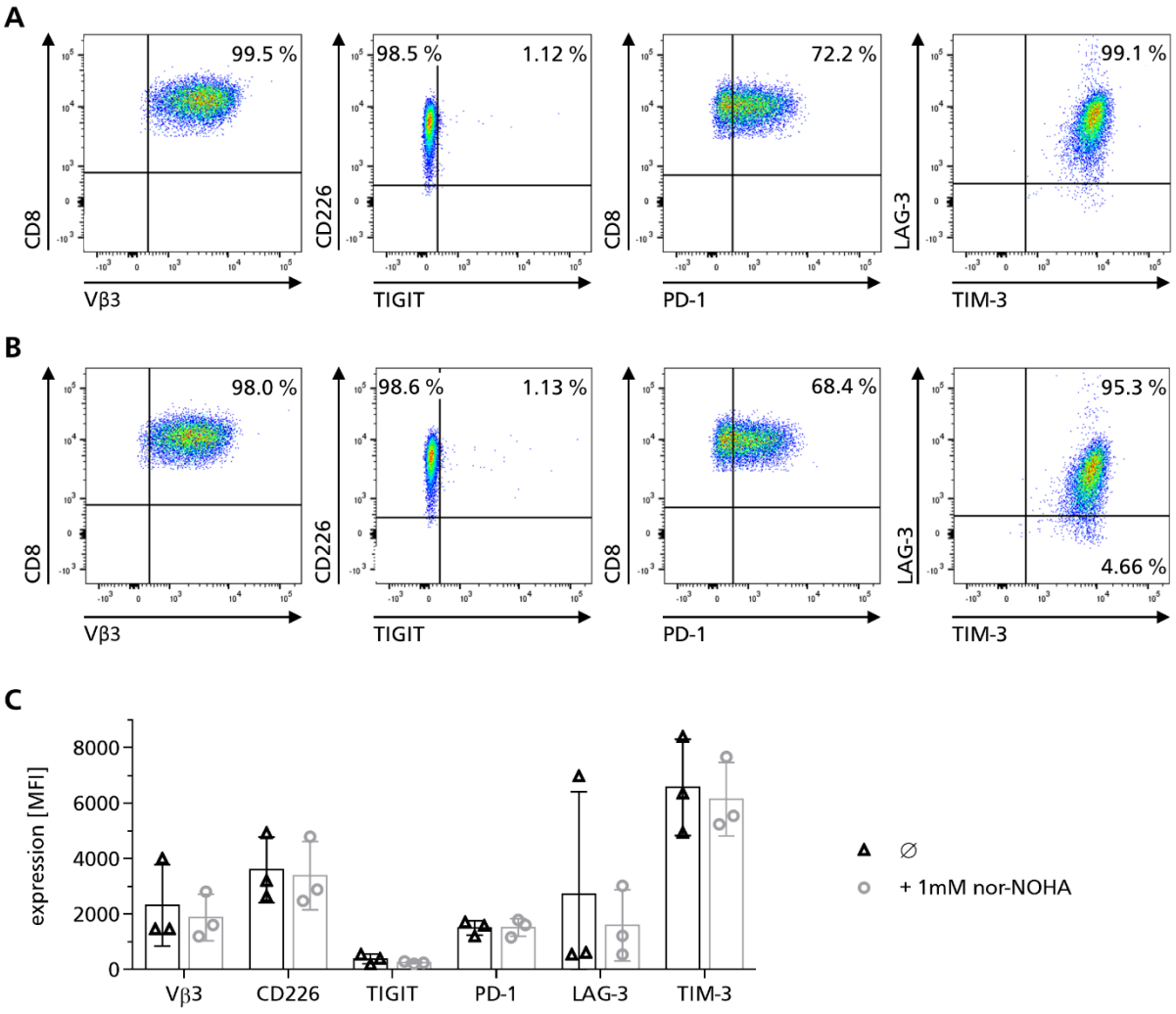

Figure 22: nor-NOHA effect on TCR and immune checkpoint expression of T cells *in vitro*
T cells were long-term cultured ± 1mM nor-NOHA and TCR as well as checkpoint receptor expression on CD8 T cell subset was determined by FACS analysis. Data are from one representative measurement of **(A)** standard conditions and **(B)** nor-NOHA treatment. **(C)** MFI of standard versus nor-NOHA cultured T cells analysed always 3 days after restimulation. n=3; Data are presented as mean ± SD.

The effect of nor-NOHA on the proliferation capacity of T cells via thymidine assay was also examined. In contrast to nor-NOHA treated MC38 tumour cells, no significant differences were detected between T cells in standard culture and T cells cultured with 1mM nor-NOHA [Figure 23A]. Additionally, T cell killing capacity was analysed. Preconditioned T cells and tumour cells (± 1 mM nor-NOHA) were co-cultured ± 1 mM nor-NOHA for 4 hrs with an E:T ratio of 10:1. As demonstrated in Figure 23B, reduced killing was observed in nor-NOHA treated conditions (~62.5 %) compared to untreated control (76 %). However, a strong reduction in tumour cell viability (37.5 %) was still achieved in the nor-NOHA treated condition.

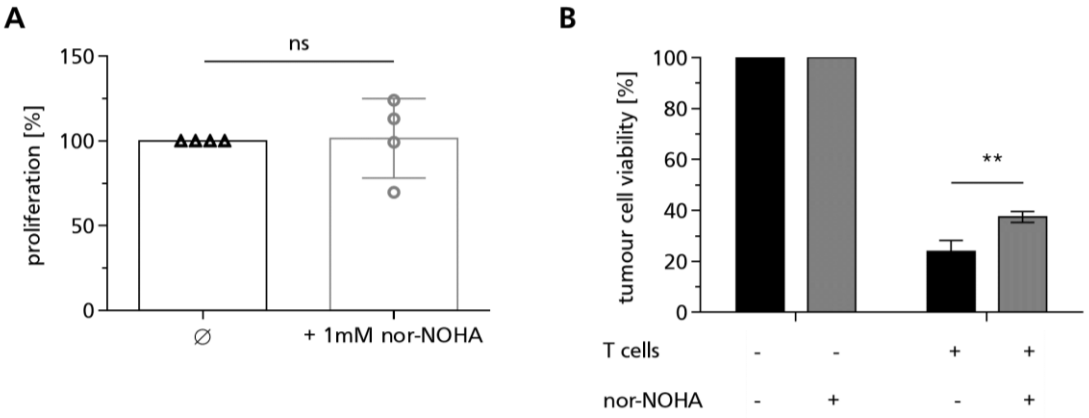

Figure 23: Effect of nor-NOHA on proliferation and killing capacity of T cells
(A) T cells were long-term cultured ± 1mM nor-NOHA and proliferation was analysed by thymidine assay. Cells were incubated with thymidine for 16 hrs. Cpm-values of untreated cells were set to 100 % proliferation. n=4; Data are presented as mean ± SD. ns=not significant. **(B)** Long-term cultured (± 1mM nor-NOHA) T cells and MC38_p53_Luc/GFP cells were used for luminescence based killing assay with an E:T ratio of 10:1. Assay was evaluated after 4 hrs. n=3 (technical replicates); Data are presented as mean ± SD. ** $p<0.005$

These data clearly show, that our p53-scTCR is antigen specific and only recognizes its cognate peptide when presented on tumour cells. In addition, T cell phenotype was reshaped when cells were co-cultured with tumour cells expressing the cognate peptide. This led to an increased TIGIT expression, reduced CD226 expression, a stabilization of PD-1 and LAG-3 and a slightly reduced TCR expression on the surface. In comparison to tumour cells, long-term treatment with nor-NOHA had no impact on proliferation and immune checkpoint expression but showed a slightly reduced killing capacity of T cells.

4.4. The impact of arginine deficiency on T cells and tumour cells *in vitro*

To investigate the consequences of arginine deficiency (mimicking high arginase I activity of the TME) on T cell effector functions, further *in vitro* experiments were conducted. Therefore, an experimental setup established by a colleague (Y. Bülbül [148]) was used. Human PMNs were isolated from peripheral blood of healthy donors and cultured. Those cells express arginase I constitutively and release the enzyme in the supernatant. The secretome (supernatant) was harvested and used for further assays. In contrast, murine PMNs only express arginase I upon specific stimuli *ex vivo* [149] and isolation of sufficient cell numbers is challenging.

Human PMNs were isolated as described [3.2.2.5] and purity (expression of CD66b marker) as well as arginase I expression of the isolated cell fraction was confirmed by FACS analysis [Figure 24]. PMNs were cultured in T cell medium ± 1 mM nor-NOHA and with 20 µM $MnCl_2$ for three days and used for experiments.

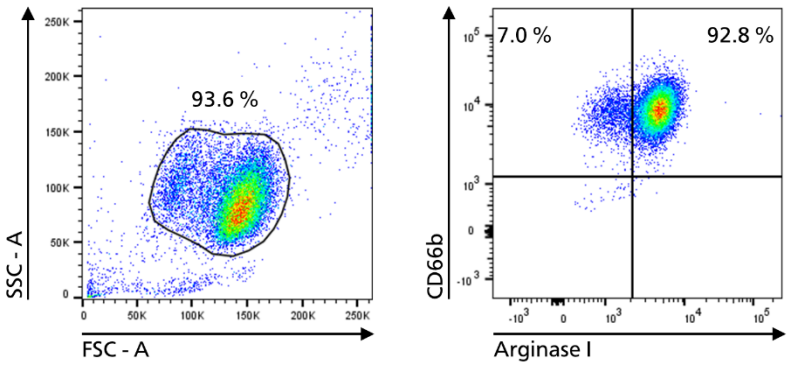

Figure 24: Representative control staining of isolated human PMNs.
Human PMNs were isolated as described in [3.2.2.5]. Cells were stained for the cell surface marker CD66b and intracellular arginase I and analysed by FACS. Viability was assessed in the FSC/SSC plot and purity was analysed by the percentage of CD66b positive cells.

4.4.1. PMN derived arginase effectively metabolises arginine

PMNs die during *in vitro* culture and release arginase I. Arginase I activity hydrolyses arginine into L-ornithine and urea in the medium resulting in arginine deficiency, whereas the addition of nor-NOHA prevents arginine degradation. For the following experiments, human PMNs were cultured in T cell medium (2.5 mio/ml to achieve a final 10:1 ratio of PMNs : T cells) ± 1 mM nor-NOHA supplemented with 20 % TCGF and 20 µM $MnCl_2$ for 3 days. Arginase I activity was verified by measuring arginine concentration in the medium by liquid chromatography–mass spectrometry (LC-MS). PMN-derived arginase I strongly reduced arginine level in the medium (PMN-SN) by 1.000-fold, whereas nor-NOHA efficiently blocked arginine degradation (PMN-SN + 1 mM nor-NOHA). The addition of 1 mM arginine (PMN-SN + 1 mM arginine) after culture and before measurement reconstituted the arginine level to control levels [Figure 25A]. In addition, T cells were restimulated (peptide specific) [3.2.2.3] and 0.5 mio cells were seeded in 2 ml/well pre-conditioned medium. After 3 days of culture, arginine levels in the culture SN were measured [Figure 25B]. Stable arginine levels with only a slight reduction in arginine concentration were measured for both control conditions (Medium and Medium + 1 mM nor-NOHA) and for PMN-SN + 1 mM nor-NOHA.

In the PMN-SN + 1 mM arginine sample, arginine was strongly reduced from $4x10^7$ to $3x10^4$ (1300-fold), compared to the same condition before T cell culture. But also, in the PMN-SN sample a 35-fold decrease from $3.5x10^4$ to $1x10^3$ was observed, whereas the other conditions showed very little changes (between 1- and 2-fold) when comparing supernatants before and after T cell culture.

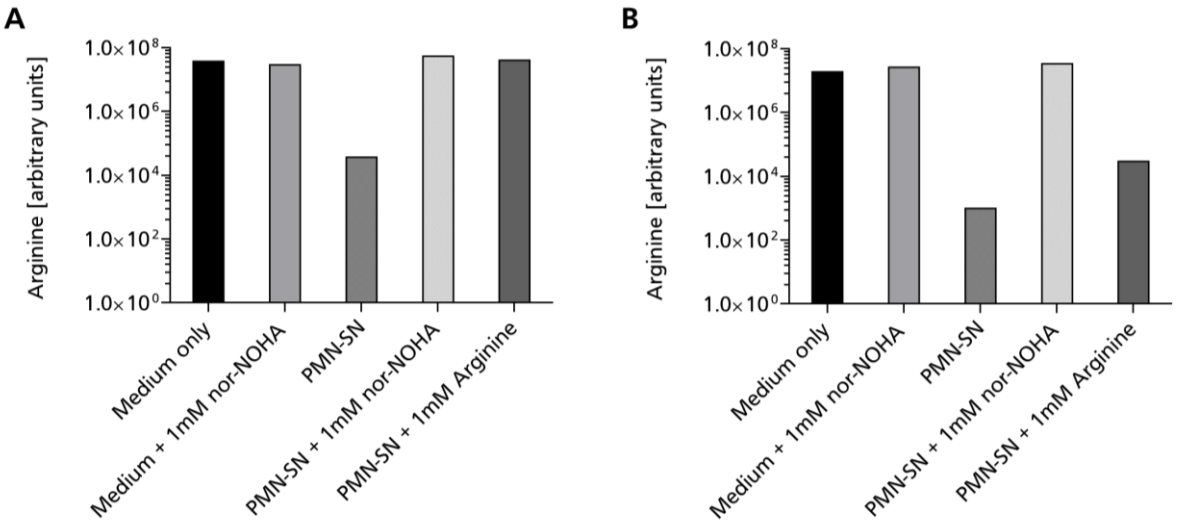

Figure 25: Representative LC-MS measurement of arginine
PMNs were cultured with 2.5 mio/ml in T cell medium ± 1 mM nor-NOHA, 20 % TCGF and 20 µM $MnCl_2$ for 3 days. Controls are T cell medium (RPMI) and RPMI + 1 mM nor-NOHA. Arginine was added after PMN incubation and before measurement (PMN-SN + 1 mM arginine). **(A)** Medium samples were analysed for arginine concentration by LC-MS. **(B)** 0.5 mio T cells were restimulated in different media from experiment (A) and arginine concentration was measured in the supernatant via LC-MS 3 days later.

4.4.2. Arginine deficiency alters T cell proliferation and immune checkpoint expression

To investigate the proliferation capacity of T cells under arginine starvation, thymidine assays were performed. T cells were restimulated (peptide specific) [3.2.2.3] and 0.5 mio cells were seeded in 2 ml/well pre-conditioned medium. The conditions were: (I) medium only, (II) medium + 1 mM nor-NOHA, (III) medium + 10 mM arginine, (IV) PMN-SN, (V) PMN-SN + 1 mM nor-NOHA, (VI) PMN-SN + 1 mM arginine (freshly added), (VII) PMN-SN + 10 mM arginine (freshly added). Arginine supplementation was shown to modulate T cell metabolism and enhance anti-tumour activity [120]. We therefore tested 10 mM arginine to evaluate a supraphysiological concentration and its potential positive impact on T cells. After 3 days of culture, proliferation was analysed. Our results are in line with published data [92,150], showing inhibition of T cell proliferation under arginine starvation (PMN-SN) [Figure 26A].

By the addition of 1 mM nor-NOHA or 1 mM arginine to PMN-SN, we were able to rescue T cell proliferation to control levels. Interestingly, the addition of 10 mM arginine to PMN-SN even further boosted the proliferation of T cells and showed significant higher cpm-values compared to its control (medium + 10 mM arginine). In contrast to the results from the proliferation assays, cell counts as determined by trypan blue exclusion were not only reduced in the PMN-SN condition (0.3 mio/ml) but also in both conditions where 10 mM arginine was added (0.45 and 0.65 mio/ml respectively). Again, PMN-SN samples with additional 1 mM nor-NOHA (1.75 mio/ml) or 1 mM arginine (2 mio/ml) demonstrated similar cell counts as controls (1.75 mio/ml) [Figure 26B].

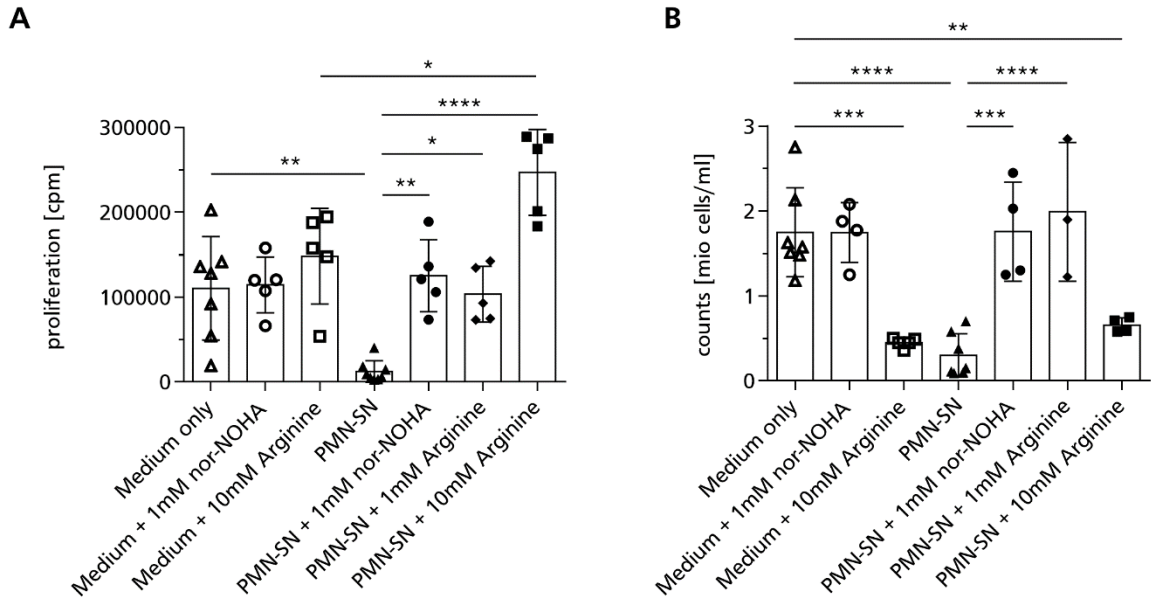

Figure 26: Proliferation and cell counts of T cells under arginine starvation
Hu PMNs (2.5 mio/ml) were cultured for 3 days in T cell medium ± 1 mM nor-NOHA, 20 % TCGF and 20 µM $MnCl_2$. T cells were restimulated according to the protocol with 0.5 mio cells/well in 2 ml conditioned medium. (I) medium only, (II) medium + 1 mM nor-NOHA, (III) medium + 10 mM arginine, (IV) PMN-SN, (V) PMN-SN + 1 mM nor-NOHA, (VI) PMN-SN + 1 mM arginine (freshly added), (VII) PMN-SN + 10 mM arginine (freshly added). **(A)** T cell proliferation was measured via thymidine assay 3 days after restimulation. **(B)** Cell counts of T cells 3 days after restimulation. n=3-7; Data are presented as mean ± SD. * $p<0.05$, ** $p<0.005$, *** $p<0.0005$, **** $p<0.0001$

For further T cell characterisation, expression of immune checkpoints as well as TCR expression was investigated. Therefore, the same experimental procedure was used as explained above. Three days after restimulation, expression of surface molecules was determined by FACS analysis. When T cells were cultured in PMN-SN, TCR expression was downregulated. This downregulation correlates well with already published data linking a CD3ζ-chain downregulation to arginine deficiency [151].

PD-1 and TIGIT expression was strongly upregulated whilst CD226 and TIM-3 expression did not change. Interestingly, LAG-3 expression was affected by high arginine concentration (10 mM), leading to significant lowered expression levels. The downregulation of the TCR and PD-1/TIGIT upregulation induced by the PMN-SN was prevented by the addition of either 1 mM nor-NOHA or arginine [Figure 27].

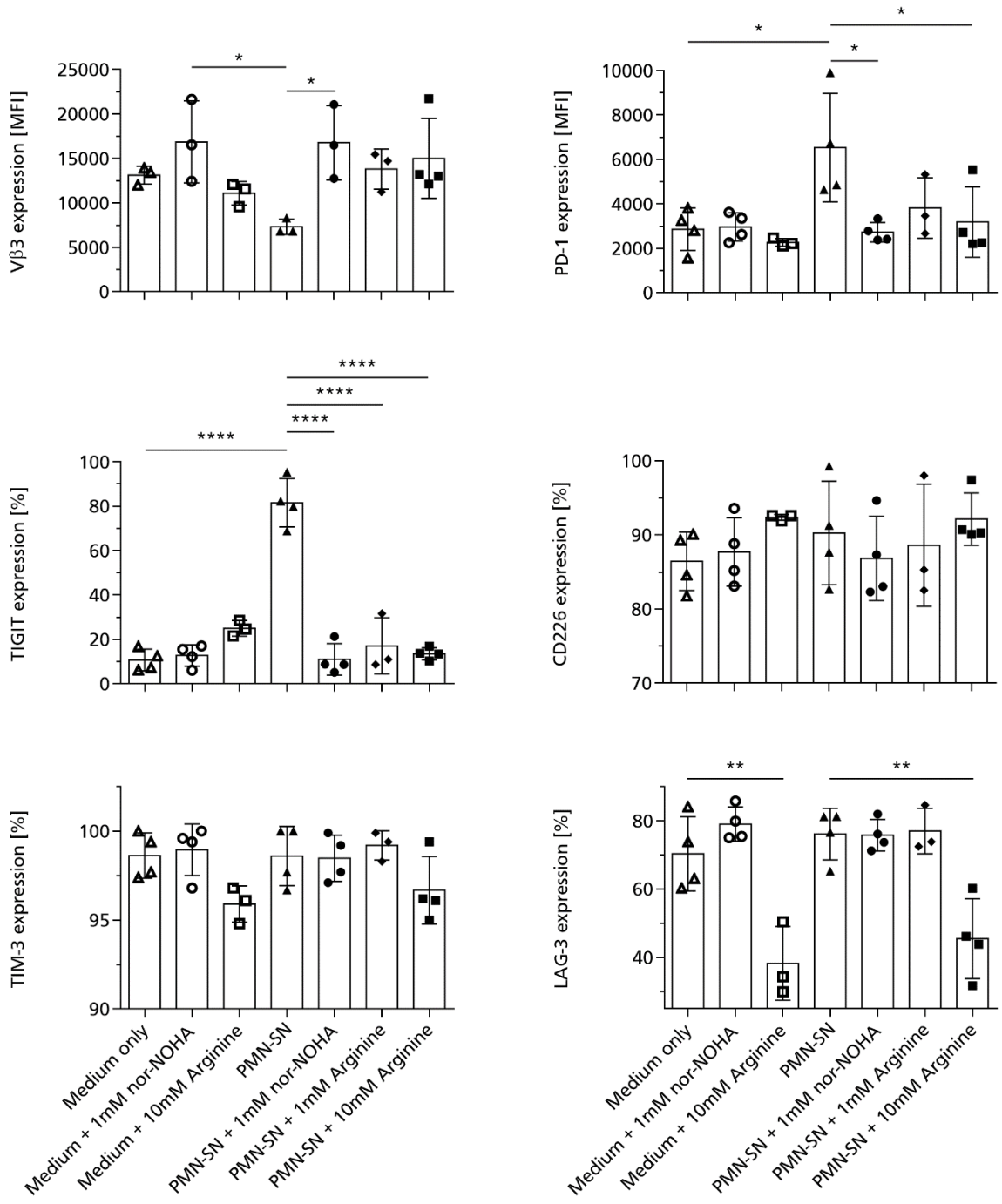

Figure 27: FACS based analysis of immune checkpoints and TCR expression under arginine starvation
T cells were cultured as explained in Figure 26 and TCR-Vβ3, PD-1, TIGIT, CD226, TIM-3 and LAG-3 expression was analysed by FACS staining 3 days after restimulation. n=3-4; Data are presented as mean ± SD. * $p<0.05$, ** $p<0.005$, **** $p<0.0001$

4.4.3. Effects of arginine deprivation on tumour cell proliferation and surface marker expression

We further analysed the effect of arginine deficiency on MC38_p53_Luc/GFP tumour cells *in vitro*. To generate PMN-SN, PMNs were cultured in DMEM complete medium (0.5 mio/ml to achieve a final 10:1 ratio of PMNs to tumour cells) ± 1 mM nor-NOHA and 20 µM $MnCl_2$ for 3 days. Afterwards, tumour cells (0.5 mio/10 ml/T75 flask) were cultured for 3 days in different conditioned media: (I) medium only, (II) medium + 1 mM nor-NOHA, (III) PMN-SN, (IV) PMN-SN + 1 mM nor-NOHA, (V) PMN-SN + 1 mM arginine (freshly added) and proliferation was measured by thymidine incorporation assay. No significant differences were observed upon addition of 1mM nor-NOHA to the culture medium (II). However, a tendency towards reduced proliferation of tumour cells cultured in PMN-SN (III) was noticed when compared to medium only (I) which became significant when compared to medium + 1 mM nor-NOHA condition (II). Reduced proliferation under arginine starvation (III) could be significantly rescued by the addition of 1 mM nor-NOHA (IV) but not by arginine (1 mM) supplementation (V) [Figure 28].

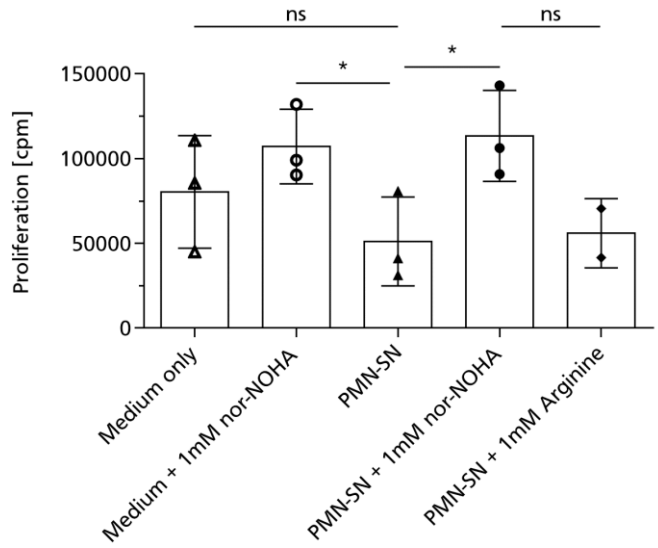

Figure 28: Proliferation of MC38_p53_Luc/GFP tumour cells under arginine deficiency
Hu PMNs (0.5 mio/ml) were cultured for 3 days in DMEM compl. medium ± 1 mM nor-NOHA and 20 µM $MnCl_2$. MC38_p53_Luc/GFP cells were seeded with 0.5 mio cells/T75 in 10 ml conditioned medium. (I) medium only, (II) medium + 1 mM nor-NOHA, (III) PMN-SN, (IV) PMN-SN + 1 mM nor-NOHA, (V) PMN-SN + 1 mM arginine (freshly added). Tumour cell proliferation was measured via thymidine incorporation after 3 days of culture. n=3; Data are presented as mean ± SD. * $p<0.05$.

Surface marker expression of HLA-A2, CD155/PVR and PD-L1 was also examined by FACS analysis after 3 days of culture. The expression pattern remained unchanged in all conditions listed above, suggesting that arginine deficiency had no effects on MC38_p53_Luc/GFP expression of surface marker, at least over this treatment period [Figure 29].

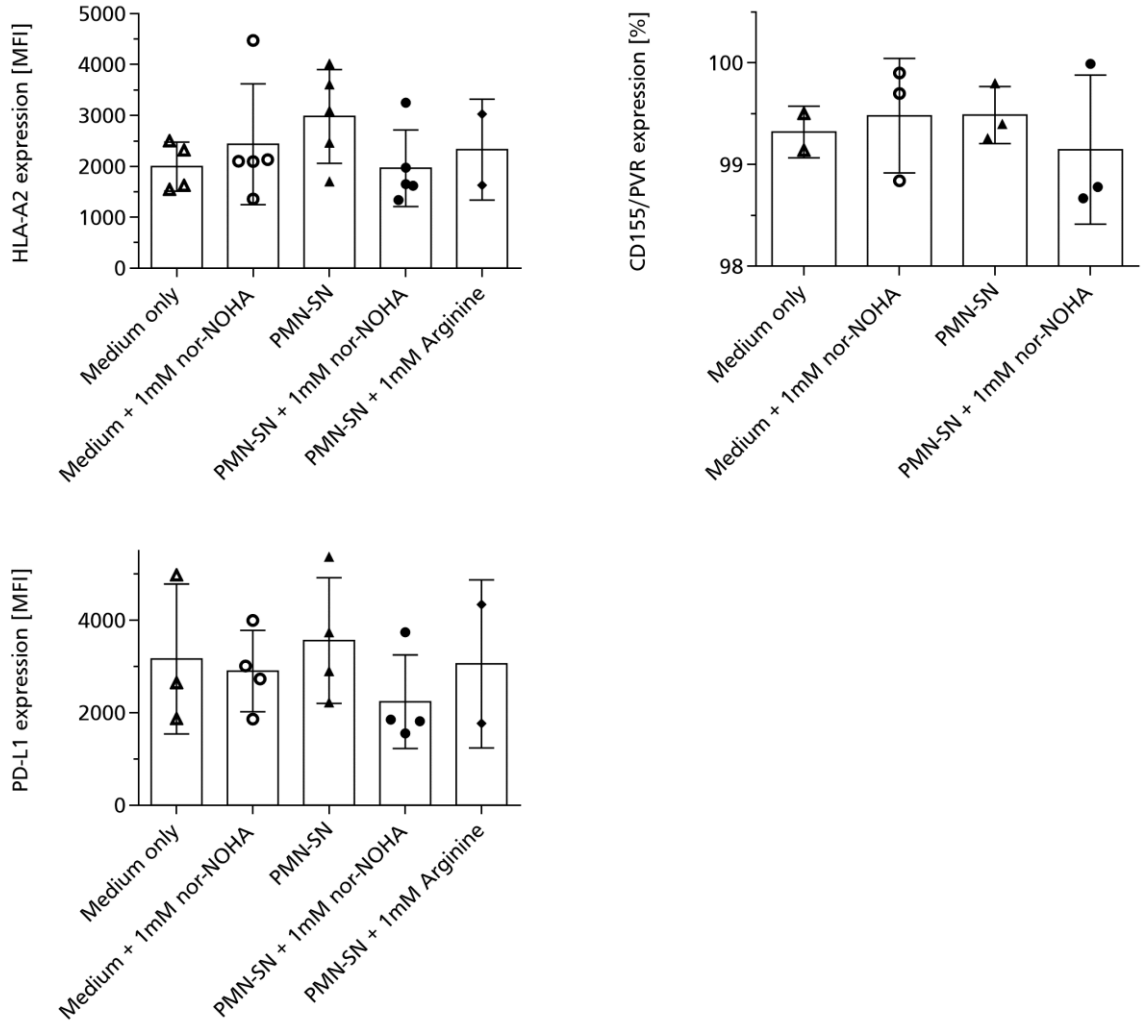

Figure 29: Surface marker expression on MC38_p53_Luc/GFP cells upon arginine deprivation
Tumour cells were cultured for 3 days in different conditioned media [Figure 28]. HLA-A2, CD155/PVR and PD-L1 expression was measured by FACS analysis. n=2-5; Data are presented as mean ± SD.

4.4.4. Killing capacity of antigen specific T cell is impaired upon arginine starvation

To assess *in vitro* killing capacity of antigen specific T cells under arginine starvation, luminescence based killing assays were performed. Therefore, T cells as well as tumour cells (MC38_p53_Luc/GFP) were pre-cultured in conditioned media as listed in 4.4.2 (I-VII) for 3 days. Killing assays were performed with tumour cells only as control (0:1) and an E:T-ratio of 2:1 and luminescence was measured after 6 hrs of co-culture. Co-cultures were prepared in conditioned DMEM complete medium (I-VII). Upon arginine starvation (PMN-SN), T cell killing capacity was significantly impaired resulting in 55.5 % tumour cell viability in comparison to control T cells (medium only: 19.5 % and medium + 1 mM nor-NOHA: 12.5 % tumour cell viability). The addition of 1 mM nor-NOHA as well as 1 mM and 10 mM arginine to PMN-SN restored T cell killing capacity to the same efficiency as control conditions. However, tumour cell viability was 3 times higher (but not significant) in arginine supplemented PMN-SN conditions (23 %) compared to PMN-SN + 1 mM nor-NOHA (7 %) [Figure 30].

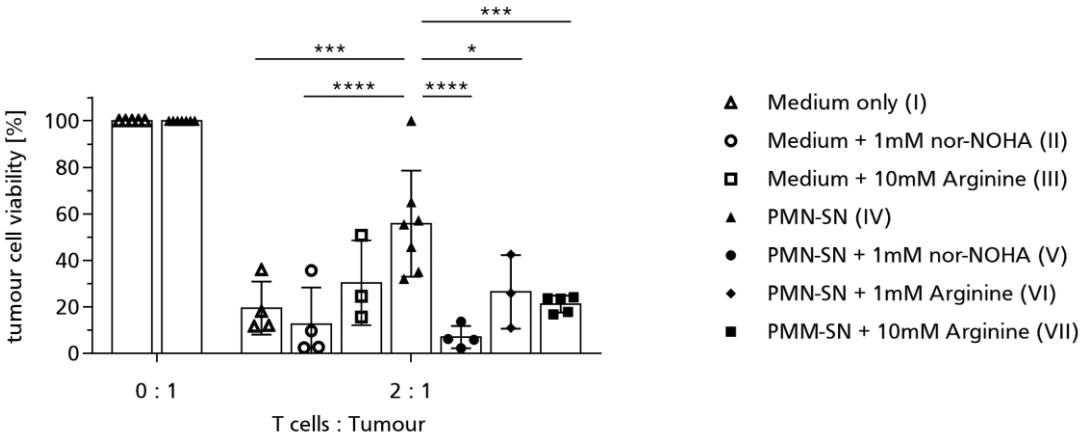

Figure 30: Killing capacity of antigen specific T cells upon arginine starvation
T cells and tumour cells were pre-cultured in the different conditions (I-VII) [see 4.4.2] for 3 days. Luminescence based killing assay was performed using MC38_p53_Luc/GFP as target cells and p53-scTCR transduced T cells as effector cells with E:T ratios of 0:1 and 2:1. Cells were prepared in conditioned DMEM compl. for the assay. Evaluation after 6 hrs. n=3-7; Data are presented as mean ± SD. * $p<0.05$, *** $p<0.0005$, **** $p<0.0001$

These findings indicate the need of arginine for T cell function as proliferation was strongly reduced when cultured in PMN-SN (arginine depleted milieu). In addition, TCR expression was downregulated and immune checkpoint expression was negatively affected resulting in increased PD-1 and TIGIT expression under arginine starvation. This arginine dependence was not visible when tumour cells were investigated for surface marker expression.

However, also in tumour cells a significant reduction in proliferation was measured when cultured in an arginine depleted milieu (PMN-SN). Finally, killing capacity of antigen specific T cells was impaired upon arginine starvation. Nevertheless, all those effects could be reverted by the addition of nor-NOHA or fresh arginine supplementation to the PMN-SN.

4.5. Effect of human PMNs on T cells in cell/cell contact setting

Not only soluble factors secreted by PMNs but also direct interactions between T cells and PMNs have distinct effects on the phenotype and function of T cells [152]. Accordingly, we wanted to extend our observations obtained with PMN-SN by testing the outcome of direct cell-cell contact experiments between human PMNs and murine T cells. This scenario mirrors a more *in vivo* situation. Nevertheless, it is important to stress the fact that we used cells from human and murine origins for those experiments. Thus, the results should be interpreted with cautious with regard to translational scientific questions. To investigate effects of PMNs on the proliferation of T cells in direct co-culture, thymidine assays were performed. T cells were seeded in a 96-well plate (50,000 cells/well) with 200 µl medium in total. For culture, T cell medium was used with 20 % TCGF and 20 µM $MnCl_2$. PMNs were added with different ratios (1:1, 5:1 and 10:1) and nor-NOHA or arginine was added as stated in Figure 31. Cells were cultured for 3 days before the thymidine assay was performed. In the control conditions no differences were detected between medium only and medium + nor-NOHA. The addition of 10 mM arginine to the medium showed a tendency (not significant) towards increased T cell proliferation compared to the control (medium only). Surprisingly, increasing PMN : T cell ratios correlated with increased T cell proliferation. This increase in proliferation became significant between 1:1 and 10:1 conditions in nor-NOHA (3.4-fold) and arginine (2.3-fold) treated samples. Furthermore, the direct comparison of the samples with 10 mM arginine ± PMNs (10:1) showed a significant increase (2-fold) of T cell proliferation when PMNs were added. Neither 1 mM nor-NOHA nor 10 mM arginine treatment proved to increase T cell proliferation when compared with PMNs alone. However, T cells cultured with PMNs and 10 mM arginine indicated the highest proliferation capacities roughly 1.5-2.0 fold higher than PMNs alone or with the addition of nor-NOHA. In addition, a synergistic effect of PMN + arginine treatment was observed when comparing to PMN or arginine alone. Taken together, those results indicate a boost of T cell proliferation in a PMN-concentration dependent manner [Figure 31].

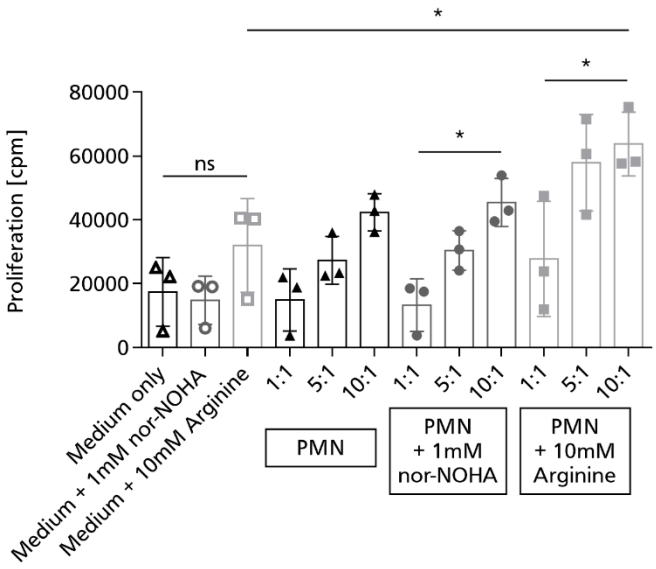

Figure 31: T cell proliferation in direct co-culture with PMNs
T cells were co-cultured with PMNs in different ratios (1:1, 5:1, 10:1) ± 1 mM nor-NOHA or ± 10 mM arginine for 3 days. Controls were T cells alone, T cells + 1 mM nor-NOHA and T cells + 10 mM arginine. Proliferation was measured via thymidine assay. n=3; Data are presented as mean ± SD. * $p<0.05$

The expression of T cell checkpoint markers like CD226, TIGIT, PD-1, LAG-3 and TIM-3 was not altered by co-culture (3 days) with PMNs ± 10 mM arginine or ± nor-NOHA. In addition, TCR expression was not affected under those two conditions compared to the control condition (T cells alone) [results not shown]. To further characterize the direct effect of PMN on T cell effector functions, luminescence based killing assays were performed. We wanted to assess, whether T cells cultured with PMNs and 10 mM arginine also result in improved killing characteristics. The four conditions as listed in Figure 32 were tested with 200 µl T cell medium (with 20 % TCGF and 20 µM $MnCl_2$) into wells of a 96-well plate. PMNs were seeded with 200,000 cells per well and T cells with 20,000 cells per well (10:1 ratio of PMNs to T cells). Cells were incubated for 3 days, and 10,000 tumour cells (MC38_p53_Luc/GFP) per well were added (2:1 ratio of T cells to tumour cells). Killing assays were evaluated (luminescence detection) after 4 hrs co-incubation. PMNs alone had no significant effect on tumour cell viability. Strong tumour killing (~90 %) of T cells was detected in the condition with T cells only. T cells co-cultured with PMNs showed significant reduced (1.8-fold) killing capacities (~50 % tumour cell viability) compared to T cells alone. This reduction in killing was not compensated by the addition of 10 mM arginine (~65 % tumour cell viability). Despite increased proliferation capacity of T cells co-cultured with PMNs ± 10 mM arginine killing capability of T cells in this condition was still impaired.

Supraphysiological arginine concentration (10 mM) was able to boost T cell proliferation in a PMN dependent manner but couldn't rescue T cell effector functions in killing assays.

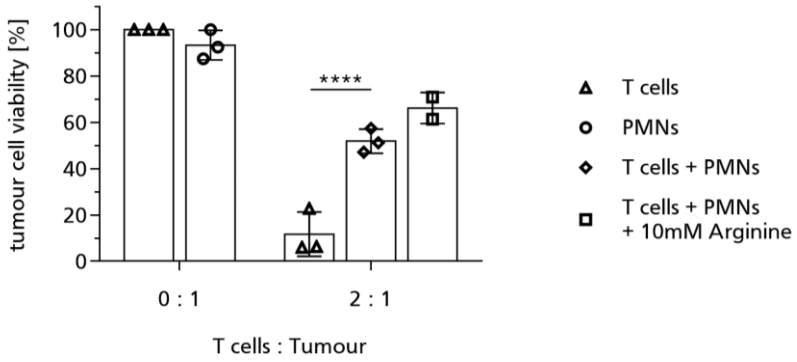

Figure 32: Impact on killing capacity of T cells co-cultured with PMNs
Cells were cultured in different conditions for 3 days. PMN to T cell ratio was 10:1. Tumour cells (MC38_p53_Luc/GFP) were added after 3 days with an E:T ratio of 2:1 and killing assay was evaluated by luminescence detection after 4 hrs. n=2-3; Data are represented as mean ± SD. **** $p<0.0001$

4.6. Impact of ACT and nor-NOHA combinatorial treatment on tumour growth *in vivo*

To further investigate the strategy of inhibiting arginase-mediated tumour immune escape and thereby support adoptive T cell transfer we conducted different *in vivo* experiments. The following experimental procedure [Figure 33] was intended to assess the impact of nor-NOHA in our tumour model.

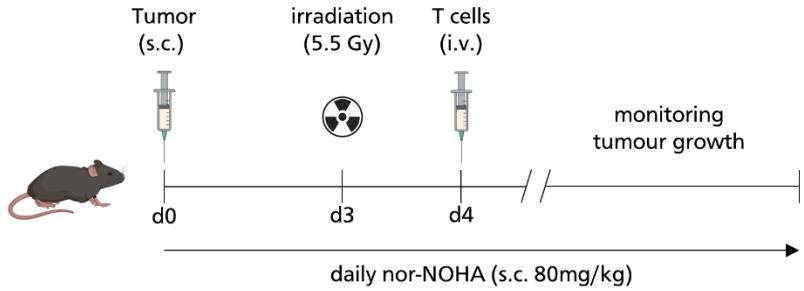

Figure 33: Experimental set up of in vivo experiments
CyA2K^b mice received 0.2 mio tumour cells (MC38_p53_Luc/GFP) s.c. into the right flank. On day 3, animals received a preconditioning regimen by total body irradiation with 5.5 Gy. One day later (d4), 5 mio TCR$^+$ T cells (p53-scTCR) were injected i.v. along with i.p. administered IL-2 (7x10^5 U/ml). Mice received a second shot of IL-2 (7x10^5 U/ml) 7 days after ACT. From day 0 on, nor-NOHA (2 mg/mouse) or 0.9 % NaCl was injected s.c. close to the tumour site on a daily basis. Tumour growth was measured by calliper and luminescence detection.

4.6.1. MC38_p53_luc/GFP tumour and p53-scTCR T cells

Mice were allocated to the following four groups (n=3): (I) control T cells + NaCl, (II) p53-scTCR T cells + NaCl, (III) control T cells + nor-NOHA, (IV) p53-scTCR T cells + nor-NOHA. T cells transduced with Katushka [Figure 45] were used as controls and 5 mio TCR$^+$ cells per mouse were injected. Tumour growth of MC38_p53_Luc/GFP cells was measured with a calliper [Figure 34A, D] and those data were additionally confirmed by luminescence detection [Figure 34B, C] starting with tumour inoculation at day 0. Mice treated with nor-NOHA had significant lowered tumour volume after 17 days compared to NaCl treated mice regardless of the T cells injected [Figure 34D]. However, there was no clear synergistic anti-tumour effect of the combination nor-NOHA and p53-TCR as animals had no advantage over those mice which received nor-NOHA and control T cells [Figure 34A, B]. The effect of nor-NOHA became clear when survival of both groups was compared. After 17 days, all nor-NOHA treated mice were still alive, whereas only 50 % of the NaCl group survived [Figure 34E].

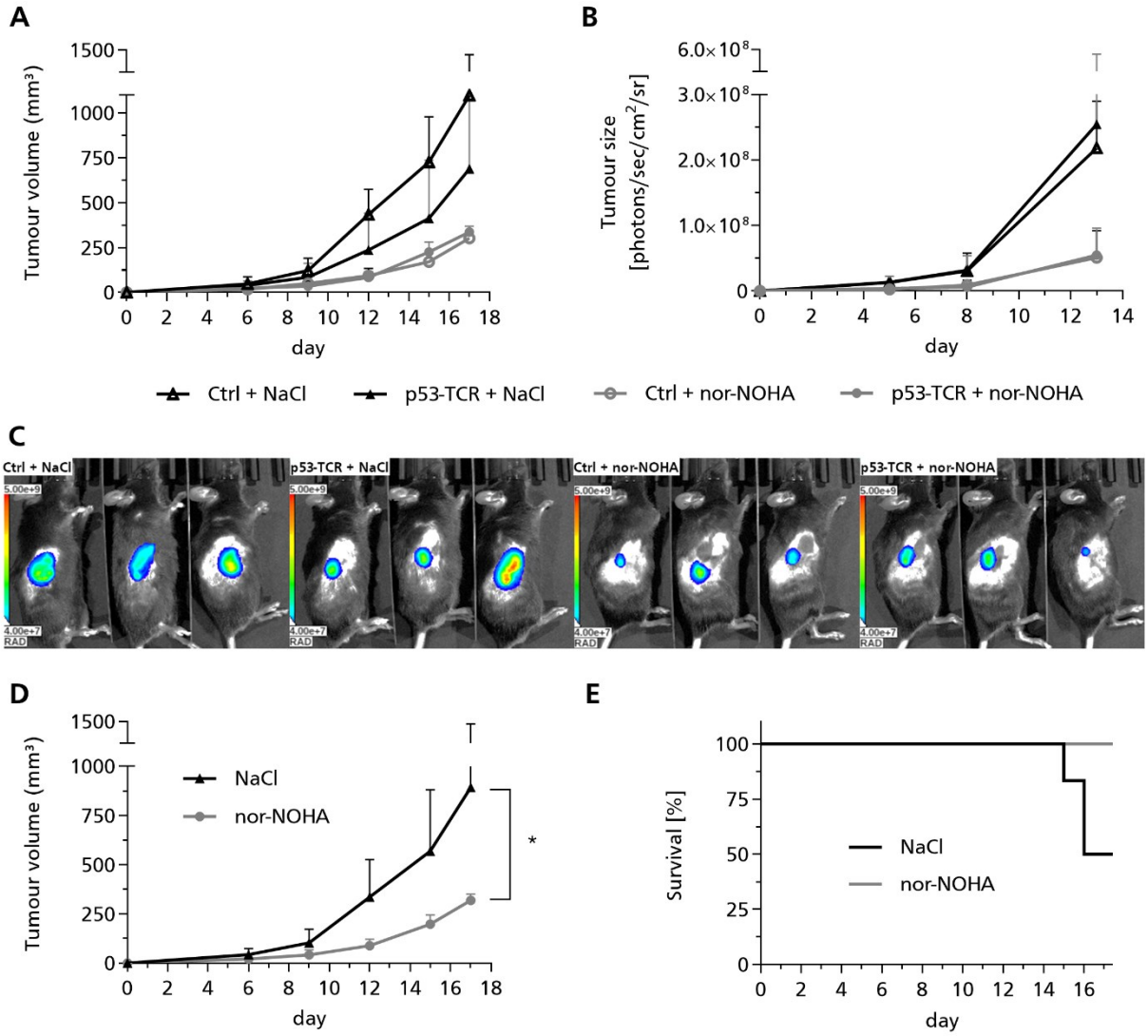

Figure 34: Tumour growth and survival of mice received ACT ± nor-NOHA treatment
Mice were organized in four groups (n=3) to study the impact of ACT and nor-NOHA treatment on tumour growth. T cells were transduced with Katushka and used as controls. **(A)** Tumour volume was determined by calliper measurement and in addition, **(B)** tumour growth was monitored by luminescence detection starting with tumour inoculation at day 0. **(C)** Luminescence measurement of tumour mass via IVIS reflecting metabolically active tumour cells at day 13. **(D)** Comparison of tumour volume (calliper measurement) in ± nor-NOHA treated animals independent of T cells and **(D)** survival analysis of those mice (n=6). Data are represented as mean ± SD. * $p<0.05$

For further analysis of the effect of nor-NOHA treatment *in vivo*, tumour infiltrating immune cells were characterized by flow cytometry. Mice were sacrificed after reaching defined tumour volume (endpoint: 1000 mm^3) and tumour mass was investigated for the presence of MDSCs, macrophages and T cells. As the focus of this experiment was on the inhibition of arginase I by nor-NOHA, we were interested whether nor-NOHA not only blocks arginase activity, but also affects arginase expression of immune cells. Therefore, tumour-associated M-MDSCs (defined as $CD11b^+$ $Ly6C^+$ $Ly6G^-$) [Figure 35A] as well as TAMs ($CD11b^+$ $F4/80^+$) [Figure 35B] were characterized for arginase expression. In mice treated with nor-NOHA, the percentage of cells expressing arginase within the MDSC- (~38 %) and macrophage-subset

(~59 %) was significantly lower compared to NaCl treated mice (~55 % and ~88 % respectively). Also, the expression levels (MFI) of arginase in both cell populations were reduced (MDSCs: 2.6-fold, TAMs: 3.7-fold) in nor-NOHA treated animals. Furthermore, the extent of tumour infiltrating CD3 positive T cells was analysed and showed a tendency (p=0.2) towards a stronger infiltration in mice treated with nor-NOHA (roughly 1.7-fold more). Here we compared only the two groups which received p53 antigen specific-TCR T cells [Figure 35C].

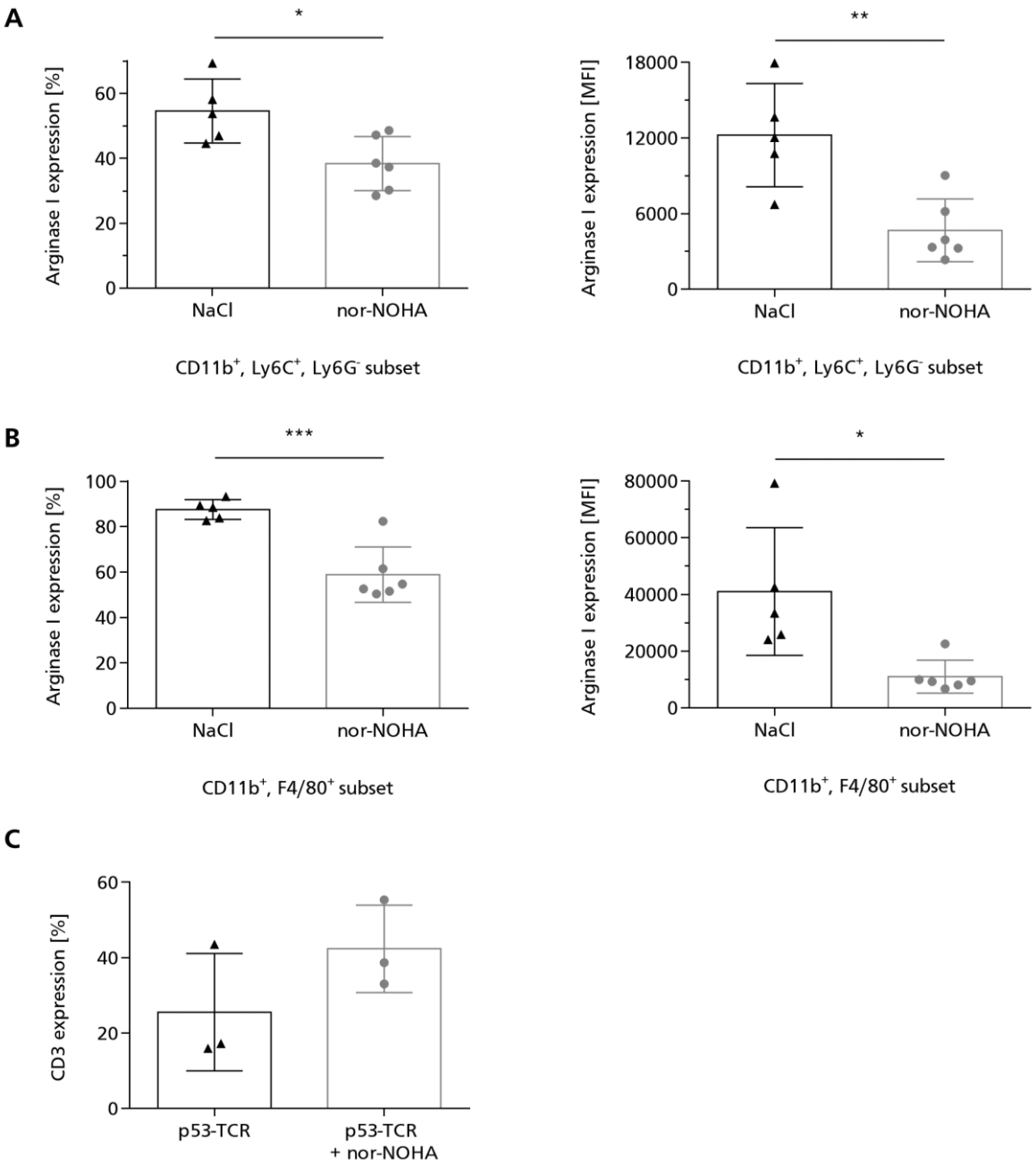

Figure 35: Tumour infiltrating immune cells and arginase I expression
Tumour mass was prepared as single cell suspension for FACS analysis. Arginase I expression in **(A)** M-MDSCs and **(B)** macrophages was investigated. Fractions of cells (%) expressing arginase I as well as expression levels (MFI) of arginase I were analysed. n=5-6; Data are represented as mean ± SD. * $p<0.05$, ** $p<0.005$, *** $p<0.0005$ **(C)** Tumour infiltrating T cells ($CD3^+$) were compared in animals treated with p53 specific T cells ± nor-NOHA treatment. n=3; Data are represented as mean ± SD.

In addition, spleen-infiltrating/resident MDSCs ($CD11b^+$, $Gr\text{-}1^+$) and cytotoxic T cells ($CD8^+$) were analysed. In line with tumour infiltrating M-MDSCs, splenic MDSCs proved to have a tendency towards reduced arginase expression in mice treated with nor-NOHA [Figure 36A]. Nor-NOHA treated animals had 2-fold reduced arginase expression (MFI) in MDSCs and only ~8 % of cells expressed arginase I compared to ~24 % in NaCl treated animals. Comparing the two groups of mice which received p53 specific T cells, FACS analysis revealed significant higher amounts (~2-fold) of CD8 positive cells in spleens of nor-NOHA treated animals [Figure 36B]. A tendency towards increased CD4 cells as well as total CD3 positive cells in spleens of nor-NOHA treated animals [results not shown] complete the picture of splenic T cells in this *in vivo* experiment.

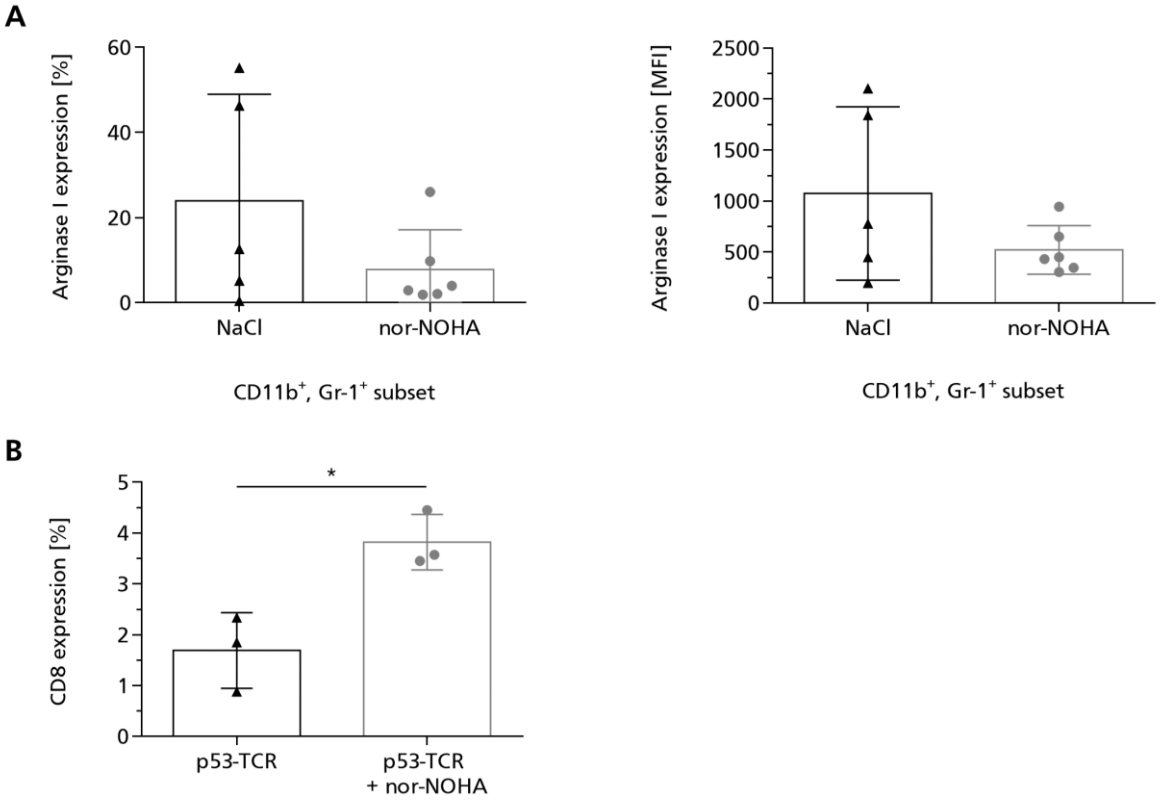

Figure 36: Splenic MDSC fractions and cytotoxic T cells
Spleens of tumour bearing mice were analysed for arginase I expressing MDSC fractions **(A)** and infiltration of cytotoxic ($CD8^+$) T cells **(B)** by FACS staining. **(A)** Animals treated with NaCl were compared with animals treated with nor-NOHA regardless of T cells. Amount of arginase I expressing cells is indicated in % and total expression levels (MFI). n=5-6 **(B)** Infiltrating CD8 positive T cells were compared in mice which received peptide specific (p53) T cells ± nor-NOHA treatment. n=3; Data are represented as mean ± SD. * $p<0.05$

The total arginase protein expression within the tumour mass was investigated by western blot analysis and revealed a tendency (p=0.094) towards reduced arginase expression (3.5-fold) in tumours of nor-NOHA treated mice as compared to control animals [Figure 37A, B]. These findings were supported by arginine measurements in plasma. Via LC-MS, arginine was detected in plasma samples of NaCl versus nor-NOHA treated mice [Figure 37C]. The trend pointed towards increased plasma arginine levels in nor-NOHA treated animals.

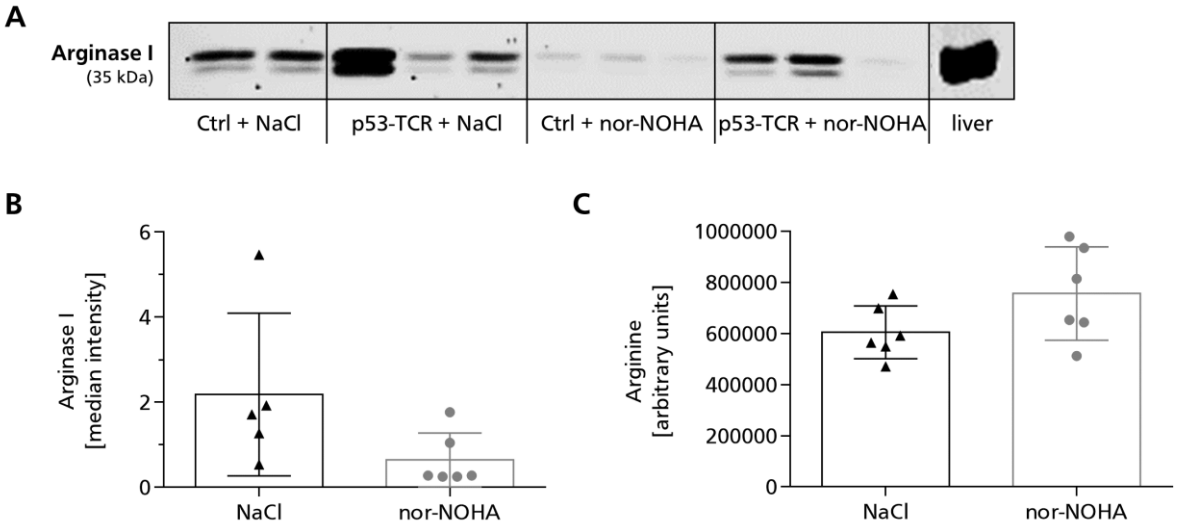

Figure 37: Total tumour arginase I quantity and plasma arginine levels
(A) Arginase I quantity in tumour lysates was investigated by western blot and liver lysate was used as positive control. **(B)** Pan Akt was used as housekeeping gene for calculation and quantification analysis (p=0.094). **(C)** LC-MS was performed to measure arginine in plasma samples (p=0.108). n=5-6; Data are represented as mean ± SD.

Taken together, nor-NOHA seemed to have a strong impact on the MC38_p53 tumour antigen model. A clear reduction in tumour growth and therefore a therapeutic benefit became obvious in nor-NOHA treated animals. Furthermore, a decreased arginase expression in tumour-infiltrating inhibitory immune cells and a tendency towards increased arginine levels in the plasma were detected in those animals. However, no effect of tumour antigen specific T cells was observed, neither in single treatment nor in combination with nor-NOHA.

4.6.2. MC38_OVA tumour and OT-1 T cells

To further extend and validate our findings we performed a second *in vivo* experiment. Therefore, we used a different well-established setting to test our strategy in a different tumour-antigen model. We used the MC38 cell line genetically engineered to express GFP and an ovalbumin peptide ($OVA_{257-264}$; SIINFEKL) on its surface (short: MC38_OVA). As effector T cells we used SIINFEKL-TCR specific OT-1 T cells which were derived from OT-1 transgenic mice. Mice were organized into the following four groups (n=5): (I) control T cells + NaCl, (II) OT-1 T cells + NaCl, (III) control T cells + nor-NOHA, (IV) OT-1 T cells + nor-NOHA. T cells from $CyA2K^b$ mice were used as controls and 10 mio T cells per mouse were injected. Tumour growth of MC38_OVA cells was measured with a calliper [Figure 38A] starting with tumour inoculation at day 0. Mice which received tumour specific OT-1 T cells showed significant lowered tumour volume after 22 days compared to mice which received control T cells [Figure 38A]. However, there was no synergistic effect in combining OT1- T cells and nor-NOHA. Those animals had no advantage over mice which received OT1-T cells and NaCl. For those two groups reduced tumour growth was independent of nor-NOHA treatment but dependent on tumour antigen specific T cells which is in sharp contrast to the previous model. Also, the survival curve at day 26 showed a prolonged survival of animals which received OT-1 T cells (dotted lines). Whilst no animals were alive in the group treated with control T cells and nor-NOHA, 60 % (n=3) were still alive in the OT1-T cells + nor-NOHA treatment group. In the NaCl groups (black lines), the effect of tumour specific T cells was even more striking (100 % versus 20 % survival). However, best survival was seen in animals which received OT1-T cells and NaCl (100 %) [Figure 38B]. Therefore, nor-NOHA seemed to have a negative impact on survival in this experiment [Figure 38B] which was additionally clearly supported by the difference in tumour growth comparing group I and III [Figure 38A]. Here, nor-NOHA treatment seemed to worsen tumour growth.

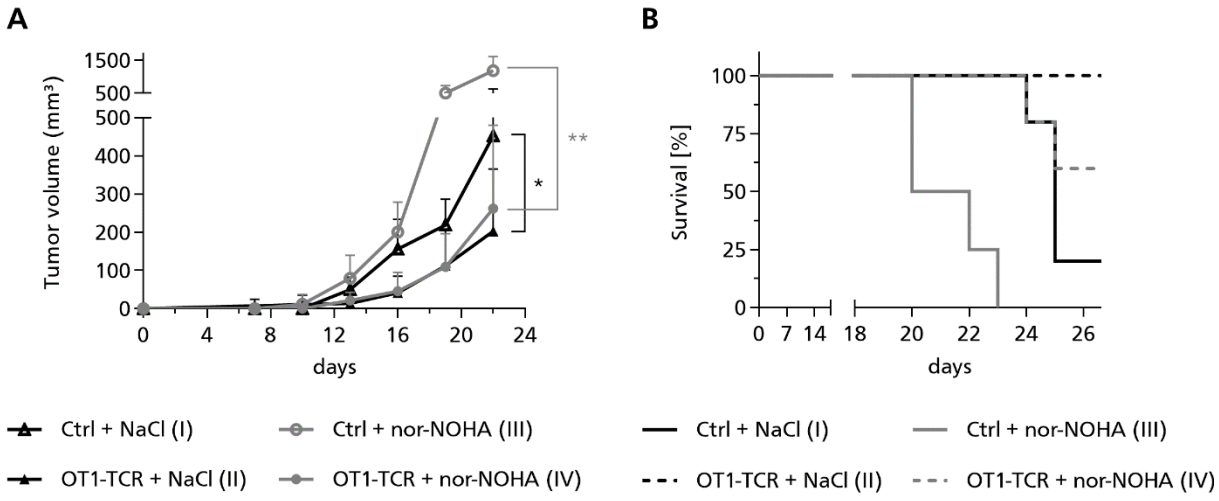

Figure 38: Tumour growth and survival of mice received ACT ± nor-NOHA treatment
Mice were organized in four groups (n=5) to study the impact of ACT and nor-NOHA treatment on tumour growth. T cells derived from CyA2K^b mice were used as controls. **(A)** Tumour volume was calculated by calliper measurement starting with tumour inoculation at day 0. **(B)** Survival analysis of mice 26 days after tumour inoculation. Data are represented as mean. * $p<0.05$, ** $p<0.005$

Two weeks after ACT, blood samples were taken and circulating T cells were investigated by FACS staining. A tendency towards more CD8$^+$ T cells in the periphery of both groups which received OT-1 T cells was observed resulting in ~7 % CD8$^+$ T cells in the OT-1 ACT groups versus ~3 % in the control ACT groups [Figure 39A]. In contrast, distribution of CD4$^+$ T cells was equal in all 4 groups ranging around 9 % [Figure 39B]. In addition, no clear effect of nor-NOHA treatment on the frequency of circulating CD8 and CD4 T cells was visible.

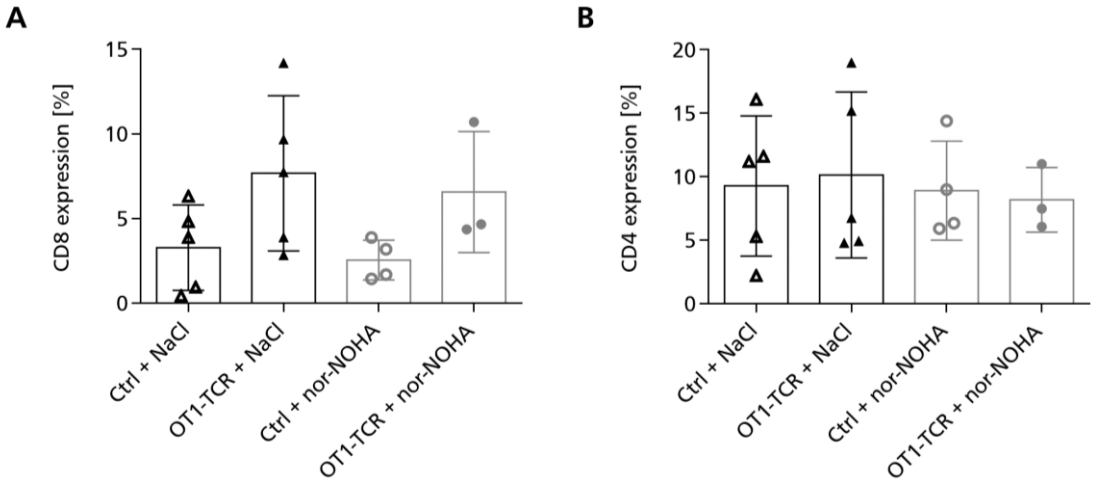

Figure 39: Investigation of circulating cytotoxic T cells in the blood
Mice were bled 2 weeks after ACT and blood samples were analysed by FACS measurement. Percentage of **(A)** CD8 and **(B)** CD4 positive cells are shown, gated on total viable cells. n=3-5; Data are represented as mean ± SD.

For further insights into the cell distribution and the potential contribution of nor-NOHA to arginase I expression *in vivo*, tumour infiltrating immune cells were characterized by FACS analysis. Mice were sacrificed after reaching defined tumour volume (endpoint: 1000 mm^3) and tumour mass was investigated for the presence of M-MDSCs ($CD11b^+$, $Ly6C^+$, $Ly6G^-$), macrophages ($CD11b^+$, $F4/80^+$) and cytotoxic T cells ($CD8^+$, $V\alpha2^+V\beta5^+$). We investigated only the groups which received peptide specific OT-1 T cells and compared NaCl vs nor-NOHA treatment. With regard to arginase I expression, a shift towards more arginase I positive cells with higher expression levels (~2-fold increase of MFI) in nor-NOHA treated animals, both in MDSCs [Figure 40A] and macrophages [Figure 40B] was observed. Due to low number of samples, statistical analysis was not possible. Nevertheless, those results are in contrast with the outcome of our previous *in vivo* experiment regarding the effect of nor-NOHA. Furthermore, nor-NOHA treatment showed no effect on the percentage and TCR expression of tumour infiltrating cytotoxic T cells [Figure 40C]. Around 10 % of all viable cells were CD8 positive whereof ~ 60 % were positive for the OT1-TCR ($V\alpha2^+V\beta5^+$). Those measurements are confirmed by the analysis of tumour infiltrating CD3 expressing cells showing again no differences between NaCl and nor-NOHA treatment [data not shown].

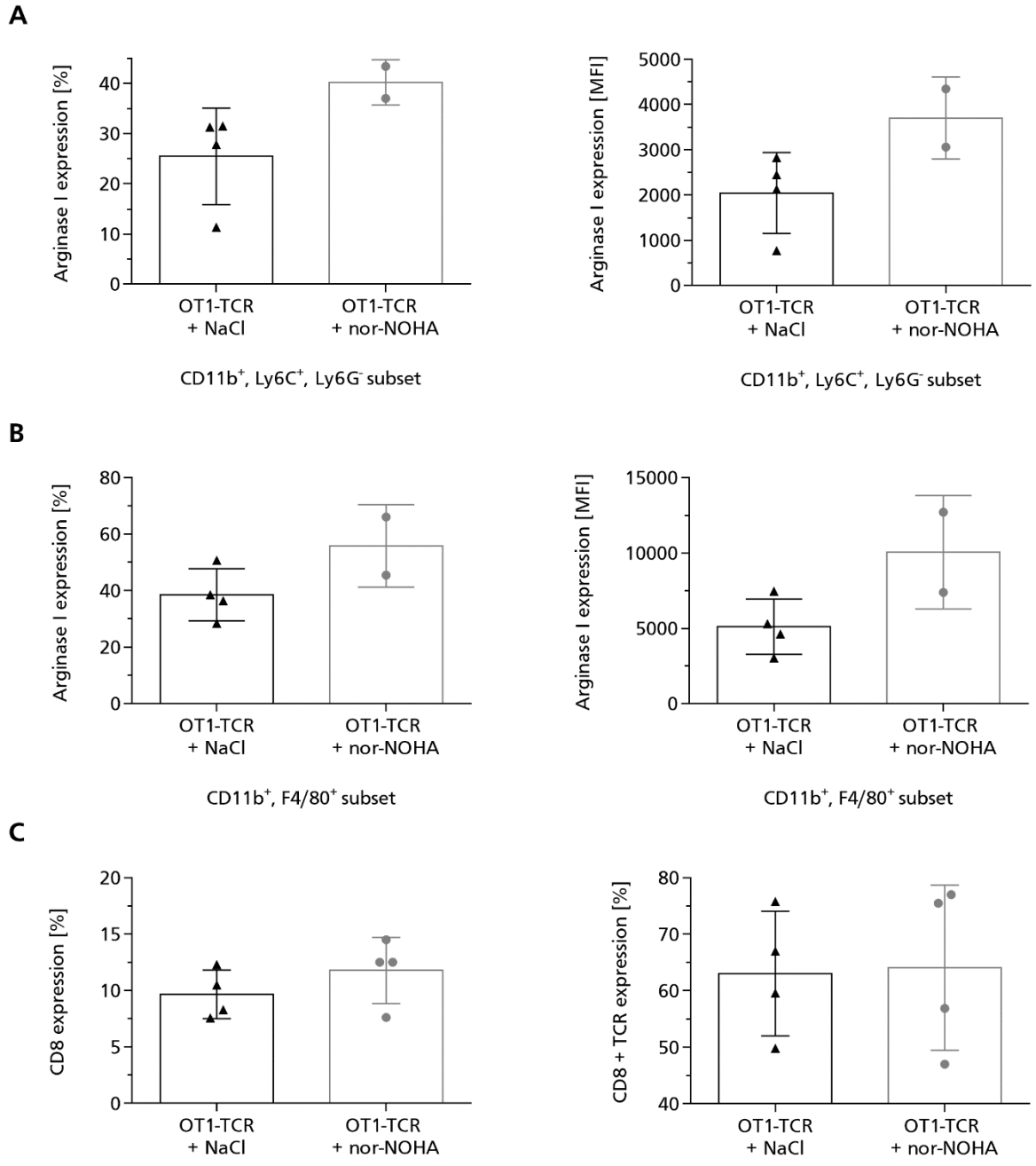

Figure 40: Tumour infiltrating immune cells and arginase I expression
Tumour mass was prepared as single cell suspension for FACS analysis. Arginase I expression in **(A)** M-MDSCs and **(B)** macrophages was investigated. Fractions of cells (%) expressing arginase I as well as expression levels (MFI) of arginase I were determined. n=2/4 **(C)** Tumour infiltrating cytotoxic T cells ($CD8^+$) were compared in animals with ACT of OT-1 specific T cells ± nor-NOHA treatment. n=4; Data are represented as mean ± SD.

Also, the fractions of cytotoxic T cells and especially OT1- T cells in the spleen were determined. In line with the results of tumour infiltrating cytotoxic T cells, FACS analysis revealed no differences in the percentage of CD8 expressing T cells when comparing OT1-T cell groups treated ± nor-NOHA [Figure 41A]. Also, percentage of cytotoxic T cells expressing the OT1-TCR were similar in both groups with a slight increase in NaCl treated animals 26 % vs. 19.5 %) [Figure 41B] suggesting that nor-NOHA treatment had no impact on the distribution of cytotoxic T cells in this experiment.

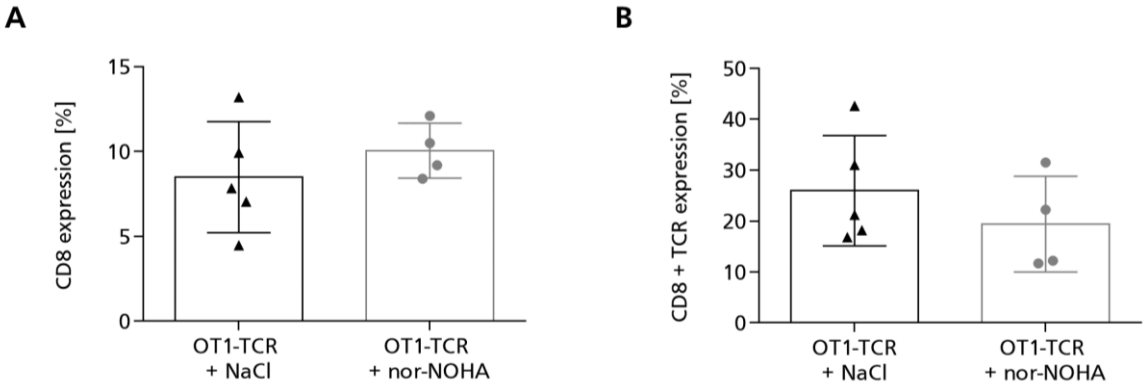

Figure 41: Splenic cytotoxic T cells
Spleens of tumour bearing mice were analysed for infiltrating cytotoxic T cells **(A)** and OT1-TCR expression **(B)** by FACS staining. Mice treated with NaCl were compared with animals treated with nor-NOHA in groups which received peptide specific OT-1 T cells. n=4-5; Data are represented as mean ± SD.

Furthermore, to complete the *in vivo* data, total tumour arginase I protein levels were measured via western blot analysis [Figure 42A]. In the overall comparison between animals treated with NaCl and nor-NOHA, no differences in arginase I levels were detected [Figure 42B]. If only nor-NOHA receiving animals were compared, a clear tendency towards higher arginase quantities in OT-1 T cell treated animals became visible [Figure 42C]. The bands on the blot [Figure 42A] seem to show a clear increase in arginase I expression in animals which received OT-1 T cells. However, this was not significant when arginase I expression levels were reported to the expression of the housekeeping gene Pan Akt. When comparing OT-1 T cell treated mice with mice which received control T cells, no differences in arginase I expression were detected [Figure 42D].

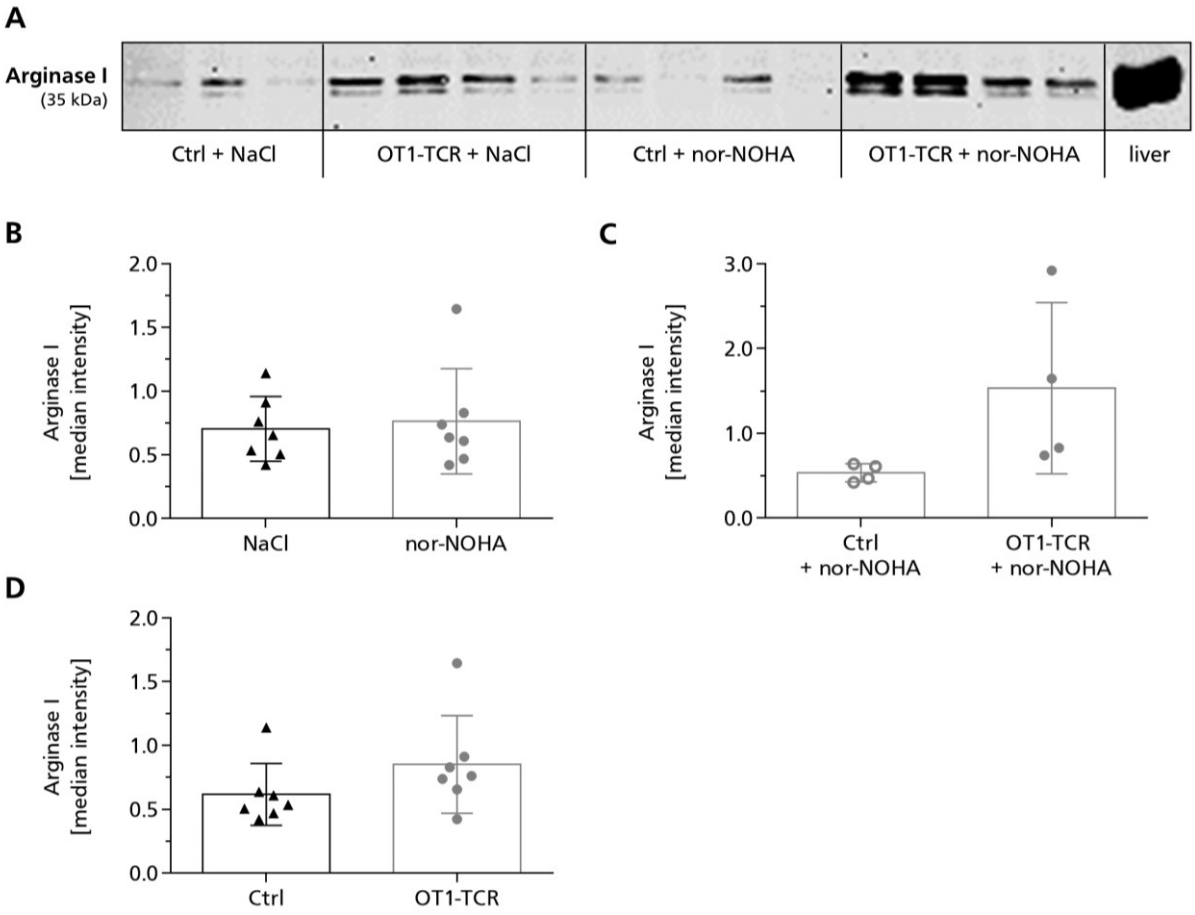

Figure 42: Total tumour arginase I quantity
(A) Arginase I quantity in tumour lysates was investigated by western blot and liver lysate was used as positive control. **(B)** Overall comparison between NaCl and nor-NOHA treated animals. n=7 **(C)** Arginase I levels in nor-NOHA treated animals comparing groups with control T cells and OT-1 T cells. n=4 **(D)** Overall comparison between Ctrl and OT1-TCR treated animals. n=7; Pan Akt was used as housekeeping gene for calculation and quantification analysis. Data are represented as mean ± SD.

Taken together, both *in vivo* experiments revealed contrasting results regarding nor-NOHA effect in combination with ACT of tumour antigen specific T cells. Whilst nor-NOHA seemed to play an important role in the MC38_p53 tumour antigen model with positive effects on impairing tumour growth, improving survival, and reducing arginase I expression, this anti-tumour effect is somehow lost or even slightly shifted towards a negative effect in the MC38_OVA tumour antigen model. Finally, none of the above conducted *in vivo* experiments proved evidence for a synergistic effect of ACT and nor-NOHA treatment as tumour therapy.

5. Discussion

In this study, we investigated the potential effect of nor-NOHA, an arginase inhibitor, in combination with adoptive T cell immunotherapy using *in vitro* and preclinical mouse tumour models. *In vivo* studies showed an inhibition of local tumour growth (lung carcinoma, fibrosarcoma, skin cancer, colon cancer) [141,142,153,154] and reduced arginase expression in tumours [153], serum [154] and MDSCs [141] after nor-NOHA treatment. Therefore, arginase inhibition is a promising strategy for an anti-tumour therapy. As monotherapy with nor-NOHA is not efficient enough in the treatment of cancer, we investigated the combination of nor-NOHA administration and ACT of tumour antigen specific T cells in tumour bearing mice. To that aim, we used an antigen-TCR model previously characterized in our lab. Echchannaoui *et al.* could already demonstrate the efficacy and safety of an HLA-A2.1 restricted single-chain TCR specific for a p53 peptide. T cells equipped with this TCR eradicated $p53^+$ $A2.1^+$ tumour cells in mouse models of ACT. However, only 50 % of mice treated with scTCR-modified T cells could eradicate tumours [55]. In this model, tumours were strongly infiltrated by TAMs and MDSCs known for their suppressive effects against T cells via arginase release in the TME. The above-mentioned combined treatment therapy was investigated in this study, to further boost the anti-tumour reactivity of T cells by targeting arginase I-mediated T cell suppression.

5.1. MHC downregulation

Downregulation of the MHC I complex on tumour cells is widely discussed in literature and reviewed by Garrido *et al.* [144]. This tumour escape mechanism is critical for the underlying treatment strategy as MHC I negative tumour cells are not recognized by TCR-cytotoxic T cells. As a consequence, therapies with immune checkpoint inhibitors like anti-CTLA-4 or anti-PD-1 can only unfold their full potential on boosting T cells if those cells can detect tumour cells via MHC bound peptide presentation. At early stage of tumour development cells remain MHC I-positive and TILs are able to infiltrate and attack the nascent tumour mass. Later, MHC I negative tumour cell variants emerge and the tumour becomes heterogeneous for MHC I expression. Finally, tumour cells become uniformly MHC I negative and TIL infiltration is strongly reduced [144]. To design efficient CTL-mediated treatment strategies in cancer patients it is necessary to analyse the patient's unique tumour MHC I expression.

Mainly alterations in the HLA / β2M genes or in the transcriptional regulation cause MHC loss or downregulation [155]. If tumour cells appear to have structural damages (like mutations or deletions) in MHC encoding genes ("hard" lesions), recovery of MHC expression is impossible. However, alterations in MHC expression caused by deregulation of transcription ("soft" lesions) can be reversed by different types of immune therapies as the treatment with Th1 cytokines for example [156].

In the first model, MEF tumour cells (MEF_p53$^{-/-}$_A2K^{b}_Mut.4_Cl.3_GFP) cultured *in vitro* showed a downregulation of the MHC I complex over time, which precluded further *in vivo* application. To overcome this downregulation on tumour cells we designed and generated a single chain construct of the MHC I molecule with a linked p53 peptide [Figure 48]. Although this does not mirror a physiological situation, the model was considered as proof of concept to evaluate our therapeutic strategy. This construct was further used to engineer MC38 cells and turn those cells into target cells for TCR recognition. Those tumour cells were strongly recognized and killed by antigen-specific TCR T cells whereas parental MC38 wild type cells were not recognized [Figure 18]. In further experiments, the specific binding and recognition of the p53-TCR to the single chain MHC I construct was demonstrated [Figure 20].

5.2. Nor-NOHA treatment *in vitro*

Arginine is essential for T cell function and their metabolism. L-arginine is avidly taken up by activated T cells and T cells with increased L-arginine levels exhibit improved anti-tumour response. In line, T cell survival is negatively affected by reduced availability of intracellular L-arginine [120]. Therefore, different strategies were investigated to overcome arginine degradation in the TME mediated by arginase I release by tumour-infiltrating suppressive cells (TAMs, MDSCs). Main research, to sustain arginine levels, focuses on two strategies: arginine supplementation or arginase inhibition. Early mouse studies with intravenous or enteral supplementation of L-arginine revealed retarded tumour growth [157–160]. In addition, MDSC frequencies were significantly reduced in an arginine supplemented breast cancer mouse model. Tumour growth was inhibited and the innate and adaptive immune response were increased [161]. It was demonstrated that mice fed with L-arginine recovered three times more TCR transgenic T cells in draining lymph nodes compared to control animals [120]. Similarly, Heys *et al.* demonstrated an enhanced infiltration of lymphocytes with anti-tumour properties in L-arginine supplemented patients with colorectal cancer [162].

In contrast, in a recently published study arginine supplementation in colorectal cancer patients had no positive effect on immunosuppression and no effect especially on the frequency of suppressor cells (M-MDSCs) [163]. Those studies show that arginine metabolism in humans is complex and pharmacokinetics of L-arginine in cancer patients is not well understood. Arginine supplementation and circulatory availability is reduced by extensive arginine metabolism by gut and liver arginase [121]. After intestinal absorption, arginine is catabolized by enterocytes [164]. A strong renal clearance of arginine after i.v. administration was measured as high concentrations of arginine exceed renal threshold for reabsorption [165]. Therefore, only a transient increase of L-arginine plasma concentration was reached after dietary intake [165]. All those aspects demonstrate the challenge of reaching high arginine availability in the TME. In addition, liberated arginase from MDSCs and M2-TAMs metabolises free arginine in the TME [112]. Based on the fact that arginine supplementation as monotherapy in cancer patients appears to be challenging, we decided to use arginase inhibition as therapeutic approach in combination with ACT. Many studies provided positive outcomes in anti-cancer treatments when arginase inhibitors were included. Inhibitors like nor-NOHA, CB-1158 or OATD-02 provided promising preclinical data when treating different cancer types like breast, colon, lung, ovarian cancer, and others in *in vivo* murine models [166]. In addition, first clinical studies were conducted to test the safety and efficacy of CB-1158 in patients mainly with advanced solid tumours. Thereby, monotherapy as well as combination of CB-1158 and checkpoint inhibition was investigated [167]. The inhibitor OATD-02 is currently also tested in a clinical trial to evaluate safety and tolerability in patients with solid tumours [168]. For further evaluation, we investigated the impact of nor-NOHA treatment on T cells and tumour cells (MC38_p53) *in vitro*. As nor-NOHA is an arginine analogue, the question arose whether the inhibitor is taken up by the cells and blocks intracellular arginase leading to altered T cell and tumour cell functions. Geiger *et al.* demonstrated that nor-NOHA led to increased intracellular L-arginine levels and reduced ornithine, putrescine, spermidine, and proline concentration in human T cells. Consequently, they concluded that L-arginine in T cells is mainly catabolized through arginase. As the cytosolic enzyme arginase I was not detected in T cells, which is in line with our findings (data not shown), the conversion of L-arginine in T cells is likely through mitochondrial arginase II [120]. It was additionally demonstrated that high intracellular L-arginine shifted T cell metabolism from glycolysis toward mitochondrial oxidative phosphorylation. This resulted in a drift towards central memory like T cells with enhanced anti-tumour activity [120].

In our study, long term treatment revealed no changes in immune checkpoint expression [Figure 22] and proliferation and only a slight reduction in killing capacity [Figure 23] of antigen specific T cells *in vitro*. Those results are in line with earlier publications showing no effect on proliferation of T cells [120,148].

On the other hand, arginine treatment reduced tumour cell proliferation in patients with colorectal adenocarcinoma [118]. This effect was linked to increased NO concentrations in the serum, as high NO concentrations have been reported to induce cytostasis and cytotoxicity in some tumour cells [169]. As nor-NOHA treatment revealed reduced MC38_p53 proliferation in our experiments [Figure 19B], it would be interesting to investigate intracellular arginine and NO levels. As explained in Figure 6, NO is metabolized from arginine via NOS. With intracellular arginase inhibition, more arginine could be available for NO production by NOS. In renal cell carcinoma cell lines (CL2, CL19, Renca), arginase expression was analysed. All three cell lines expressed arginase II while arginase I was not expressed at all [170]. Similarly, also in MC38_p53 cells no arginase I expression was detected (data not shown). The CL19 cell line expressed significantly higher arginase II levels and enzyme activity (increased ornithine) compared to CL2 and Renca cells. In contrast, CL2 and Renca cells significantly reduced L-glutamine levels in the medium in comparison to CL19 cells after 72 hrs. The authors inferred that CL2 and Renca cells metabolize ornithine, needed for cell growth, by converting L-glutamine to L-glutamate and thereby bypassing arginase for the production of ornithine. Therefore, only CL19 cells reacted to nor-NOHA treatment by a significant reduction in cell proliferation [170]. Those findings are supported by Singh *et al.* as they published similar results by investigating arginase expression in breast cancer cell lines [171]. In comparison, also our MC38_p53 cells revealed a significant reduction in cell proliferation when cells were cultured in 1 mM nor-NOHA [Figure 19B]. To further characterise the MC38_p53 cell line and its intracellular arginine metabolism, it would be necessary to investigate arginase II expression and intracellular NO production in those cells. Our results, in this specific experimental model (MC38_p53 cells and p53sc TCR T cells) demonstrated that nor-NOHA treatment *in vivo*, could support enhanced killing capacity of T cells and in addition directly inhibit tumour growth.

5.3. Arginine deficiency on T cells and tumour cells

To confirm previously published findings, we investigated the impact of arginine deficiency on murine T cells and tumour cells in our experimental models. Human PMNs were pre-incubated in medium to metabolise arginine in the medium by PMN released arginase I. T cells cultured in arginine low medium showed almost no proliferation. This inhibition in proliferation could be rescued by the supplementation of arginine or by nor-NOHA which was added when PMNs were pre-incubated [Figure 26A]. In addition, a downregulation of the p53-scTCR was observed [Figure 27]. Those are established effects of arginine deprivation on T cells [112]. It is important to mention, that TIGIT and especially PD-1 were upregulated on T cells when cultured in arginine low medium *in vitro* [Figure 27]. This needs to be considered for further evaluation for combinatorial treatment strategies (i.e. immune checkpoint inhibitors). This approach is already tested in clinical studies where the orally available small-molecule compound CB-1158 (arginase inhibitor) is being tested in combination with immune checkpoint inhibitors in solid tumours [131,172] and multiple myeloma [173]. In the present study, we could clearly demonstrate that arginine deficiency reduced T cell killing capacity which was rescued by the addition of nor-NOHA or fresh arginine [Figure 30]. Those results demonstrated that nor-NOHA treatment *in vitro* was able to efficiently block arginase I activity and thereby restored T cell proliferation, TCR expression and killing capacity. In collaboration with the research team of Prof. Munder (co-principal investigator in this CRC1292 TP06 funded project) we further investigated the effect of human PMNs on murine T cells. The group recently published their findings where they demonstrated a yet not elucidated mechanism by which supernatant of human PMNs induced hyper proliferation of human T cells in the presence of an arginase inhibitor [148]. In our setup with human PMNs and murine T cells we were not able to confirm those findings. Interestingly we could detect a significantly increased proliferation of T cells in PMN-SN + 10 mM arginine which was not seen in control medium + 10 mM arginine [Figure 26]. This increase in proliferation was also observed when murine T cells were co-cultured with human PMNs + 10 mM arginine in a cell-cell contact assay. In those co-culture experiments a tendency towards an increase in T cell proliferation was observed with increasing PMN to T cell ratio. But only T cells cultured with the highest concentration of PMNs + 10 mM arginine revealed significant higher proliferation capacities [Figure 31]. However, this combination was not able to rescue tumour killing capacity of T cells in a direct co-culture assay.

Those results demonstrated that other mechanisms of PMNs in direct co-culture block T cell killing capacity which couldn't be overcome by excess of arginine. Despite the fact, that we used human PMNs and murine T cells and tumour cells it is worth investigating further those inhibitory mechanisms. As human and mouse PD-L1 share similar molecular structures [174], the PD-L1/PD-1 pathway could be the reason for inhibition of T cells resulting in reduced killing capacity. It was shown that peritumoural neutrophils regulate immunity via this pathway [175]. Therefore, a further phenotypic characterisation of PMNs and T cells in this assay could give information about the surface expression of PD-1 and PD-L1. In addition, PD-1/PD-L1 inhibitors could be used in the assay to verify this assumption. If it turns out that the PD-1/PD-L1 axis is affecting T cell killing capacity in this setup it still wouldn't explain why we see no suppression in a cell-cell contact proliferation assay. It was shown, that T cell proliferation was blocked when co-cultured with murine MDSCs independent of arginase I expression suggesting other additional mechanisms being responsible for the suppressive capacity of murine MDSCs [176]. Furthermore, it was evidenced, that suppression is cell contact dependent, as co-culture of T cells and arginase negative MDSCs in transwell plates failed to suppress T cell proliferation. Finally, blocking PD-L1 did not rescue proliferation in direct co-culture proving that other direct cell-cell contact mechanisms were responsible for MDSC mediated inhibition of proliferation [176]. It is obvious that human PMNS can't be compared with murine MDSCS in those assays and therefore it is difficult to discuss our results.

Nevertheless, the question persists why proliferation of murine T cells cultured in supernatant of human PMNs in the presence of an arginase inhibitor was not positively affected as compared to human T cells. Therefore, it remains unclear and further research is needed to uncover the PMN-secreted factor(s) which is/are boosting human T cell proliferation in this setup but not murine T cells.

5.4. Investigation of ACT and nor-NOHA treatment *in vivo*

Our group could already demonstrate the antitumour efficacy of the p53-scTCR *in vivo* [55]. When antigen-specific T cells were simultaneously injected with tumour cells, 50 % of mice could eradicate tumours resulting in a prolonged tumour-free survival [55]. However, when ACT was conducted in mice with established tumours, only a delay in tumour growth was observed but no control or eradication of the tumour.

To improve ACT, we focused on the inhibition of arginase I. The results discussed above demonstrated the positive impact of the arginase inhibitor nor-NOHA *in vitro*. In our first in vivo setup [4.6.1], we could only detect a slight delay in tumour growth in mice receiving ACT. This difference was only evident when tumour size was measured by a calliper [Figure 34A] and became negligible in luminescence-based tumour measurement [Figure 34B, C]. Nevertheless, the combination of ACT and nor-NOHA treatment further reduced tumour growth clearly. Surprisingly, nor-NOHA treatment alone was as efficient as in combination with ACT. Those results demonstrated a positive effect of nor-NOHA treatment on tumour growth whereas ACT had no effect. It seems likely, that nor-NOHA had a direct effect on tumour cell proliferation also *in vivo* as we demonstrated it already in our *in vitro* experiments [Figure 19B]. Therefore, it is important to further characterize the intracellular arginase and NOS expression and the effect of nor-NOHA on those pathways especially in the MC38 tumour cell line. Those results are necessary to better understand the underlying mechanisms leading to reduction in tumour cell growth *in vitro* and *in vivo* under nor-NOHA treatment. Globally, nor-NOHA treatment significantly reduced tumour growth and survival of nor-NOHA treated mice was clearly prolonged [Figure 34D, E]. Additionally, it was demonstrated that overexpression of arginase I in ovarian carcinoma cells led to an increased tumour progression in mice in comparison to unmodified tumour cells. When mice were treated with the arginase inhibitor OATD-02, tumour growth was significantly reduced [177]. In line, arginase mediated suppression of adoptively transferred OT-1 T cells was partially reverted in OATD-02 treated mice. However, the combination of ACT and arginase inhibition in the context of an established tumour is missing in this publication [177]. Hu *et. al* tested the combination of ACT and docetaxel, a chemotherapeutic agent inhibiting MDSC function. In two mouse tumour models (colon cancer and mammary carcinoma) they demonstrated that ACT and docetaxel synergistically inhibited tumour growth [178]. Another publication by Sierra *et. al* further supports the idea of dual ACT and arginase inhibition. By combining ACT and the anti-Jagged1/2 blocking antibody CTX0145, tumour growth was decreased, and MDSC activity was inhibited due to reduced expression of arginase I and iNOS. The study highlighted, that anti-Jagged therapy increased the infiltration of reactive $CD8^+$ cells into tumours and thereby enhanced the efficacy of T cell-based immunotherapy [179].

It was evidenced, that macrophages are the predominant source of arginase in the MC38 model and that a progressive accumulation of arginase positive myeloid cells takes place [180]. Therefore, further analysis of tumour infiltrating immune cells in our mouse model was performed. In nor-NOHA treated mice, a significant reduction in arginase I-expressing MDSCs as well as macrophages was measured which supported our strategy [Figure 35A, B]. Those results were confirmed by the findings of Rodriguez *et al.* showing a reduced arginase I expression in tumour associated myeloid cells after nor-NOHA treatment [141]. A tendency towards more CD3 positive cells in ACT + nor-NOHA treated animals was observed when compared with ACT alone [Figure 35C]. This tendency was supported by a significant increase of cytotoxic $CD8^+$ T cells in the spleen [Figure 36B].

We could demonstrate that nor-NOHA treatment was significantly reducing tumour growth but was not able to fully control and reject the tumour. Despite less arginase in the tumour microenvironment, higher plasma arginine concentration [Figure 37C] and more tumour infiltrating T cells, no synergistic effect of nor-NOHA treatment and ACT was observed. This could be explained by the low TCR expression of transferred T cells. As transduction efficiency was around 20 % [data not shown], the high TCR^- to TCR^+ ratio could implicate an *in vivo* overgrowth of TCR negative T cells. Furthermore, around 10 % of TILs were TCR positive on average at the end of the experiment [data not shown], suggesting a poor infiltration of tumour-specific T cells. In addition, the fitness of transferred T cells may have contributed to this low anti-tumour response. To verify this statement, one would need to investigate in more detail the TIL phenotype by including the analysis of exhaustion markers. Another factor could be the increased expression of immune checkpoints, as we observed in this model a high PD-1 expression on TILs and high PD-L1 expression on tumour cells *in vivo* [data not shown]. This well-known tumour suppressive mechanism may have played a role in inhibiting T cell proliferation and function and could be further investigated by blocking the PD-1/PD-L1 axis in this tumour model. Lastly, downregulation of the MHC complex and thereby reduced peptide presentation by the tumour cells could be an additional factor that affected the outcome of ACT.

To further investigate our treatment approach, an additional *in vivo* experiment was conducted. We used the MC38 cell line genetically engineered to express an ovalbumin peptide ($OVA_{257-264}$; SIINFEKL) on its surface. Peptide specific OT-1 T cells were isolated from OT-1 transgenic mice and used as antigen effector cells for ACT in this setup. As opposed to the previous model, 100 % of injected T cells were antigen-specific TCR positive.

In contrast to the above discussed *in vivo* experiment, tumour growth was significantly reduced in animals which received peptide specific OT-1 T cells. Whereas nor-NOHA treatment even accelerated tumour growth in control T cell groups [Figure 38A]. This became more prominent when survival of animals was investigated. Nor-NOAH treatment resulted into a reduced survival rate of animals compared to animals which received T cells only [Figure 38B]. Two weeks after ACT, proportions of circulating cytotoxic T cells ($CD8^+$) in the peripheral blood were increased in OT-1 treated mice compared to control animals regardless of nor-NOHA treatment [Figure 39A]. The increase in $CD8^+$ T cells in OT-1 T cell treated animals could be explained by the fact, that those cells recognized their cognate antigen, were stimulated and proliferated whereas control T cells received no TCR specific stimulus. However, nor-NOHA treatment seemed not to further boost this proliferation. In this experimental setup OT-1 T cells delayed tumour growth but could not fully eradicate the tumours. Nor-NOHA treatment showed no positive synergistic effect on tumour growth in combination with tumour antigen specific T cells [Figure 38A]. Furthermore, nor-NOHA treatment did not impact the frequency of cytotoxic OT-1 T cells infiltrating the spleen [Figure 41] and the tumour [Figure 40C] and even slightly shifted arginase I expression in tumour infiltrating MDSCs and macrophages towards higher expression levels [Figure 40A, B]. Those results were in sharp contrast to our earlier findings where nor-NOHA positively affected the outcome of the *in vivo* experiment and showed a strong impact on arginase I expression. The absence of a synergistic effect of nor-NOHA plus OT-1 T cells on tumour growth after 22 days could be explained by the hypothesis that OT-1 T cells alone were already strongly hampering tumour expansion and thereby potential positive effects of nor-NOHA treatment were not visible yet. To investigate this hypothesis, we may need to compare OT-1 TCR receiving mice ± nor-NOHA injection for a longer time to detect eventual benefits of nor-NOHA treatment at later time points. Nevertheless, it remained unclear why there were no noticeable or even negative effects of nor-NOHA on arginase expression and distribution of cytotoxic T cells in this experiment.

It was shown that different tumour models react differently to the anti-arginase inhibitor CB-1158 [181]. However, it was already proven that the MC38_OVA tumour model responded to arginase targeted treatment strategies [182,183]. Other *in vivo* experiments clearly demonstrated arginase related inhibition of proliferation of adoptively transferred OT-1 T cells. This inhibition was partially reverted by the arginase inhibitor OATD-02 [177].

As we have not performed any *in vitro* experiments to investigate the effect of nor-NOHA on MC38_OVA and OT-1 cells we cannot draw any conclusion from those results. Differences in arginase and NOS expression between our MC38_p53 and MC38_OVA cell lines could lead to different reactions to nor-NOHA treatment *in vitro* and *in vivo*. Further investigations in this direction would be necessary and could help to better understand the outcome of the conducted *in vivo* experiment. The absence of a significant effect of nor-NOHA in the OVA model could be the result of an already dramatically lowered arginase I expression in tumour infiltrating cells when comparing control conditions to the p53 model. Arginase I expression was roughly 50 % less in MDSCs (25.5 % vs. 54.5 %) and macrophages (38.5 % vs. 87.5 %) compared to the p53 model [Figure 40A, B vs. Figure 35A, B]. Yet, values for nor-NOHA treated groups are comparable in both cell populations (~40 % in MDSCs and ~60 % in macrophages). Therefore, arginase I might had a very low contribution in this experimental model and T cell function was therefore not affected. To test this hypothesis, it would have been interesting to measure total tumour arginase levels (concentration or total quantity) and even more important to analyse the enzymatic activity of tumour arginase. Yet, the mechanism by which arginase I is expressed in MDSCs is widely discussed with different results. T cell produced cytokines as well as tumour-released factors can have an effect on arginase I expression in MDSCs. However, controversial study results ruled out the one or the other option dependent on the experimental model [184–188]. In the MC38 tumour model it was shown, that bone marrow derived MDSCs were arginase I negative whereas myeloid cells from tumour tissue and spleen displayed strong arginase I expression. Interestingly, bone marrow derived MDSCs proved to have the same T cell inhibitory capacity compared to arginase I positive tumour and spleen MDSCs. Tumour cells had no capacity to induce arginase I expression in bone marrow derived MDSCs whereas TCR stimulated T cells were able to trigger arginase I expression in MDSCs. In this model, mainly IL-4 and IL-10 were critical cytokines necessary to induce arginase I expression, via JAK-STAT signalling, whereas IL-17 and / or IFNγ weakened the induction [176].

Different cytokine portfolios of our T cells (p53 vs. OT-I T cells) could explain the differences in arginase I expression in MDSCs [Figure 40A vs. Figure 35A]. However, MDSC mediated inhibition of T cell proliferation was shown to be arginase I independent, but cell contact dependent [176]. This could partially explain the inefficiency of nor-NOHA treatment in the OVA-tumour model but not the clear positive effect of nor-NOHA treatment in the p53-tumour model. Furthermore, in the above-mentioned publication, it was shown that PD-L1 blockade didn't rescue T cell proliferation in a direct cell-cell contact assay, suggesting other inhibitory contact mechanisms [176].

All together, those results demonstrate the complex mechanisms in the TME and the challenge to develop treatment strategies which are effective in every patient and even more difficult to be effective in different tumours. Further investigations on our models are necessary to understand the underlying mechanisms and the different responses upon treatment with nor-NOHA in combination with ACT. The number of parameters that differed between the two models made it difficult to compare both *in vivo* experiments. Different numbers of TCR positive T cells were injected, the purity of TCR positive fractions differed strongly and we used transduced versus endogenous transgenic TCR expressing T cells. The transduction process could have had a negative impact on T cell fitness as compared to freshly isolated and directly injected OT-1 T cells. Another important difference between both experiments was the distribution of $CD8^+$ T cells. In the first *in vivo* experiment only ~45 % of p53-TCR^+ cells accounted for CD8 T cells (~25 % of all viable cells) whereas ~95 % of OT1-TCR^+ cells were CD8 T cells (~70 % of all viable cells) in the second *in vivo* experiment. However, whether the total number of TCR^+ CD8 T cells influenced the outcome of our in vivo experiments remains unclear and needs to be further investigated. In general, the group sizes were quite small which made it difficult to draw robust conclusions out of these two small experiments.

However, several publications support the idea of targeting arginase in cancer patients. Steggerda *et al.* demonstrated in various experiments the effectiveness of the arginase inhibitor CB-1158. In a number of tumour models, they observed an increase in tumour infiltrating CD8 positive T cells, combined with increased T cell and NK cell markers and an increase in interferon response genes. In addition, myeloid cells ($CD11b^+$ / $CD68^+$) were reduced. Those findings resulted in a reduction of tumour growth already in single treatment therapies (CB-1158) and the anti-tumour effect was even more pronounced in combined treatment therapies of CB-1158 and anti-PD-L1 or CB-1158 and adoptive T cell transfer [189].

In other tumour models, the presence of arginase positive myeloid cells in more advanced tumours was associated with a systemic loss of arginine in WT mice [180]. Those findings were supported by a clear correlation of increased plasma arginase and decreased plasma arginine concentrations in cancer patients compared to healthy donors [189,190]. For example, an increase of plasma arginase in ovarian cancer patients was measured which was significantly reduced after chemotherapy [191]. This indicates that the existing murine models to some extent correspond to clinical data. Also our p53 tumour model revealed a tendency towards increased plasma arginine levels in nor-NOHA treated animals [Figure 37C] which could be explained by the fact, that arginase I expression was clearly reduced in MDSC and macrophages and tumour lysates [Figure 35A,B; Figure 36A; Figure 37B]. Safety and efficacy of single CB-1158 treatment or the combination of CB-1158 and PD-1 inhibition (pembrolizumab) in patients with colorectal carcinoma was already shown in a clinical phase I study [132]. Moreover, response rates and progression-free survival suggested a benefit of the combined treatment of CB-1158 and chemotherapy for some patients with biliary tract cancer in a clinical phase I/II study [167]. Another arginase inhibitor (OATD-02) has been shown to delay ovarian cancer, colorectal and kidney carcinomas (CT26 and Renca, respectively), as well as leukaemia (K562) progression and to revert arginase-mediated inhibition of antigen-specific T-cell proliferation in preclinical mouse models [192]. A significant antitumour efficacy in multiple tumour models as a monotherapy and in combinations with checkpoint inhibitors and gemcitabine was demonstrated [193,194]. All in all, different arginase inhibitors were shown to exert modest antitumour effects, but inhibition of arginase activity as monotherapy failed to trigger strong antitumour response leading to tumour eradication. Further efforts were made, and combination therapies of arginase inhibitors and checkpoint inhibitors were evaluated. It was shown that arginase inhibition significantly potentiated checkpoint blockade (anti-PD-L1) in strong immunogenic tumour models like CT-26 colon adenocarcinoma [189]. In less immunogenic tumours like 4T1 breast cancer or 3LL lung carcinoma only minor effects were observed [180,181]. Interestingly, it was shown that a combined treatment of arginase inhibition (by ABH) and PD-1 blockade in the MC38 tumour model failed to provide potentiated antitumour efficacy when compared to single treatment [195]. In glioblastomas, the treatment with oral arginase inhibitor OATD-02 unblocked antitumour responses and improved the efficacy of PD-1 inhibition in mice [196].

In a murine pancreatic cancer model, arginase inhibition by CB-1158 was also found to sensitize the tumour to anti-PD1 immune checkpoint blockade [197]. Similar findings were reported in a cutaneous squamous cell carcinoma mouse model. Arginase inhibition using nor-NOHA reduced tumour growth and arginase activity and increased dendritic and T cell tumour infiltration. Likewise our p53 in vivo model, PD-1 expression was high on TILs. This was counteracted by anti PD-1 therapy (nivolumab) which resulted in reduced tumour growth already as single treatment and was additionally boosted by the combination with nor-NOHA [153].

Although many experiments were published testing different combination approaches targeting tumour escape mechanisms, therapeutic effects are still insufficient to induce complete responses in mice. Additionally, in most of the above-mentioned animal studies arginase inhibitor administration was started soon after tumour inoculation. As a more therapeutically relevant approach it would be important to test those treatment strategies once the tumour is fully established to determine whether similar antitumour effects can be reached or if the therapeutic effects would be even more reduced. Furthermore, very high concentrations of arginase inhibitors were used in mouse models whereas concentrations in human trials were much lower.

Nevertheless, further improvement of antitumour therapies and prolonged survival of tumour-bearing mice demonstrated that ongoing tumour research is providing new promising strategies to fight cancer in humans [180]. This is substantiated by further attractive antitumour approaches that have emerged within the last few years which could boost combinatorial treatment strategies. Emerging approaches, including the mRNA technology, provided promising data. After the big breakthrough as vaccination method against COVID-19, the mRNA technology became very popular. Already in 1996, first mRNA-based cancer vaccine studies were tested *in vitro* [198]. During the last years, mRNA vaccines became promising candidates for future cancer treatments, especially in combination with additional immunotherapies. Many clinical trials in phase 1 and 2 are ongoing testing different mRNA formulations in various combinations with other existing immunotherapies [199]. One promising strategy against solid tumours is BioNTech's CARVac approach. Like our ACT approach with TCR engineered T cells, CART cell therapies are extensively studied. They have shown to eradicate very advanced leukaemias and lymphomas [200]. As of October 2021, there are seven CAR T cell therapies approved by the American Food and Drug Administration [201]. However, in patients with solid tumours the efficacy of CAR T cell therapy is much more challenging and less effective [202].

BioNTech designed a CAR against the oncofoetal surface antigen claudin 6 (CLDN6) which is widely expressed in various human tumours [64]. To overcome the rapid decline of CAR T cells in the solid tumour setting they introduced liposomal antigen-encoding mRNA to stimulate CLDN6 CAR T cells. The nanoparticle vaccine delivered the antigen to APCs in the spleen, lymph nodes and bone marrow and initiated an immune stimulatory program. This promoted priming and strong expansion of antigen specific T cells [64]. They were able to collect promising data out of a clinical phase 1/2 study, with strongest responses seen in testicular cancer patients. They reached an overall response rate of 57% and a disease control rate of 85% [203].

In cooperation with research partners, we tested OT-1 T cell transfer in combination with SIINFEKL encoding mRNA and nor-NOHA treatment in a small mouse cohort with OVA-expressing tumours (MC38_OVA). After three mRNA injections (once a week) we found increased CD8 positive T cells circulating in blood with a strong TCR expression. In addition, TCR positive CD8 T cells were highly increased in the spleen and the TME. Consequently, a reduced tumour growth was measured. Importantly, this combinatorial approach resulted in a further reduction of tumour growth as compared to ACT + nor-NOHA treatment [data not shown]. Those results underline the power of mRNA vaccines as an additional treatment strategy in cancer therapy.

Overall, we could demonstrate to a certain extent, that a combination of ACT with tumour specific T cells and inhibition of arginase I reduced tumour growth and increased survival. However, this strategy needs to be further evaluated in different tumour models and combined with other approaches to significantly increase the therapeutic effect. Last but not least it became clear that a combination treatment approach is currently necessary to overcome escape mechanisms and efficiently target tumour growth. In the future, further research will be indispensable to improve existing strategies and explore new approaches for cancer immunotherapy.

6. Bibliography

1. Sung, H. *et al.* Global Cancer Statistics 2020: GLOBOCAN Estimates of Incidence and Mortality Worldwide for 36 Cancers in 185 Countries. *CA Cancer J Clin* **71**, (2021).
2. White, M. C. *et al.* Age and Cancer Risk: A Potentially Modifiable Relationship. *Am J Prev Med* **46**, S7 (2014).
3. AM, L., M, R., S, R., T, L. & B, L. Environmental risk factors for cancer - review paper. *Ann Agric Environ Med* **26**, 1–7 (2019).
4. Sudhakar, A. History of Cancer, Ancient and Modern Treatment Methods. doi:10.4172/1948-5956.100000e2.
5. Grubbé, E. H. Priority in the Therapeutic Use of X-rays. *https://doi.org/10.1148/21.2.156* **21**, 156–162 (1933).
6. Arruebo, M. *et al.* Assessment of the Evolution of Cancer Treatment Therapies. *Cancers 2011, Vol. 3, Pages 3279-3330* **3**, 3279–3330 (2011).
7. Falzone, L., Salomone, S. & Libra, M. Evolution of Cancer Pharmacological Treatments at the Turn of the Third Millennium. *Front Pharmacol* **0**, 1300 (2018).
8. Delaney, G., Jacob, S., Featherstone, C. & Barton, M. The role of radiotherapy in cancer treatment. *Cancer* **104**, 1129–1137 (2005).
9. Baumann, M. *et al.* Radiation oncology in the era of precision medicine. *Nature Reviews Cancer 2016 16:4* **16**, 234–249 (2016).
10. Bernstein, M. B., Krishnan, S., Hodge, J. W. & Chang, J. Y. Immunotherapy and stereotactic ablative radiotherapy (ISABR): a curative approach? *Nat Rev Clin Oncol* **13**, 516 (2016).
11. F, K. *et al.* Low-dose irradiation programs macrophage differentiation to an iNOS^{+}/M1 phenotype that orchestrates effective T cell immunotherapy. *Cancer Cell* **24**, 589–602 (2013).
12. R, M. *et al.* Targeting the mechanisms of resistance to chemotherapy and radiotherapy with the cancer stem cell hypothesis. *J Oncol* **2011**, (2011).
13. Sullivan, R. *et al.* Global cancer surgery: delivering safe, affordable, and timely cancer surgery. *Lancet Oncol* **16**, 1193–1224 (2015).
14. Damyanov, C. A. Conventional Treatment of Cancer Realities and Problems. **1**, (2018).

15. Wilson, B. E. *et al.* Estimates of global chemotherapy demands and corresponding physician workforce requirements for 2018 and 2040: a population-based study. *Lancet Oncol* **20**, 769–780 (2019).
16. Amjad, M. T., Chidharla, A. & Kasi, A. Cancer Chemotherapy. *Fundamentals of Pharmaceutical Nanoscience* 401–427 (2021).
17. Schirrmacher, V. From chemotherapy to biological therapy: A review of novel concepts to reduce the side effects of systemic cancer treatment (Review). *Int J Oncol* **54**, 407 (2019).
18. RC, L. *et al.* Single-agent versus combination chemotherapy in advanced non-small-cell lung cancer: the cancer and leukemia group B (study 9730). *J Clin Oncol* **23**, 190–196 (2005).
19. Solinas, G., Germano, G., Mantovani, A. & Allavena, P. Tumor-associated macrophages (TAM) as major players of the cancer-related inflammation. *J Leukoc Biol* **86**, 1065–1073 (2009).
20. A, M., F, M., A, M., L, L. & P, A. Tumour-associated macrophages as treatment targets in oncology. *Nat Rev Clin Oncol* **14**, 399–416 (2017).
21. A, M., S, S., M, L., P, A. & A, S. Macrophage polarization: tumor-associated macrophages as a paradigm for polarized M2 mononuclear phagocytes. *Trends Immunol* **23**, 549–555 (2002).
22. QW, Z. *et al.* Prognostic significance of tumor-associated macrophages in solid tumor: a meta-analysis of the literature. *PLoS One* **7**, (2012).
23. A, M. *et al.* Recognition of tumors by the innate immune system and natural killer cells. *Adv Immunol* **122**, 91–128 (2014).
24. Cooper, M. A., Fehniger, T. A. & Caligiuri, M. A. The biology of human natural killer-cell subsets. *Trends Immunol* **22**, 633–640 (2001).
25. Mandelboim, O. *et al.* Human CD16 as a lysis receptor mediating direct natural killer cell cytotoxicity. *Proc Natl Acad Sci U S A* **96**, 5640 (1999).
26. R, C. & GM, G. Lytic granules, secretory lysosomes and disease. *Curr Opin Immunol* **15**, 516–521 (2003).
27. L, Z. *et al.* Natural killer (NK) cell-mediated cytotoxicity: differential use of TRAIL and Fas ligand by immature and mature primary human NK cells. *J Exp Med* **188**, 2375–2380 (1998).

28. I, M. & RM, S. Dendritic cells: specialized and regulated antigen processing machines. *Cell* **106**, 255–258 (2001).
29. Wieczorek, M. *et al.* Major Histocompatibility Complex (MHC) Class I and MHC Class II Proteins: Conformational Plasticity in Antigen Presentation. *Front Immunol* **0**, 292 (2017).
30. J, K. & DH, R. Events that regulate differentiation of alpha beta TCR+ and gamma delta TCR+ T cells from a common precursor. *Semin Immunol* **9**, 171–179 (1997).
31. Rossjohn, J. *et al.* T Cell Antigen Receptor Recognition of Antigen-Presenting Molecules. *http://dx.doi.org/10.1146/annurev-immunol-032414-112334* **33**, 169–200 (2015).
32. Mariuzza, R. A., Agnihotri, P. & Orban, J. The structural basis of T-cell receptor (TCR) activation: An enduring enigma. *J Biol Chem* **295**, 914 (2020).
33. Li, Y. & Mariuzza, R. Structural and Biophysical Insights into the Role of CD4 and CD8 in T Cell Activation. *Front Immunol* **0**, 206 (2013).
34. Glatzová, D. & Cebecauer, M. Dual role of CD4 in peripheral T lymphocytes. *Frontiers in Immunology* vol. 10 Preprint at https://doi.org/10.3389/fimmu.2019.00618 (2019).
35. What are T Cell Receptors- CUSABIO. https://www.cusabio.com/receptor/T-Cell-Receptor.html.
36. Reiser, J. & Banerjee, A. Effector, Memory, and Dysfunctional CD8+ T Cell Fates in the Antitumor Immune Response. *J Immunol Res* **2016**, (2016).
37. DM, P. & SL, T. The role of CD4+ T cell responses in antitumor immunity. *Curr Opin Immunol* **10**, 588–594 (1998).
38. WH, F., F, P., C, S.-F. & J, G. The immune contexture in human tumours: impact on clinical outcome. *Nat Rev Cancer* **12**, 298–306 (2012).
39. Togashi, Y., Shitara, K. & Nishikawa, H. Regulatory T cells in cancer immunosuppression — implications for anticancer therapy. *Nature Reviews Clinical Oncology 2019 16:6* **16**, 356–371 (2019).
40. D, H. & RA, W. The hallmarks of cancer. *Cell* **100**, 57–70 (2000).
41. TA, B. Targeted Cancer Therapy: The Next Generation of Cancer Treatment. *Curr Drug Discov Technol* **12**, 3–20 (2015).
42. Seidel, J. A., Otsuka, A. & Kabashima, K. Anti-PD-1 and Anti-CTLA-4 Therapies in Cancer: Mechanisms of Action, Efficacy, and Limitations. *Front Oncol* **0**, 86 (2018).

43. Morante, M., Pandiella, A., Crespo, P. & Herrero, A. Immune Checkpoint Inhibitors and RAS–ERK Pathway-Targeted Drugs as Combined Therapy for the Treatment of Melanoma. *Biomolecules* vol. 12 Preprint at https://doi.org/10.3390/biom12111562 (2022).

44. MC, L. & TG, H. Identification of responders to immune checkpoint therapy: which biomarkers have the highest value? *J Eur Acad Dermatol Venereol* **33 Suppl 8**, (2019).

45. Mahoney, K. M., Rennert, P. D. & Freeman, G. J. Combination cancer immunotherapy and new immunomodulatory targets. *Nature Reviews Drug Discovery 2015 14:8* **14**, 561–584 (2015).

46. A, H. & V, P. Estimation of the Percentage of US Patients With Cancer Who Are Eligible for and Respond to Checkpoint Inhibitor Immunotherapy Drugs. *JAMA Netw Open* **2**, (2019).

47. Fares, C. M., Van Allen, E. M., Drake, C. G., Allison, J. P. & Hu-Lieskovan, S. Mechanisms of Resistance to Immune Checkpoint Blockade: Why Does Checkpoint Inhibitor Immunotherapy Not Work for All Patients? *Am Soc Clin Oncol Educ Book* **39**, 147–164 (2019).

48. Groisberg, R., Maymani, H. & Subbiah, V. Immunotherapy and next-generation sequencing guided therapy for precision oncology: What have we learnt and what does the future hold? *Expert Rev Precis Med Drug Dev* **3**, 205 (2018).

49. Zhao, Y. *et al.* Tumor Infiltrating Lymphocyte (TIL) Therapy for Solid Tumor Treatment: Progressions and Challenges. *Cancers (Basel)* **14**, (2022).

50. Yang, F. *et al.* Adoptive cellular therapy (ACT) for cancer treatment. *Adv Exp Med Biol* **909**, 169–239 (2016).

51. Kishton, R. J., Sukumar, M. & Restifo, N. P. Metabolic Regulation of T Cell Longevity and Function in Tumor Immunotherapy. *Cell Metab* **26**, 94–109 (2017).

52. CC, L., H, Y., R, Z., JJ, Z. & DJ, H. Tumour-associated antigens and their anti-cancer applications. *Eur J Cancer Care (Engl)* **26**, (2017).

53. Theobald, M., Biggs, J., Dittmer, D., Levine, a J. & Sherman, L. a. Targeting p53 as a general tumor antigen. *Proc Natl Acad Sci U S A* **92**, 11993–11997 (1995).

54. Duffy, M. J., Synnott, N. C. & Crown, J. Mutant p53 as a target for cancer treatment. *Eur J Cancer* **83**, 258–265 (2017).

55. Echchannaoui, H. *et al.* A potent tumor-reactive p53-specific single-chain TCR without on- or off-target autoimmunity in vivo. *Molecular Therapy* **27**, 1–11 (2018).

56. Ö, M., KM, J., CA, C., M, D. & IM, S. Principles of adoptive T cell therapy in cancer. *Semin Immunopathol* **41**, 49–58 (2019).

57. CH, J., SR, R. & TN, S. Adoptive cellular therapy: a race to the finish line. *Sci Transl Med* **7**, (2015).

58. Alnefaie, A. *et al.* Chimeric Antigen Receptor T-Cells: An Overview of Concepts, Applications, Limitations, and Proposed Solutions. *Front Bioeng Biotechnol* **10**, (2022).

59. First-Ever CAR T-cell Therapy Approved in U.S. *Cancer Discov* **7**, OF1 (2017).

60. FDA-approved CAR T-cell Therapies | UPMC Hillman. https://hillman.upmc.com/mario-lemieux-center/treatment/car-t-cell-therapy/fda-approved-therapies.

61. Sengsayadeth, S., Savani, B. N., Oluwole, O. & Dholaria, B. Overview of approved CAR-T therapies, ongoing clinical trials, and its impact on clinical practice. *EJHaem* **3**, 6 (2022).

62. Tsai, H. J. Clinical cancer chemoprevention: From the hepatitis B virus (HBV) vaccine to the human papillomavirus (HPV) vaccine. *Taiwan J Obstet Gynecol* **54**, 112–115 (2015).

63. Miao, L., Zhang, Y. & Huang, L. mRNA vaccine for cancer immunotherapy. *Molecular Cancer 2021 20:1* **20**, 1–23 (2021).

64. Reinhard, K. *et al.* An RNA vaccine drives expansion and efficacy of claudin-CAR-T cells against solid tumors. *Science (1979)* **367**, 446–453 (2020).

65. Mackensen, A. *et al.* CLDN6-specific CAR-T cells plus amplifying RNA vaccine in relapsed or refractory solid tumors: the phase 1 BNT211-01 trial. *Nat Med* **29**, 2844–2853 (2023).

66. Rojas, L. A. *et al.* Personalized RNA neoantigen vaccines stimulate T cells in pancreatic cancer. *Nature 2023 618:7963* **618**, 144–150 (2023).

67. Study Details | Study of Personalized Tumor Vaccines (PCVs) and a PD-L1 Blocker in Patients With Pancreatic Cancer That Can be Treated With Surgery | ClinicalTrials.gov. https://clinicaltrials.gov/study/NCT04161755#publications.

68. Marusyk, A. & Polyak, K. Tumor heterogeneity: causes and consequences. *Biochim Biophys Acta* **1805**, 105 (2010).

69. Miller, F. R. Intratumor immunologic heterogeneity. *Cancer and Metastasis Review* **1**, 319–334 (1982).

70. Li, H. & Shi, B. Tolerogenic dendritic cells and their applications in transplantation. *Cellular & Molecular Immunology 2014 12:1* **12**, 24–30 (2014).

71. Gabrilovich, D. Mechanisms and functional significance of tumour-induced dendritic-cell defects. *Nat Rev Immunol* **4**, 941–952 (2004).

72. Gabrilovich, D. I. *et al.* Production of vascular endothelial growth factor by human tumors inhibits the functional maturation of dendritic cells. *Nat Med* **2**, 1096–1103 (1996).

73. Algarra, I., García-Lora, A., Cabrera, T., Ruiz-Cabello, F. & Garrido, F. The selection of tumor variants with altered expression of classical and nonclassical MHC class I molecules: implications for tumor immune escape. *Cancer Immunol Immunother* **53**, 904–910 (2004).

74. Labani-Motlagh, A., Ashja-Mahdavi, M. & Loskog, A. The Tumor Microenvironment: A Milieu Hindering and Obstructing Antitumor Immune Responses. *Front Immunol* **11**, 940 (2020).

75. Boussiotis, V. A. Molecular and Biochemical Aspects of the PD-1 Checkpoint Pathway. *New England Journal of Medicine* **375**, 1767–1778 (2016).

76. Azuma, T. *et al.* B7-H1 is a ubiquitous antiapoptotic receptor on cancer cells. *Blood* **111**, 3635–3643 (2008).

77. Boutros, C. *et al.* Safety profiles of anti-CTLA-4 and anti-PD-1 antibodies alone and in combination. *Nature Reviews Clinical Oncology 2016 13:8* **13**, 473–486 (2016).

78. Andrews, L. P., Marciscano, A. E., Drake, C. G. & Vignali, D. A. A. LAG3 (CD223) as a cancer immunotherapy target. *Immunol Rev* **276**, 80–96 (2017).

79. Tang, R., Rangachari, M. & Kuchroo, V. K. Tim-3: A co-receptor with diverse roles in T cell exhaustion and tolerance. *Semin Immunol* **42**, 101302 (2019).

80. Anderson, A. C., Joller, N. & Kuchroo, V. K. Lag-3, Tim-3, and TIGIT: Co-inhibitory Receptors with Specialized Functions in Immune Regulation. *Immunity* **44**, 989–1004 (2016).

81. Solomon, B. L. & Garrido-Laguna, I. TIGIT: a novel immunotherapy target moving from bench to bedside. *Cancer Immunology, Immunotherapy 2018 67:11* **67**, 1659–1667 (2018).

82. Pasche, B. Role of Transforming Growth Factor Beta in Cancer. *J Cell Physiol* **186**, 153–168 (2001).

83. Palomares, O. *et al.* Regulatory T cells and immune regulation of allergic diseases: roles of IL-10 and TGF-β. *Genes & Immunity 2014 15:8* **15**, 511–520 (2014).

84. Togashi, Y., Shitara, K. & Nishikawa, H. Regulatory T cells in cancer immunosuppression — implications for anticancer therapy. *Nature Reviews Clinical Oncology 2019 16:6* **16**, 356–371 (2019).

85. Turnis, M. E. *et al.* Interleukin-35 Limits Anti-Tumor Immunity. *Immunity* **44**, 316–329 (2016).

86. Lindqvist, C. A. *et al.* T regulatory cells control T-cell proliferation partly by the release of soluble CD25 in patients with B-cell malignancies. *Immunology* **131**, 371–376 (2010).

87. Smyth, M. J. *et al.* CD4+CD25+ T Regulatory Cells Suppress NK Cell-Mediated Immunotherapy of Cancer. *The Journal of Immunology* **176**, 1582–1587 (2006).

88. Wilke, C. M., Wu, K., Zhao, E., Wang, G. & Zou, W. Prognostic significance of regulatory T cells in tumor. *Int J Cancer* **127**, 748–758 (2010).

89. Colegio, O. R. *et al.* Functional polarization of tumour-associated macrophages by tumour-derived lactic acid. *Nature 2014 513:7519* **513**, 559–563 (2014).

90. Hao, N. B. *et al.* Macrophages in tumor microenvironments and the progression of tumors. *Clin Dev Immunol* **2012**, (2012).

91. Cassetta, L. & Pollard, J. W. Targeting macrophages: therapeutic approaches in cancer. *Nature Reviews Drug Discovery 2018 17:12* **17**, 887–904 (2018).

92. Munder, M. Arginase: an emerging key player in the mammalian immune system. *Br J Pharmacol* **158**, 638–651 (2009).

93. Otsuji, M., Kimura, Y., Aoe, T., Okamoto, Y. & Saito, T. Oxidative stress by tumor-derived macrophages suppresses the expression of CD3 ζ chain of T-cell receptor complex and antigen-specific T-cell responses. *Proceedings of the National Academy of Sciences* **93**, 13119–13124 (1996).

94. Li, B. H., Garstka, M. A. & Li, Z. F. Chemokines and their receptors promoting the recruitment of myeloid-derived suppressor cells into the tumor. *Mol Immunol* **117**, 201–215 (2020).

95. Gabrilovich, D. I. & Nagaraj, S. Myeloid-derived suppressor cells as regulators of the immune system. *Nat Rev Immunol* **9**, 162–174 (2009).

96. Bronte, V. *et al.* Recommendations for myeloid-derived suppressor cell nomenclature and characterization standards. *Nat Commun* **7**, (2016).

97. Yu, J. *et al.* Myeloid-derived suppressor cells suppress antitumor immune responses through IDO expression and correlate with lymph node metastasis in patients with breast cancer. *J Immunol* **190**, 3783–3797 (2013).

98. Guerra, L., Bonetti, L. & Brenner, D. Metabolic Modulation of Immunity: A New Concept in Cancer Immunotherapy. *Cell Rep* **32**, 107848 (2020).

99. Brosnan, M. E. & Brosnan, J. T. Renal Arginine Metabolism. *J Nutr* **134**, 2791S-2795S (2004).

100. Wu, G. Amino acids: metabolism, functions, and nutrition. *Amino Acids* **37**, 1–17 (2009).

101. Wang, W. & Zou, W. Amino Acids and Their Transporters in T Cell Immunity and Cancer Therapy. *Mol Cell* **80**, 384–395 (2020).

102. Chen, C.-L., Hsu, S.-C., Ann, D. K., Yen, Y. & Kung, H.-J. Arginine Signaling and Cancer Metabolism. (2021) doi:10.3390/cancers13143541.

103. Shaibe, E., Metzer, E. & Halpern, Y. S. Control of utilization of L-arginine, L-ornithine, agmatine, and putrescine as nitrogen sources in Escherichia coli K-12. *J Bacteriol* **163**, 938 (1985).

104. Minois, N., Carmona-Gutierrez, D. & Madeo, F. Polyamines in aging and disease. *Aging (Albany NY)* **3**, 716 (2011).

105. Szefel, J., Danielak, A. & Kruszewski, W. J. Metabolic pathways of L-arginine and therapeutic consequences in tumors. *Adv Med Sci* **64**, 104–110 (2019).

106. Husson, A., Brasse-Lagnel, C., Fairand, A., Renouf, S. & Lavoinne, A. Argininosuccinate synthetase from the urea cycle to the citrulline–NO cycle. *Eur J Biochem* **270**, 1887–1899 (2003).

107. Levenbergt, B. Role of L-Glutamine as Donor of Carbamyl Nitrogen for the Enzymatic Synthesis of Citrulline in Agaricus bisporus *. *Journal of Biological Chemistry* **237**, 2590–2598 (1962).

108. Cohen, P. P. & Grisolia, S. THE INTERMEDIATE ROLE OF CARBAMYL-L-GLUTAMIC ACID IN CITRULLINE SYNTHESIS* sirs. *Journal of Biological Chemistry* **174**, 389–390 (1948).

109. Hamilton, P. B. PROLINE: SYNTHESIS FROM ORNITHINE, CITRULLINE, OR ARGININE. *Journal of Biological Chemistry* **198**, 587–597 (1952).

110. Feldmeyer, N. *et al.* Arginine deficiency leads to impaired cofilin dephosphorylation in activated human T lymphocytes. *Int Immunol* **24**, 303–313 (2012).

111. Rodriguez, P. C. *et al.* L-arginine deprivation regulates cyclin D3 mRNA stability in human T cells by controlling HuR expression. *J Immunol* **185**, 5198–5204 (2010).

112. Grzywa, T. M. *et al.* Myeloid Cell-Derived Arginase in Cancer Immune Response. *Frontiers in Immunology* vol. 11 938 Preprint at https://doi.org/10.3389/fimmu.2020.00938 (2020).

113. Miraki-Moud, F. *et al.* Arginine deprivation using pegylated arginine deiminase has activity against primary acute myeloid leukemia cells in vivo. *Blood* **125**, 4060–4068 (2015).

114. Kelly, M. P. *et al.* Arginine deiminase PEG20 inhibits growth of small cell lung cancers lacking expression of argininosuccinate synthetase. *Br J Cancer* **106**, 324–332 (2012).

115. Izzo, F. *et al.* Pegylated arginine deiminase treatment of patients with unresectable hepatocellular carcinoma: results from phase I/II studies. *J Clin Oncol* **22**, 1815–1822 (2004).

116. Savaraj, N. *et al.* Targeting argininosuccinate synthetase negative melanomas using combination of arginine degrading enzyme and cisplatin. *Oncotarget* **6**, 6295–6309 (2015).

117. Kim, R. H. *et al.* Arginine deiminase as a novel therapy for prostate cancer induces autophagy and caspase-independent apoptosis. *Cancer Res* **69**, 700–708 (2009).

118. Ma, Q., Wang, Y., Gao, X., Ma, Z. & Song, Z. l-Arginine Reduces Cell Proliferation and Ornithine Decarboxylase Activity in Patients with Colorectal Adenoma and Adenocarcinoma. *Clinical Cancer Research* **13**, 7407–7412 (2007).

119. Yim, C.-Y., Bastian, N. R., Smith, J. C., Hibbs, J. B. & Samlowski, W. E. Macrophage Nitric Oxide Synthesis Delays Progression of Ultraviolet Light-induced Murine Skin Cancers. *Cancer Res* **53**, (1993).

120. Geiger, R. *et al.* L-Arginine Modulates T Cell Metabolism and Enhances Survival and Anti-tumor Activity. *Cell* **167**, 829-842.e13 (2016).

121. Nieves, C. & Langkamp-Henken, B. Arginine and immunity: a unique perspective. *Biomed Pharmacother* **56**, 471–482 (2002).

122. Curis, E. *et al.* Almost all about citrulline in mammals. *Amino Acids 2005 29:3* **29**, 177–205 (2005).

123. Schwedhelm, E. *et al.* Pharmacokinetic and pharmacodynamic properties of oral L-citrulline and L-arginine: impact on nitric oxide metabolism Correspondence. (2007) doi:10.1111/j.1365-2125.2007.02990.x.

124. Werner, A. *et al.* Reconstitution of T cell proliferation under arginine limitation: Activated human T cells take up citrulline via L-Type amino acid transporter 1 and use it to regenerate arginine after induction of argininosuccinate synthase expression. *Front Immunol* **8**, 864 (2017).

125. Pudlo, M., Demougeot, C. & Girard-Thernier, C. Arginase Inhibitors: A Rational Approach Over One Century. *Med Res Rev* **37**, 475–513 (2017).

126. di Costanzo, L., Ilies, M., Thorn, K. J. & Christianson, D. W. Inhibition of human arginase I by substrate and product analogues. *Arch Biochem Biophys* **496**, 101–108 (2010).

127. Baggio, R. *et al.* Biochemical and Functional Profile of a Newly Developed Potent and Isozyme-Selective Arginase Inhibitor. *Journal of Pharmacology and Experimental Therapeutics* **290**, (1999).

128. Kim, N. N. *et al.* Probing Erectile Function: S-(2-Boronoethyl)-l-Cysteine Binds to Arginase as a Transition State Analogue and Enhances Smooth Muscle Relaxation in Human Penile Corpus Cavernosum†,‡. *Biochemistry* **40**, 2678–2688 (2001).

129. Custot, J. *et al.* The New α-Amino Acid Nω-Hydroxy-nor-l-arginine: a High-Affinity Inhibitor of Arginase Well Adapted To Bind to Its Manganese Cluster. *J Am Chem Soc* **119**, 4086–4087 (1997).

130. Miret, J. J. *et al.* Suppression of Myeloid Cell Arginase Activity leads to Therapeutic Response in a NSCLC Mouse Model by Activating Anti-Tumor Immunity. *J Immunother Cancer* **7**, 32 (2019).

131. Arginase Inhibitor INCB001158 as a Single Agent and in Combination With Immune Checkpoint Therapy in Patients With Advanced/Metastatic Solid Tumors - Full Text View - ClinicalTrials.gov. https://www.clinicaltrials.gov/ct2/show/NCT02903914.

132. Naing, A. *et al.* Phase I study of the arginase inhibitor INCB001158 (1158) alone and in combination with pembrolizumab (PEM) in patients (Pts) with advanced/metastatic (adv/met) solid tumours. *Annals of Oncology* **30**, v160 (2019).

133. Steggerda, S. M. *et al.* Inhibition of arginase by CB-1158 blocks myeloid cell-mediated immune suppression in the tumor microenvironment. *J Immunother Cancer* **5**, 101 (2017).

134. Arikan-Ayyildiz, Z. *et al.* Beneficial effects of arginase inhibition and inhaled l-arginine administration on airway histology in a murine model of chronic asthma. *Allergol Immunopathol (Madr)* **42**, 316–323 (2014).

135. Takahashi, N. *et al.* Direct inhibition of arginase attenuated airway allergic reactions and inflammation in a Dermatophagoides farinae-induced NC/Nga mouse model. *Am J Physiol Lung Cell Mol Physiol* **299**, 17–24 (2010).

136. Olivon, V. C. *et al.* Arginase inhibition prevents the low shear stress-induced development of vulnerable atherosclerotic plaques in ApoE−/− mice. *Atherosclerosis* **227**, 236–243 (2013).

137. Prati, C., Berthelot, A., Kantelip, B., Wendling, D. & Demougeot, C. Treatment with the arginase inhibitor Nw-hydroxy-nor-L-arginine restores endothelial function in rat adjuvant-induced arthritis. *Arthritis Res Ther* **14**, 1–11 (2012).

138. Bagnost, T. *et al.* Treatment with the arginase inhibitor Nω-hydroxy-nor-L-arginine improves vascular function and lowers blood pressure in adult spontaneously hypertensive rat. *J Hypertens* **26**, 1110–1118 (2008).

139. Jung, C., Gonon, A. T., Sjöquist, P. O., Lundberg, J. O. & Pernow, J. Arginase inhibition mediates cardioprotection during ischaemia–reperfusion. *Cardiovasc Res* **85**, 147–154 (2010).

140. Pudlo, M., Demougeot, C. & Girard-Thernier, C. Arginase Inhibitors: A Rational Approach Over One Century. *Med Res Rev* **37**, 475–513 (2017).

141. Rodriguez, P. C. *et al. Arginase I Production in the Tumor Microenvironment by Mature Myeloid Cells Inhibits T-Cell Receptor Expression and Antigen-Specific T-Cell Responses*. *CANCER RESEARCH* vol. 64 (2004).

142. Narita, Y. *et al.* The key role of IL-6-arginase cascade for inducing dendritic cell-dependent CD4(+) T cell dysfunction in tumor-bearing mice. *J Immunol* **190**, 812–820 (2013).

143. Secondini, C. *et al.* Arginase inhibition suppresses lung metastasis in the 4T1 breast cancer model independently of the immunomodulatory and anti-metastatic effects of VEGFR-2 blockade. *Oncoimmunology* **6**, (2017).

144. Garrido, F., Ruiz-Cabello, F. & Aptsiauri, N. Rejection versus escape: the tumor MHC dilemma. *Cancer Immunology, Immunotherapy* **66**, 259–271 (2017).

145. Patil, M., Bhaumik, J., Babykutty, S., Banerjee, U. & Fukumura, D. Arginine dependence of tumor cells: targeting a chink in cancer's armor. *Oncogene* **35**, 4957 (2016).

146. Zhou, F. Molecular mechanisms of IFN-gamma to up-regulate MHC class I antigen processing and presentation. *Int Rev Immunol* **28**, 239–260 (2009).

147. OT I Mouse | Charles River Laboratories. https://www.criver.com/products-services/find-model/ot-i-mouse?region=23.

148. Vonwirth, V. *et al.* Inhibition of Arginase 1 Liberates Potent T Cell Immunostimulatory Activity of Human Neutrophil Granulocytes. *Front Immunol* **11**, 1 (2021).

149. Munder, M. *et al.* Arginase I is constitutively expressed in human granulocytes and participates in fungicidal activity. *Blood* **105**, 2549–2556 (2005).

150. Munder, M. *et al.* Suppression of T-cell functions by human granulocyte arginase. *Blood* **108**, 1627–1634 (2006).

151. Rodriguez, P. C., Zea, A. H., Culotta, K. S., Zabaleta, J. & Ochoa Augusto C Ochoa, J. B. Regulation of T Cell Receptor CD3ζ Chain Expression byl-Arginine *. *Journal of Biological Chemistry* **277**, 21123–21129 (2002).

152. Minns, D., Smith, K. J., Hardisty, G., Rossi, A. G. & Gwyer Findlay, E. The Outcome of Neutrophil-T Cell Contact Differs Depending on Activation Status of Both Cell Types. *Front Immunol* **12**, 1049 (2021).

153. Mittal, A. *et al.* Topical arginase inhibition decreases growth of cutaneous squamous cell carcinoma. *Scientific Reports 2021 11:1* **11**, 1–11 (2021).

154. Wang, X. *et al.* Arginase-1 inhibition reduces migration ability and metastatic colonization of colon cancer cells. *Cancer & Metabolism 2022 11:1* **11**, 1–14 (2023).

155. Garrido, F. *et al.* Implications for immunosurveillance of altered HLA class I phenotypes in human tumours. *Immunol Today* **18**, 89–95 (1997).

156. Garrido, F., Cabrera, T. & Aptsiauri, N. '"Hard"' and ' "soft"' lesions underlying the HLA Class I alterations in cancer cells: implications for immunotherapy. doi:10.1002/ijc.25270.

157. Reynolds, J. v. *et al.* Immunologic effects of arginine supplementation in tumor-bearing and non-tumor-bearing hosts. *Ann Surg* **211**, 202 (1990).

158. Lubec, B. *et al.* Decreased tumor incidence and increased survival by one year oral low dose arginine supplementation in the mouse. *Life Sci* **58**, 2317–2325 (1996).

159. Millis, R. M., Diya, C. A., Reynolds, M. E., Dehkordi, O. & Bond, V. Growth inhibition of subcutaneously transplanted hepatomas without cachexia by alteration of the dietary arginine-methionine balance. *Nutr Cancer* **31**, 49–55 (1998).

160. Szende, B., Tyihák, E. & Trézl, L. Role of arginine and its methylated derivatives in cancer biology and treatment. *Cancer Cell Int* **1**, (2001).

161. Cao, Y., Feng, Y., Zhang, Y., Zhu, X. & Jin, F. L-Arginine supplementation inhibits the growth of breast cancer by enhancing innate and adaptive immune responses mediated by suppression of MDSCs in vivo. *BMC Cancer* **16**, 1–11 (2016).

162. Heys, S. D. *et al.* Dietary supplementation with L-arginine: modulation of tumour-infiltrating lymphocytes in patients with colorectal cancer. *British Journal of Surgery* **84**, 238–241 (1997).

163. Szefel, J. *et al.* The effect of l-arginine supplementation and surgical trauma on the frequency of myeloid-derived suppressor cells and T lymphocytes in tumour and blood of colorectal cancer patients. *Adv Med Sci* **67**, 66–78 (2022).

164. Reyes, A. A., Karl, I. E. & Klahr, S. Role of arginine in health and in renal disease. *Am J Physiol* **267**, (1994).

165. Tangphao, O., Grossmann, M., Chalon, S., Hoffman, B. B. & Blaschke, T. F. *Pharmacokinetics of Intravenous and Oral L-Arginine in Normal Volunteers*. (1999).

166. Niu, F. *et al.* Arginase: An emerging and promising therapeutic target for cancer treatment. *Biomedicine and Pharmacotherapy* **149**, (2022).

167. Javle, M. M. *et al.* A phase I/II study of safety and efficacy of the arginase inhibitor INCB001158 plus chemotherapy in patients (Pts) with advanced biliary tract cancers. *https://doi.org/10.1200/JCO.2021.39.3_suppl.311* **39**, 311–311 (2021).

168. Study Details | First-in-human Phase I Study to Evaluate Safety, Tolerability and Antineoplastic Activity of OATD-02 in Patients With Selected Advanced and/or Metastatic Solid Tumours | ClinicalTrials.gov. https://clinicaltrials.gov/study/NCT05759923?intr=OATD-02&rank=1.

169. Xu, W., Liu, L. Z., Loizidou, M., Ahmed, M. & Charles, I. G. The role of nitric oxide in cancer. *Cell Research 2002 12:5* **12**, 311–320 (2002).

170. Tate, D. J. *et al.* Effect of arginase II on L-arginine depletion and cell growth in murine cell lines of renal cell carcinoma. *J Hematol Oncol* **1**, (2008).

171. Singh, R., Pervin, S., Karimi, A., Cederbaum, S. & Chaudhuri, G. *Activity in Human Breast Cancer Cell Lines: N(ω)-Hydroxy-L-Arginine Selectively Inhibits Cell Proliferation and Induces Apoptosis in MDA-MB-468 Cells Arginase Activity in Human Breast Cancer Cell Lines: N-Hydroxy-L-Arginine Selectively Inhibits Cell Proliferation and Induces Apoptosis in MDA-MB-468 Cells 1*. *CANCER RESEARCH* vol. 60 https://www.researchgate.net/publication/12453138 (2000).

172. A Study of INCMGA00012, INCB001158, and the Combination in Japanese Participants With Advanced Solid Tumors - Full Text View - ClinicalTrials.gov. https://clinicaltrials.gov/ct2/show/NCT03910530?term=INCB001158&draw=2&rank=2.

173. INCB001158 Combined With Subcutaneous (SC) Daratumumab, Compared to Daratumumab SC, in Relapsed or Refractory Multiple Myeloma - Full Text View - ClinicalTrials.gov. https://clinicaltrials.gov/ct2/show/NCT03837509?term=INCB001158&draw=2&rank=1.

174. Magiera-Mularz, K. *et al.* Human and mouse PD-L1: similar molecular structure, but different druggability profiles. *iScience* **24**, (2021).

175. He, G. *et al.* Peritumoural neutrophils negatively regulate adaptive immunity via the PD-L1/PD-1 signalling pathway in hepatocellular carcinoma. *Journal of Experimental and Clinical Cancer Research* **34**, 1–11 (2015).

176. Bian, Z. *et al.* Arginase-1 is neither constitutively expressed in nor required for myeloid-derived suppressor cell-mediated inhibition of T-cell proliferation. *Eur J Immunol* 1046–1058 (2018) doi:10.1002/eji.201747355.

177. Czystowska-Kuzmicz, M. *et al.* Small extracellular vesicles containing arginase-1 suppress T-cell responses and promote tumor growth in ovarian carcinoma. doi:10.1038/s41467-019-10979-3.

178. Hu, Y. *et al.* Synergistic effect of adoptive immunotherapy and docetaxel inhibits tumor growth in a mouse model. *Cell Immunol* **348**, (2020).

179. Sierra, R. A. *et al.* Anti-Jagged immunotherapy inhibits MDSCs and overcomes tumor-induced tolerance. *Cancer Res* **77**, 5628 (2017).

180. Sosnowska, A. *et al.* Inhibition of arginase modulates T-cell response in the tumor microenvironment of lung carcinoma. (2021) doi:10.1080/2162402X.2021.1956143.

181. Steggerda, S. M. *et al.* Inhibition of arginase by CB-1158 blocks myeloid cell-mediated immune suppression in the tumor microenvironment. doi:10.1186/s40425-017-0308-4.

182. Schuller, A. *et al.* Abstract 4523: Inhibition of arginase in combination with anti-PDL1 leads to increased infiltration and activation of CD8+ T cells, NK cells, and CD103+ dendritic cells in mouse syngeneic tumor models. *Cancer Res* **80**, 4523–4523 (2020).

183. Martí i Líndez, A. A. *et al.* Mitochondrial arginase-2 is a cell-autonomous regulator of CD8+ T cell function and antitumor efficacy. *JCI Insight* **4**, (2020).

184. Rodriguez, P. C. *et al.* Arginase I in myeloid suppressor cells is induced by COX-2 in lung carcinoma. *J Exp Med* **202**, 931–939 (2005).

185. Gallina, G. *et al.* Tumors induce a subset of inflammatory monocytes with immunosuppressive activity on CD8+ T cells. *J Clin Invest* **116**, 2777–2790 (2006).

186. Sinha, P., Parker, K. H., Horn, L. & Ostrand-Rosenberg, S. Tumor-induced myeloid-derived suppressor cell function is independent of IFN-γ and IL-4Rα. *Eur J Immunol* **42**, 2052–2059 (2012).

187. Sinha, P., Clements, V. K. & Ostrand-Rosenberg, S. Interleukin-13-regulated M2 macrophages in combination with myeloid suppressor cells block immune surveillance against metastasis. *Cancer Res* **65**, 11743–11751 (2005).

188. Munder, M. *et al.* Th1/Th2-Regulated Expression of Arginase Isoforms in Murine Macrophages and Dendritic Cells. *The Journal of Immunology* **163**, 3771–3777 (1999).

189. Steggerda, S. M. *et al.* Inhibition of arginase by CB-1158 blocks myeloid cell-mediated immune suppression in the tumor microenvironment. *J Immunother Cancer* **5**, 1–18 (2017).

190. Peyraud, F. *et al.* Circulating L-arginine predicts the survival of cancer patients treated with immune checkpoint inhibitors. *Annals of Oncology* **33**, 1041–1051 (2022).

191. Coosemans, A. *et al.* Immunosuppressive parameters in serum of ovarian cancer patients change during the disease course. (2016) doi:10.1080/2162402X.2015.1111505.

192. Grzybowski, M. M. *et al.* OATD-02 Validates the Benefits of Pharmacological Inhibition of Arginase 1 and 2 in Cancer. *Cancers (Basel)* **14**, 3967 (2022).

193. Grzybowski, M. M. *et al.* Novel dual arginase 1/2 inhibitor OATD-02 (OAT-1746) improves the efficacy of immune checkpoint inhibitors. *Annals of Oncology* **28**, xi20–xi21 (2017).

194. Stanczak, P. S. *et al.* Development of OAT-1746, a novel arginase 1 and 2 inhibitor for cancer immunotherapy. *Annals of Oncology* **28**, v418 (2017).

195. Arlauckas, S. P. *et al.* Arg1 expression defines immunosuppressive subsets of tumor-associated macrophages. *Theranostics* **8**, 5842–5854 (2018).

196. Pilanc, P. *et al.* A Novel Oral Arginase 1/2 Inhibitor Enhances the Antitumor Effect of PD-1 Inhibition in Murine Experimental Gliomas by Altering the Immunosuppressive Environment. *Front Oncol* **11**, (2021).

197. Menjivar, R. E. *et al.* Arginase 1 is a key driver of immune suppression in pancreatic cancer. *Elife* **12**, (2023).

198. Boczkowski, D., Nair, S. K., Snyder, D. & Gilboa, E. Dendritic cells pulsed with RNA are potent antigen-presenting cells in vitro and in vivo. *J Exp Med* **184**, 465–472 (1996).

199. L Lorentzen, D. C. *et al.* Clinical advances and ongoing trials of mRNA vaccines for cancer treatment. *Lancet Oncology* **23**, e450–e458 (2022).

200. Melenhorst, J. J. *et al.* Decade-long leukaemia remissions with persistence of CD4+ CAR T cells. *Nature 2022 602:7897* **602**, 503–509 (2022).

201. Sengsayadeth, S., Savani, B. N., Oluwole, O. & Dholaria, B. Overview of approved CAR-T therapies, ongoing clinical trials, and its impact on clinical practice. *EJHaem* **3**, 6–10 (2022).

202. Scarfò, I. & Maus, M. v. Current approaches to increase CAR T cell potency in solid tumors: targeting the tumor microenvironment. *J Immunother Cancer* **5**, 28 (2017).

203. BioNTech Presents Encouraging Phase 1/2 Follow-up Data for CAR-T Candidate BNT211 in Hard-To-Treat Solid Tumors at ESMO. (2022).

7. Appendix

7.1. Vector maps and constructs

7.1.1. pMx_puro RTV-014 vector

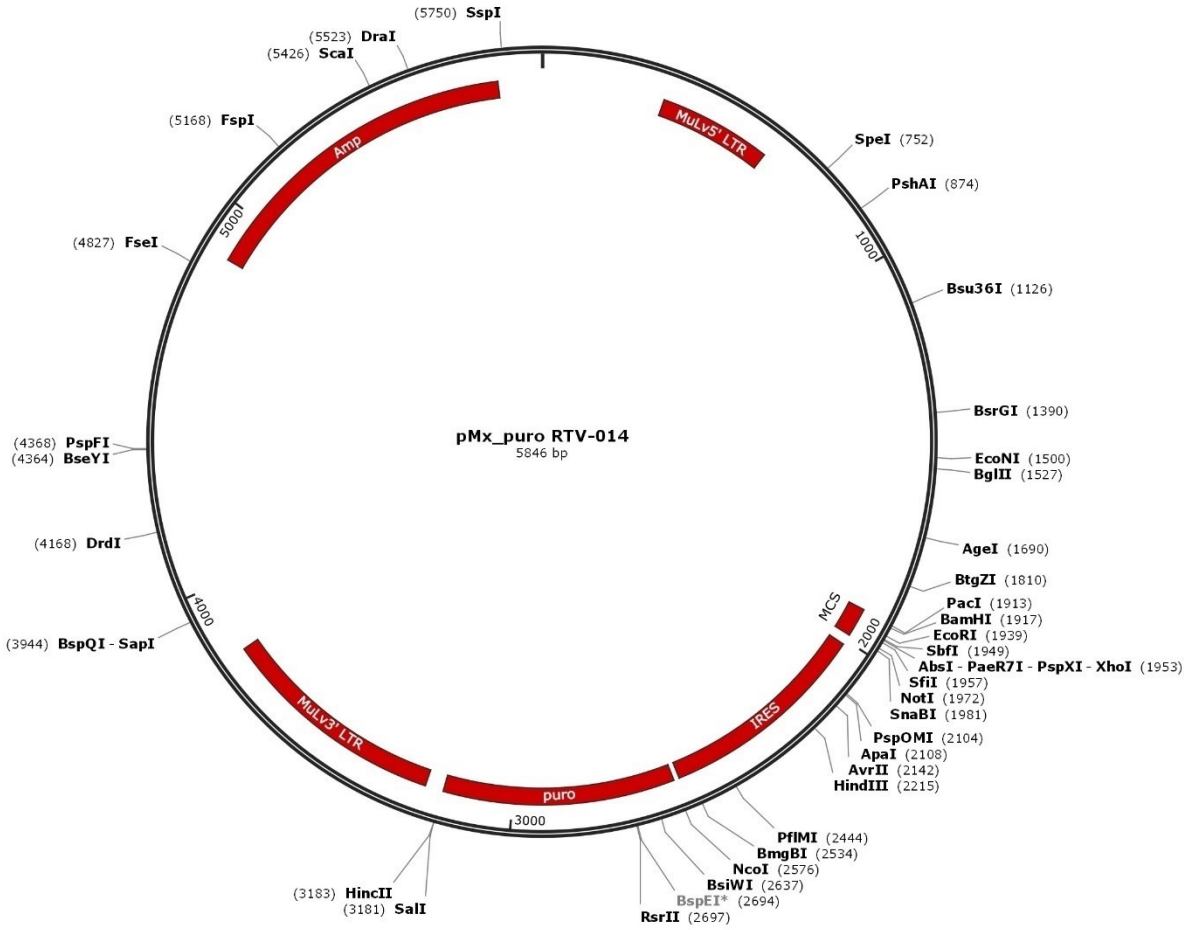

Figure 43: Vector map of the pMx_puro RTV-014 plasmid
This vector was used as a plasmid-backbone for the scA2Kb_β2M_p53.

7.1.2. pMx-Luciferase-IRES-GFP vector

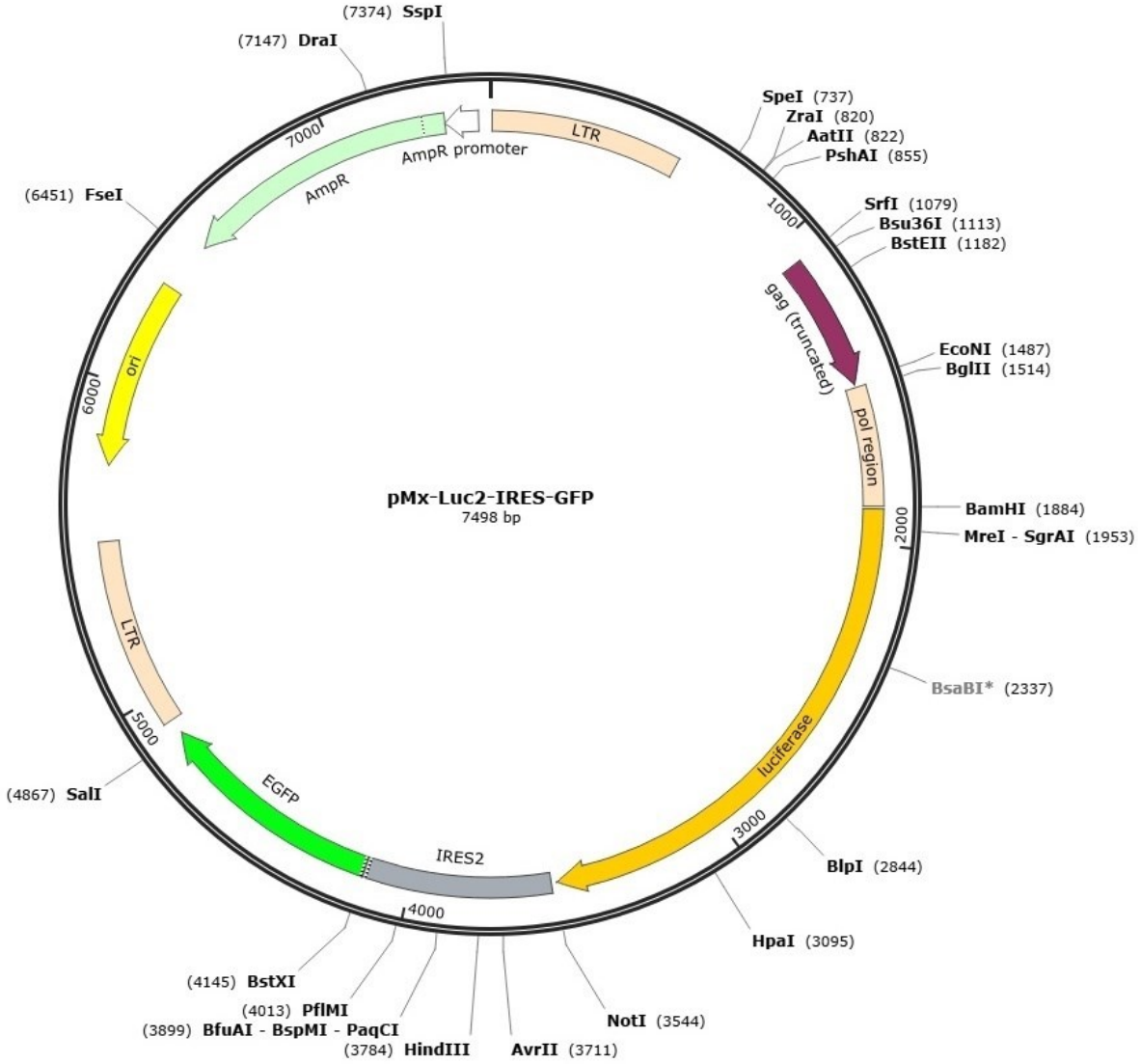

Figure 44: Vector map of the pMx-Luciferase-IRES-GFP plasmid
Luciferases are oxidative enzymes producing bioluminescence by metabolising its substrate luciferin. GFP is a green fluorescence protein originally derived and isolated from the jellyfish Aequorea Victoria. Both genes are frequently used as reporter genes of expression in cell and molecular biology.

7.1.3. pMx_Katushka vector

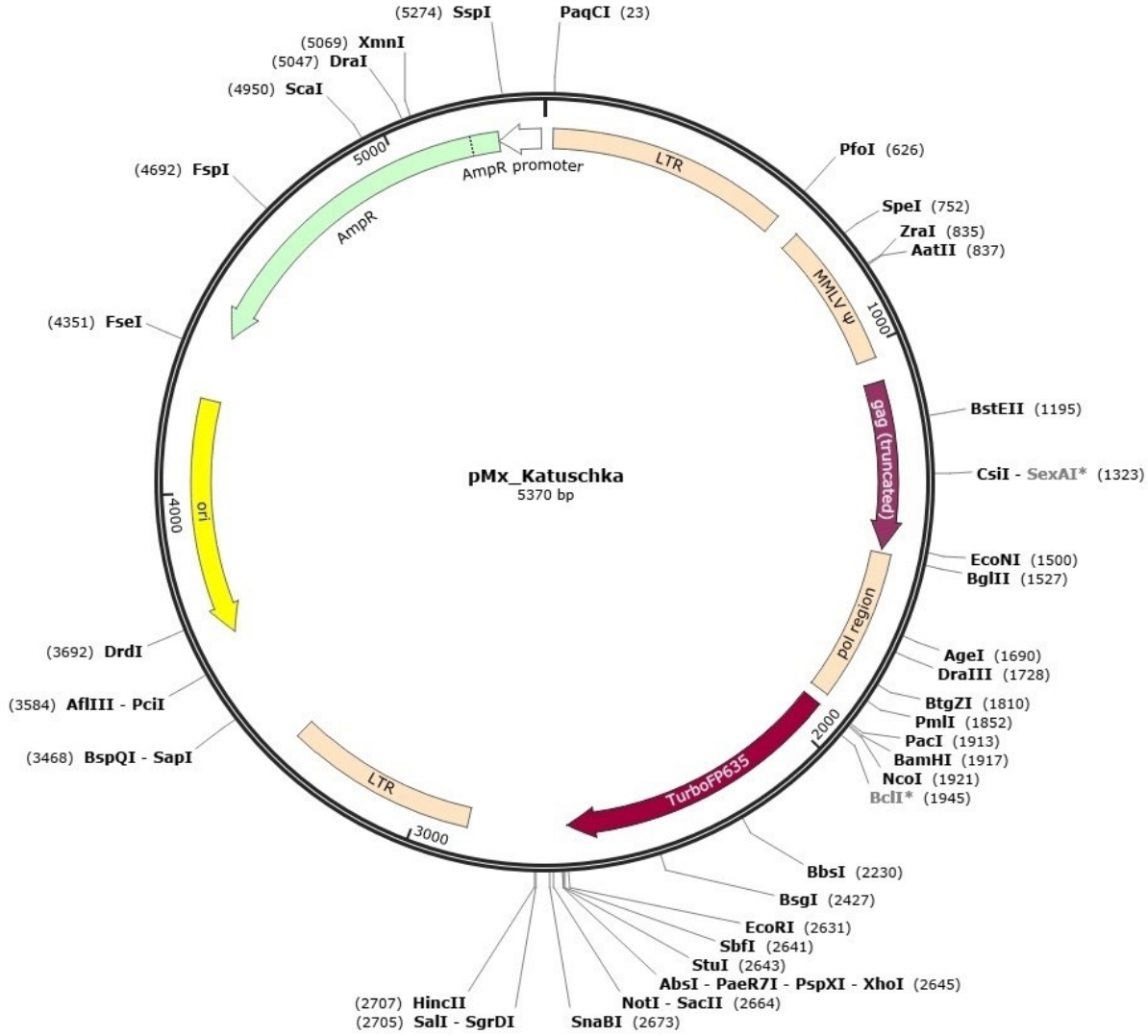

Figure 45: Vector map of the pMx-Katushka plasmid
Katushka is a basic (constitutively fluorescent) red fluorescent protein, derived from the Bubble-tip anemone Entacmaea quadricolor.

7.1.4. p53-scTCR_pGMP93 vector

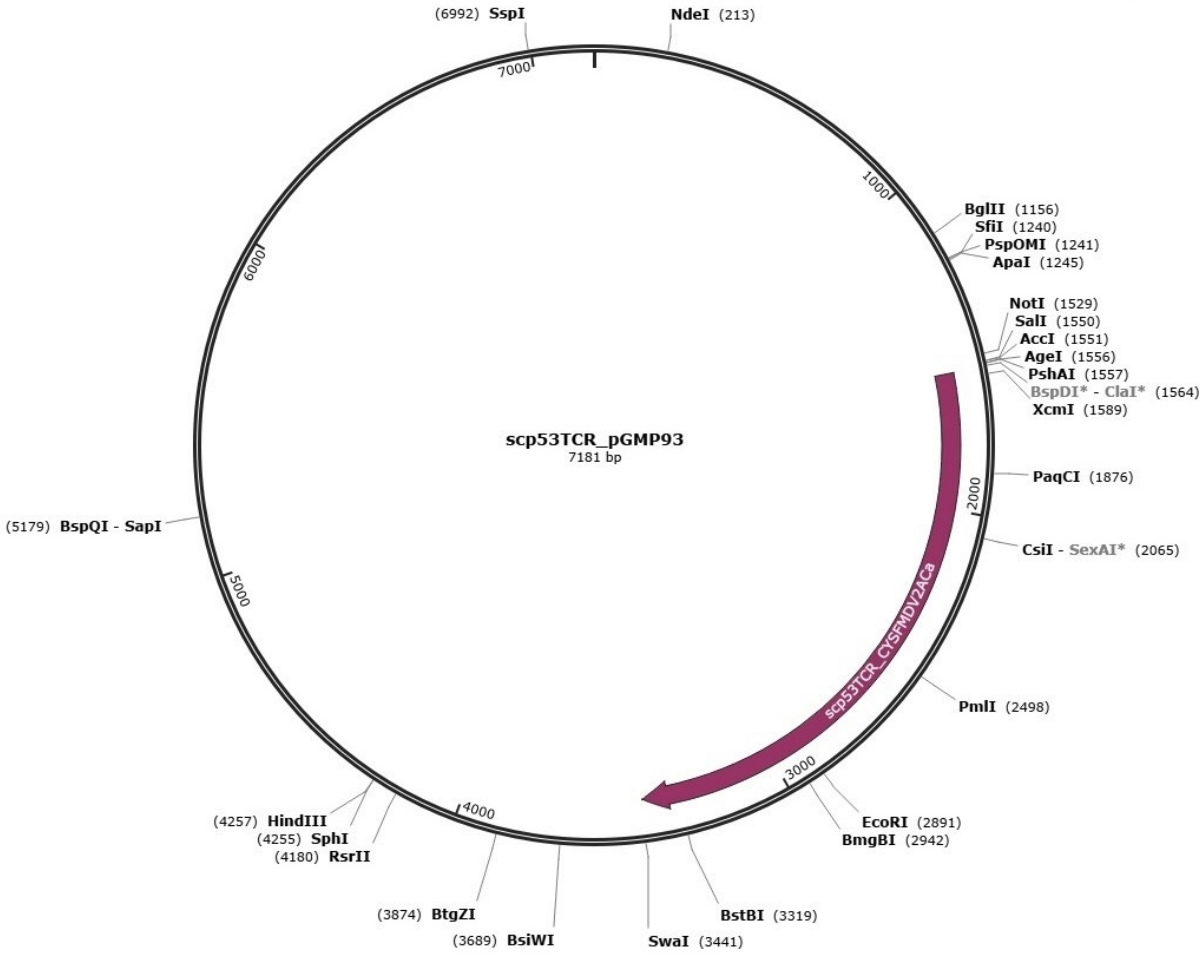

Figure 46: Vector map of the p53-scTCR_pGMP93 plasmid

7.1.5. pMx_scA2Kb-b2M-p53_puro

Codon-optimized sequence

GAA*GGATCC*ACC**ATG**GTTCCCTGCACACTGTTGTTGCTGCTGGCTGCTGCTCTGGCCCCTACAC
AGACAAGAGCCCTGCTGGGCAGAAACAGCTTTGAAGTCGGAGGCGGAGGATCTGGTGGTGGT
GGATCTGGCGGCGGAGGCTCTATTCAGAAAACCCCTCAGATCCAGGTGTACAGCAGACACCC
TCCTGAGAACGGCAAGCCCAACATCCTGAACTGCTACGTAACCCAGTTTCACCCTCCTCACAT
CGAGATCCAGATGCTGAAGAACGGGAAGAAGATCCCCAAGGTCGAGATGAGCGACATGAGC
TTCAGCAAGGACTGGTCCTTCTACATCCTGGCTCACACCGAG**TTC**ACCCCTACCGAGACAGAC
ACATACGCCTGTAGAGTGAAGCACGCCAGCATGGCCGAGCCTAAGACAGTGTACTGGGACA
GAGATATGGGAGGTGGCGGTAGTGGTGGCGGAGGTTCAGGCGGAGGTGGAAGCGGAAGCCA
CAGCATGAGATACTTTTTCACCAGCGTGTCCAGACCTGGCAGAGGCGAGCCTAGATTCATTGC
TGTGGGCTACGTGGACGACACCCAGTTCGTCAGATTCGACTCTGATGCCGCCAGCCAGAGAA
TGGAACCTAGGGCTCCTTGGATCGAGCAAGAGGGCCCTGAGTATTGGGACGGCGAGACAAGA
AAAGTGAAGGCCCACAGCCAGACACACAGAGTGGACCTTGGAACCCTGAGAGGCTACTACA
ACCAGTCTGAGGCCGGCTCTCACACCGTGCAGAGGATGTATGGCTGTGACGTGGGCAGCGAT
TGGAGATTCCTGAGGGGATACCACCAGTACGCCTACGACGGCAAGGACTATATCGCCCTGAA
AGAGGACCTGAGAAGCTGGACAGCCGCCGATATGGCCGCTCAGACAACAAAGCACAAGTGG
GAAGCCGCTCACGTGGCCGAGCAGCTGAGAGCTTATCTGGAAGGCACCTGTGTGGAATGGCT
GCGGAGATACCTGGAAAACGGCAAAGAGACACTGCAGAGAACAGACAGCCCCAAGGCTCA
CGTGACACACCACAGCAGACCTGAGGACAAAGTGACCCTGAGATGCTGGGCTCTGGGCTTCT
ACCCTGCCGACATTACACTGACATGGCAGCTGAACGGCGAGGAACTGATCCAGGACATGGAA
CTGGTGGAAACCAGACCTGCTGGCGACGGCACATTCCAGAAATGGGCAAGTGTGGTGGTGCC
CCTGGGCAAAGAGCAGTACTACACCTGTCACGTGTACCACCAGGGACTGCCTGAGCCTCTGA
CACTGAGATGGGAACCTCCACCTAGCACCGTGTCTAACATGGCCACAGTGGCTGTGCTGGTGG
TGCTGGGAGCTGCTATTGTGACAGGCGCTGTGGTGGCCTTCGTGATGAAGATGAGAAGAAGA
AACACCGGCGGCAAAGGCGGCGATTATGCTCTGGCTCCTGGCTCTCAGACAAGCGACCTTAG
CCTGCCTGACTGCAAAGTGATGGTGCACGATCCTCACAGCCTGGCC**TGATAA***GCGGCCGC*TTC

Figure 47: Schematic representation of the sequence encoding for scA2K^b_β$_2$M_p53
Murine sequences in light orange and grey, human sequences in orange and green.

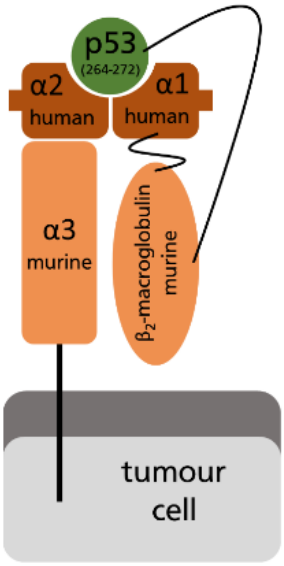

Figure 48: Structural representation of the chimeric single chain MHC I molecule including the p53 (264-272) peptide

7.2. Primer

Table 15: Primer for pMx_scA2K^b_β$_2$M_p53_puro DNA amplification

Primer	Sequence 5′-3′
Forward (SE206)	TTACACAGTCCTGCTGACCACC
Reverse (R_pMxRTV014_2036)	AAGCGGCTTCGGCCAGTAAC

Acknowledgement

First of all, I would like to express my gratitude to my boss and mentor [redacted]. Thank you for giving me the opportunity to work on this challenging, interesting, and exciting project as part of my PhD thesis. You had always an open door for problems and scientific discussions which was highly appreciated. Thank you for your input and for proof-reading my doctoral thesis.

Second, I would like to thank the members of the examination board for their time and willingness to read my thesis and examine me during my defence. Special thanks to [redacted] for being my first correspondent and for your scientific input during my research.

Additionally, I want to thank the whole team of AG Echchannaoui/Theobald and all the research members of the III. Medical Department for their constant assistance during my PhD studies but also for the great time we had together at work and at after-work events.

Last but not least, I want to express my deepest gratefulness to my family and friends. Your sustained support and sympathy were key to pass my studies and now finally finish my PhD.